

Microwave Electronics

**DEVELOPMENT OF COMPACT MICROWAVE FILTERS USING MICROSTRIP LOOP
RESONATORS**

Thesis submitted by

JITHA B

in partial fulfillment of the requirements for the degree of

DOCTOR OF PHILOSOPHY

Under the guidance of

Dr. C. K. AANANDAN



**DEPARTMENT OF ELECTRONICS
FACULTY OF TECHNOLOGY
COCHIN UNIVERSITY OF SCIENCE AND TECHNOLOGY
COCHIN-22, INDIA**

March 2010

Dedicated

to

The Almighty




DEPARTMENT OF ELECTRONICS,
COCHIN UNIVERSITY OF SCIENCE AND TECHNOLOGY,
KOCHI, INDIA

Dr. C. K. Aanandan,
(Supervising Guide)
Professor,
Department of Electronics,
Cochin University of Science and Technology

CERTIFICATE

Certified that this thesis entitled “**DEVELOPMENT OF COMPACT MICROWAVE FILTERS USING MICROSTRIP LOOP RESONATORS**” is a bonafide record of the research work carried by Ms. Jitha B under my supervision in the Centre for Research in ElectroMagnetics and Antennas, Department of Electronics, Cochin University of Science and Technology. The results presented in this thesis or part of it have not been presented for the award of any other degree.

Cochin - 22
5th March 2010


Dr. C. K. Aanandan

DECLARATION

I hereby declare that the work presented in this thesis entitled “**DEVELOPMENT OF COMPACT MICROWAVE FILTERS USING MICROSTRIP LOOP RESONATORS**” is a bonafide record of the research work done by me under the supervision of Prof. C.K. Anandan, Department of Electronics, Cochin University of Science and Technology, India and that no part thereof has been presented for the award of any other degree.

Cochin-22
March 2010



JITHA B

Acknowledgement

I remember with gratitude,

My supervising guide, Dr. C.K. Aanandan, Professor, Department of Electronics, Cochin University of Science and Technology, for his valuable guidance, advice and timely care extended to me during my research period. His imminent way of thinking has helped me to explore my research abilities and encouraged in implementing the ideas with absolute satisfaction. I was able to successfully complete this research work and deliver this thesis because of his able guidance and immense patience.

Dr. K.G. Nair, Director, Centre for Science in Society, Cochin University of Science and Technology and the founder of Center for Research in Electromagnetics and Antennas, for his vision and commitment for the research that has led to this great establishment with wonderful teachers, resources and facilities.

Prof. K. Vasudevan, Head, Department of Electronics, Cochin University of Science and Technology for his constant encouragement, concern and extending the facilities of the department.

Dr. P Mohanan, Professor, Department of Electronics, Cochin University of Science and Technology for the advice and timely care rendered during these years. He has been always there with tremendous support and as a steady source of inspiration.

Prof. K.T. Mathew, Prof. P.R.S. Pillai, Dr. Tessamma Thomas, Dr. James Kurian and Dr. Supriya M.H and other faculties of Department of Electronics, Cochin University of Science and Technology for their support.

All non-teaching staff of Department of Electronics for their friendly relation, sincere cooperation and timely help. Special thanks to Mr. C.P. Muraleedharan and Mr. Ibrahimkutty and Mr. Siraj for their amicable relation and valuable helps.

All my senior research scholars who have pursued good career after their research work and are excellent evidences for a successful occupation ahead.

My colleagues and friends Ms. Raji, Laila Miss, Ms. Nisha, Mr. Sujith, Mr. Deepu, Ms. Shameena, Mr. Sarin, Mr. Gopikrishnan, Ms. Deepti, Mr. Sreejith, Mr. Sreenath, Ms. Anju, Mr. Lindo, Mr. Paulbert, Toni Sir, Mr. Dineshan and Sarah Miss at Centre

Acknowledgement

for Research in Electromagnetics and Antennas for their fruitful discussions, open hearted help and creating a homely environment in the laboratory.

Mrs. Anju Pradeep, Dr. Binu Paul and Dr. S. Mridula, , School of Engineering, for their whole hearted rapport. Anju Miss has always attended me with immense patience and spent her precious time for fruitful discussions

My friends in, Cochin University Centre for Ocean Electronics (CUCENTOL) and Microwave Tomography and Material Research (MTMR) for extending their noble friendship. I would specially thank Mr. Ananthakrishnan and Mr. Ullas for their timely help with patience.

My friend Ms. Nimisha C.S, Research Scholar, IISc Bangalore, for being a good companion during the initial period of my research work, helping and supporting me with valuable suggestions.

Ms. Prabha Anil and Dr. Beena Mary John for including me in their prayers and being a constant source of inspiration in completing my research work in time.

University Grants Commission for the financial assistance in the form of Research fellowship for meritorious students (RJ'SMS).

The matron and staff of Athulya Ladies Hostel, Cochin University of Science and Technology, for their help and cooperation during my stay.

My friend and roommate Ms. Cilla Sanjay for her love, support, care and prayers that rendered me a warm atmosphere for the successful completion of the work.

My friend Mr. Rakesh V.V for his help, constant encouragement and sincere support throughout the research period.

My words are limitless to express my thanks to my friend Dr. Ameer Krishnakumar, for her great support that helped me to complete my work in time. She was instrumental in relentless encouragement and thrust to keep me in full pace of my thesis work. She has always been with me as a sincere friend giving valuable suggestions and also as an unwavering supporter.

Dr. Gijo Augustin, and his wife Ms. Bybi P.C. for being with me through the thick and thin of my research life. Gijo, who was my senior, has been a constant support as an affectionate brother and a good motivator as a researcher. My friend Bybi, also my

Acknowledgement

colleague, has helped me in my work and in my odd days with her sincere advice, care and affection.

Achan, Amma, Jayakutty and Ammamma for their deep love, care and patience to move on with my research work. They were always with me as a constant source of energy without whose prayers and blessings I would never been able to achieve my aim.

Jitha B

Chapter One

INTRODUCTION

| | | |
|------------|---|-----------|
| 1.1 | Microwave Communication | 3 |
| 1.1.1 | Microwave frequency bands | 4 |
| 1.2 | Filters | 4 |
| 1.2.1 | Need for filters in microwave communication | 5 |
| 1.2.2 | Evolution of filters | 5 |
| 1.2.3 | Filter classification | 7 |
| 1.2.4 | Filter specifications | 10 |
| 1.2.5 | Applications of filters | 11 |
| 1.3 | Resonators for Microwave Communication | 17 |
| 1.3.1 | Bulk wave, Surface Acoustic Wave and helical resonator | 17 |
| 1.3.2 | Coaxial, dielectric, waveguide and stripline resonators | 17 |
| 1.3.3 | Planar resonators | 18 |
| 1.4 | Outline of Present Work | 23 |
| 1.5 | Organisation of the Thesis | 23 |
| | References | 25 |

Chapter Two

REVIEW OF LITERATURE

| | | |
|------------|--|-----------|
| 2.1 | Microwave Filters | 31 |
| 2.2 | Microstrip Bandstop filters | 31 |
| 2.3 | Microstrip Band Pass Filters | 38 |
| 2.4 | Waveguide Filter Using Planar Loop Resonator Insert | 51 |

| | |
|------------|----|
| References | 53 |
|------------|----|

Chapter Three**METHODOLOGY**

| | | |
|------------|---|-----------|
| 3.1 | Techniques for Modelling and Optimization of Filters | 69 |
| 3.1.1 | Ansoft HFSS | 69 |
| 3.1.2 | Zealand IE3D | 72 |
| 3.2 | Filter Fabrication | 74 |
| 3.2.1 | Photolithographic technique | 76 |
| 3.3 | Filter Characteristics Measurement | 77 |
| 3.3.1 | HP 8510c Vector Network Analyzer | 77 |
| 3.3.2 | E8362B Precision Network Analyzer (PNA) | 79 |
| 3.3.3 | Measurement procedure | 80 |
| 3.3.4 | S Parameters, Resonant Frequency and Band width | 80 |
| | References | 80 |

Chapter Four**COMPACT PLANAR LOOP RESONATOR FILTERS**

| | | |
|------------|------------------------------------|------------|
| 4.1 | Introduction | 83 |
| 4.1.1 | Open loop resonator | 94 |
| 4.1.2 | Compact Microstrip Bandstop Filter | 100 |
| 4.2 | Bandpass Filters | 111 |

| | | |
|-------|---|-----|
| 4.2.1 | Bandpass Characteristics of closed loop resonator | 113 |
| 4.2.2 | Bandpass Characteristics Of Open Loop Resonator | 120 |
| 4.2.3 | Bandpass Filter: Slits along L ($L < W$) | 125 |
| 4.2.4 | Bandpass Filter: Slits along L ($L > W$) | 130 |
| 4.3 | Compact Bandpass Filter using Folded Loop Resonator | 133 |
| 4.3.1 | Folded Loop Resonator | 133 |
| 4.3.2 | Compact Folded Open Loop Resonator Filter | 136 |
| 4.4 | Conclusion | 144 |

Chapter Five

SRR BASED MICROSTRIP BANDSTOP FILTER

| | | |
|-------|--|-----|
| 5.1 | Introduction | 149 |
| 5.1.1 | Transmission characteristics Of SRR loaded microstrip Line | 150 |
| 5.2 | Conclusion | 158 |
| | References | 158 |

Chapter Six

SRR BASED WAVEGUIDE FILTER

| | | |
|-------|--|-----|
| 6.1 | Intoduction | 161 |
| 6.1.1 | Bandstop characteristics of SRR in waveguide | 164 |
| 6.1.2 | Bandpass characteristics of SRR in waveguide: Waveguide miniaturization | 170 |

| | | |
|------------|-------------------|-----|
| 6.2 | Conclusion | 171 |
| | References | 171 |

Chapter Seven**CONCLUSIONS**

| | | |
|------------|--|-----|
| 7.1 | Thesis Highlights | 174 |
| 7.2 | Compact Planar Loop Resonator Filters | 174 |
| 7.3 | Parallel Coupled Loop Resonators | 175 |
| 7.4 | Compact Bandpass Filter Using Folded Loop Resonator | 176 |
| 7.5 | SRR Based microstrip Bandstop Filter | 176 |
| 7.6 | SRR Based Waveguide Bandstop Filter | 176 |
| 7.7 | SRR Based Waveguide Bandpass Filter | 177 |
| 7.8 | Suggestions for Future Work | 177 |

INTRODUCTION

Filters are essential components in any communication system. They are used to select or confine the RF microwave signals within assigned spectral limits so as to share the limited electromagnetic spectrum. Emerging applications in wireless communication demand RF-microwave filter with even more stringent requirements: smaller size, lighter weight, lower cost along with better performance. Depending on the requirements and specification, RF microwave filters may be designed and realized in various transmission line structures, such as waveguide, coaxial line or microstrip line. Development of compact filters using resonators in microstrip configuration is discussed in this thesis.

1.1 Microwave Communication

Microwaves are electromagnetic radiation of frequencies from several hundred MHz to several hundred GHz. Microwave technology owes its origin to the development of radar, which started before World War II by necessity. Various investigators were trying to solve the problem of UHF/microwave bands with high power. At the heart of their investigation was the conventional vacuum tube, which at the time seem to be the best approach. The high frequency shorting at these frequencies and longer transit time in the vacuum tube limited its operation in the lower frequencies. A solution to this problem was proposed in 1920 by German scientists H Barkhausen and K. Kurz through their Barkhausen- Kurz oscillator, a new type of vacuum tube that generated high frequency signals, but with a limited output power. The limitations of these devices paved way to the invention of new microwave device such as magnetron followed by klystron vacuum tube. With the production of these microwave devices, radar was finally a commercially, albeit a military, success at microwave frequencies. In the decades that followed, the use of microwaves was limited to telephone companies in the commercial sectors. By 1960's, microwave communication has replaced 40% of the telephone circuits between the major cities. 1990's have seen a continuous evolution of microwave developments, particularly in the consumer marketplace. Direct broadcast satellite services (DBS) to the home at high frequencies and power have occurred. Personal communicators, cellular phones and the like which are under the general category of personal communication systems (PCS), continue to be heavy growth areas. Microwaves have found applications in areas other than those in communications and in radar. They are also used in medicine, remote sensing, heating, industrial quality control, radio astronomy, in navigation via global positioning systems etc.

1.1.1 Microwave frequency bands

The IEEE standard frequency allocation for various applications is illustrated in table 1.1.

| Band Designation | Frequency range | Usage |
|------------------|-----------------|--|
| VLF | 3-30KHz | Long distance telegraphy and navigation |
| LF | 30-300 KHz | Aeronautical navigation services, Radio broadcasting, Long distance communication, |
| MF | 300-3000 | Regional broadcasting, AM radio |
| HF | 3-30MHz | Communications, broadcasting, surveillance, CB radio |
| VHF | 30-300 MHz | Surveillance, TV broadcasting, FM radio |
| UHF | 300-1000MHz | Cellular communications |
| L | 1-2 GHz | Long range surveillance, remote sensing |
| S | 2-4 GHz | Weather detection, Long range tracking |
| C | 4-8 GHz | Weather detection, long-range tracking |
| X | 8-12 GHz | Satellite communications, missile guidance, mapping |
| Ku | 12-18 GHz | Satellite communications, altimetry, high resolution mapping |
| K | 18-27 GHz | Very high resolution mapping |
| Ka | 27-40 GHz | Air port surveillance |

Table 1.1 Frequency bands allocation for various applications

1.2 Filters

A filter is a two port network used to control the frequency response at a certain point in the electromagnetic spectrum by providing low loss transmission at frequencies for the desired band and high attenuation in the rest of the frequencies. Filters find applications virtually in any type of communication, radar or test and measurement systems.

1.2.1 Need for filters in microwave communication

Filters are essential in separating and sorting signals in communication systems. The electromagnetic spectrum is limited and has to be shared; filters are used to select or confine the RF/microwave signals within assigned spectral limits. They are used in a variety of communication systems which typically transmit and receive amplitude and/or phase modulated signals across a communication channel. Radio transmitters and receivers require filters to remove or suppress unwanted frequencies from being transmitted or received. Emerging applications such as wireless communication continue to challenge RF/microwave filters with even more stringent requirements smaller size, lighter weight, and lower cost with better performance. Filters used in communication and radar applications, are implemented in different kinds of transmission lines including rectangular waveguide, microstrip line and stripline. Filters are also the integral part of multiplexers which are of major demand in the broad band wireless access communication systems.

1.2.2 Evolution of filters

Filters in electric circuits have played an important role since the early stages of telecommunication and have progressed steadily in accordance with advancement of communication technology. The introduction of telephony which drastically reformed the technological landscape surrounding telecommunication system required the development of new technology to extract and detect signals contained within a specific frequency band. This technological advance further accelerated the research and development of filter technology.

The foundation of modern filter theory and practice took place during the period of World War II and the years immediately following, especially by such pioneers as P. L Richards (1948). Work on microwave filters commenced prior to the war, a particularly significant paper being published by Mason and Sykes(1937). They used ABCD parameters, although not in matrix form, to derive the image impedance and image phase and attenuation functions of a rather large variety of

useful filter sections. Network theory was probably the most advanced topic in engineering at that time, Darlington having published his famous cascade synthesis theory as far back as 1939 (Darlington,1939) .

The direct-coupled cavity filter theory was one of the first great contributions from the group formed at Stanford Research Institute, among whose workers were Leo Young. The direct-coupled cavity filters have excessive length in coaxial or stripline form. This dimension was reduced by a factor of 2 with the introduction of parallel coupled lines (Ozaki et al., 1958; Cohn et al., 1958). Parallel coupling is much stronger than end coupling, so that realizable bandwidths could be much greater. The prime mover here was George Matthaei, who published the theory and practical realizations of interdigital filters (Matthaei,1962) and the combline filter in the following year [Matthaei,1962]. Turning to other types of filters, waveguide bandstop filters were described by Fano and Lawson (1948). Low-pass filters in both waveguide and coaxial form are very important components in microwave systems, being used to reject unwanted harmonics in both high- and low-power systems. A very good account of the early development is given in the classic volume of Matthaei, Young, and Jones [1964]. The previous reference leads naturally to the examination of the history of dielectric resonator filters.

Most of the early research was carried out in the early 1960's, as summarized in (Cohn, 1968). These filters consist of a number of coupled dielectric disks mounted in a waveguide beyond cut off. In order to give important size reduction, a high dielectric constant must be used, but originally such dielectrics possessed excessive temperature sensitivity. Now this drawback has been overcome with the development of high-Q ceramics with temperature coefficients of expansion comparable to those of invar. One of the first dielectrics having improved frequency stability was reported by workers at Raytheon (Masse and Pucel, 1972). Considerable improvements carried out at Bell Telephone Laboratories and Murata Manufacturing Company of Japan were reported at the Workshop on Filter Technology during the 1979 MTT-S International Microwave Symposium. Bell uses

a barium titanate ceramic ($\text{Ba}_2\text{Ti}_{90}\text{Zr}_{10}\text{O}$) having a relative permittivity of 40, and achieves resonator Q's between 5000 and 10000 in the 2-7-GHz frequency range (Plourde and Linn, 1977; Ren, 1978). Filters may be constructed in all the common transmission media ranging from waveguides to microstrip, and the technique is, therefore, quite versatile. Substantial size reductions have been made, particularly in the 3.7–4.2 GHz and 5.9–6.4GHz waveguide bands, and the filters are stated to have low cost.

Emerging applications such as wireless communications continue to challenge RF/microwave filters with ever more stringent requirements. The recent advances in novel materials and fabrication technologies, including high-temperature superconductors (HTS), low-temperature co-fired ceramics (LTCC), monolithic microwave integrated circuits (MMIC), micro-electromechanic system (MEMS), and micromachining technology, have stimulated the rapid development of new microstrip and other filters for RF/microwave applications. In the meantime, advances in computer-aided design (CAD) tools such as full-wave electromagnetic (EM) simulators have revolutionized filter design.

1.2.3 Filter classification

- **Classification of filters based on passband types**

Filters are used in all frequency ranges and are categorized into four main groups:

- Lowpass filter (LPF) that transmits all signals from DC to a cut-off value, ω_c and attenuates all signals with frequencies above ω_c .
- Highpass filter (HPF) that passes all signals with frequencies above the cutoff value ω_c and rejects signal below ω_c .
- Bandpass filter (BPF) that passes signal with frequencies in the range of ω_1 to ω_2 and rejects frequencies outside this range.
- The complement to bandpass filter is the bandstop filter (BSF).

Figure 1.1(a) to Fig.1.1 (d) shows the characteristics of the four filter categories. Note that the characteristics shown are for passive filter.

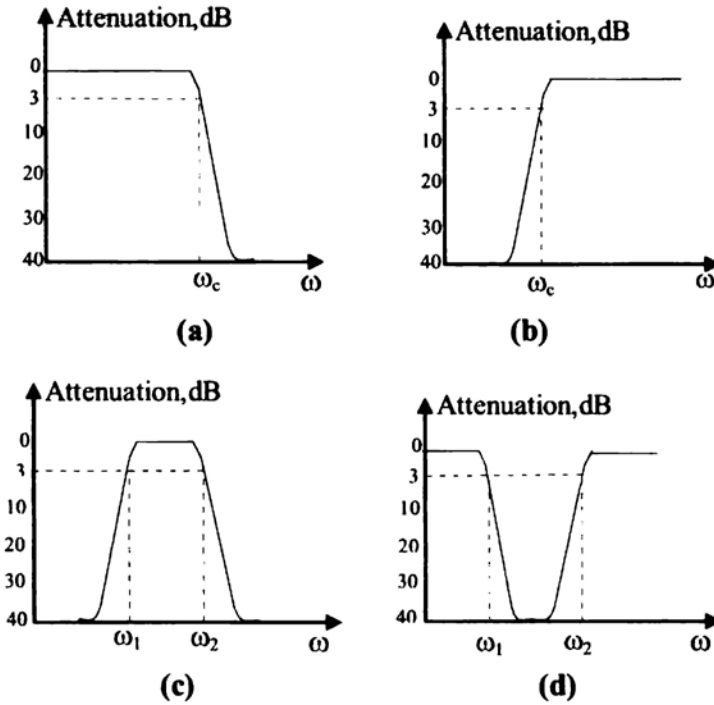


Fig. 1.1 Frequency responses of (a) Lowpass filter (b) Highpass filter (c) Bandpass filter (d) bandstop filter.

The characteristic of a passive filter can be described using the transfer function approach or the attenuation function approach. In low frequency circuit the transfer function ($H(\omega)$) description is used while at microwave frequencies the attenuation function description is preferred.

▪ **Classification of filters based on fractional bandwidth**

Fractional bandwidth or percentage bandwidth is a simple calculation, and gives a normalized measure of how much frequency variation a system or component can handle. If you know the center frequency and the bandwidth, the percentage bandwidth is:

$$BW\% = \frac{BW}{f_c} * 100$$

Here "BW" is the *absolute* bandwidth and f_c is the center frequency.

- Narrow Band Filters : below 5%
- Moderate Band Width : between 5% to 25%
- Wide Band Filters : greater than 25%

▪ **Classification of filters by transmission media**

The transmission media are characterized into two: Lumped elements and distributed elements. When the behavior of a resistor, capacitor, or inductor can be fully described by a simple linear equation, microwave engineers refer it to as a lumped element where operation is restricted to lower frequencies where they are physically much smaller than a quarter-wavelength.

At microwave frequencies, other factors must also be considered. To accurately calculate the behavior of **the** same 50-ohm resistor, you need to consider its length, width, and thickness of metal (due to the skin effect), and its proximity to the ground plane. This is when we must consider it as a distributed element. The transmission media at microwave frequencies include the following:

- Coaxial transmission lines
- Microstrip lines
- Strip lines
- Waveguides

Most transmission media that use two conductors, where one is considered ground include coaxial, microstrip and stripline. The transmission line that does not use a pair of conductors is waveguide.

1.2.4 Filter specifications

- **Frequency specifications:**
 - Center frequency and bandwidth (f_0 & BW) for BPF and BSF
 - Cut-off frequency (f_c) For LPF and HPF
 - Passband insertion loss
 - Return Loss and Flatness (ripple level)
 - Selectivity or skirt sharpness
 - Out of band rejection levels
 - Harmonic Rejection
- **Power handling capability**
 - Multipactor effects & voltage breakdown
 - Environmental specifications
 - Operational temperature limits
 - Pressure & humidity environments
 - Shock & vibration levels
- **Mechanical specifications**
 - Size, shape & weight
 - Type Of Input / Output connectors
 - Mechanical mounting interfaces

- **Lower frequency techniques limitations**

- Lumped element sizes (R,L,C) become comparable to wavelength
- Radiation from elements causes undesirable effects and increased losses
- Wire connections between elements become part of circuit (parasitic)

1.2.5 Applications of filters

- **Radar systems**

World War II and the invention of radar led to significant developments in filters at various laboratories in the U.S. Work concentrated on narrow-band waveguide filters for radar systems. Advances on broad-band TEM filters for electronic support measures (ESM) systems and tunable narrow-band filters for search receivers were made. Most of this work is described in (Fano and Lawson, 1948).

Military applications required wide-band and tunable devices for electronic support measures receivers, which led to the development of highly selective wide-band waveguide filters, coaxial resonator and suspended-substrate multiplexers, and electronically tunable filters. One of the critical parts of any military system is the electronic counter measures (ECM) system and its associated ESM system. The ESM system detects and classifies incoming radar signals by amplitude, frequency, pulse width, etc., and the ECM system can then take appropriate countermeasures, such as jamming. One method of classifying signals by frequency is to split the complete microwave band of interest into smaller sub-bands. This can be done using a contiguous multiplexer, which consists of separate bandpass filters whose pass bands crossover at their 3-dB frequencies. The outputs of the individual channels can be detected, giving coarse frequency information while retaining unity probability of intercept (Tsui, 1992).

- **Communication systems:**
 - **Mobile and cellular systems**

Cellular communications base-stations demanded low-loss high power-handling selective filters with small physical size, capable of being manufactured in tens of thousands at a reasonable cost. These demands led to advances in coaxial resonator, dielectric resonator, and superconducting filters, and also methods of cost-reduction, including computer-aided alignment. Cellular radio handsets have required the manufacture of hundreds of millions of extremely small very low-cost filters, still with reasonably low loss and high selectivity. The filters used in cellular radio handsets have completely different requirements. The original analog handsets in the 1980s were large, bulky, and manufactured in relatively small volumes. However, these phones used an FDMA access scheme; thus, they were transmitting and receiving simultaneously. Handsets for second-generation TDMA systems, such as GSM, transmit and receive in different time slots.

This has driven significant advances in integrated ceramic, surface, and bulk acoustic-wave active and passive filters using micromachined electromechanical systems (MEMS). Cellular radio has provided a significant driver for filter technology since the analog systems were launched in the early 1980s. This has resulted in various innovations in filter technology for both base-stations and handsets, which have depended upon the frequency planning of the various systems standards. In the U.S., the analog Advanced Mobile Phone Service (AMPS) used a frequency-division multiple-access (FDMA) scheme, and was allocated 869–894 MHz for base-station transmit (mobile receive) and 824–849 MHz for base-station receive (mobile transmit). The digital time-division multiple-access (TDMA) system (IS136) occupies the personal communications system (PCS) band from 1930 to 1990 MHz and 1850 to 1910 MHz and each 60-MHz band is sub-banded and allocated to operators in three 15-MHz and three 5-MHz segments. The American code-division multiple-access (CDMA) system (IS95) occupies both of the above

bands and is sub-banded into 5-, 10-, or 15-MHz segments. In Europe, the original analog total access communication system (TACS) occupied 890–905 and 935–950MHz. This was extended (ETACS) to 872–905 and 917–950MHz. The digital TDMA global system for mobile communications (GSM) (Glover, 1997) occupies 925–969 and 880–915 MHz and the bands from 1710 to 1785 and 1805 to 1880 MHz. These systems are not sub-banded. The third-generation universal mobile telecommunications system (UMTS) uses CDMA in the bands from 1920 to 1980 MHz and 2110 to 2170 MHz. The first analog systems required filters with percentage bandwidths in the region of 2% and with reasonable guard bands between channels. These specifications may be met with asymmetric generalized Chebyshev bandpass filters, typically with six resonators with a Q of 3000 and one or possibly two transmission zeros located on one side of the passband (Hunter, 2002).

Much smaller filters may be constructed using TEM transmission lines, which do not need a minimum cross sectional dimension to ensure propagation. The most significant developments were the parallel coupled-line filter (Cohn, 1958), which has found numerous applications in microstrip sub assemblies, the interdigital filter (Matthaei, 1962), and the combline filter (Matthaei, 1963).

The combline filter is of particular interest, as it has stood the test of time and variants of it are widely used in cellular radio base-stations. It consists of an array of equal-length parallel coupled conductors, each of which is short circuited to ground at the same end with capacitive loading on opposite ends. Here, we see that the capacitive loading will drive the resonant frequency of the resonators below that of the series couplings so that relatively strong inter-resonator couplings can occur. The combline filter has several advantages; firstly, it is compact, as the coupled conductors are typically one-eighth wavelength long. Secondly, the electrically short resonators will not re-resonate until typically six times the center frequency of the filter, giving a broad spurious-free stopband, which is not possible with wide-band interdigital filters. Thirdly, it is easier to manufacture than the interdigital filter, as

all the tuning screws required for electrical alignment can be on the same face of the filter. Finally, the center frequency of the combline filter may be tuned by an octave or more without causing significant distortion to its frequency response (Hunter and Rhodes, 1982). An accurate design method for wide-band combline filters is described in (Wenzel, 1971). The design of multiplexers using wide-band combline filters is reported in (Schumacher, 1976; La-Tourette, 1977; La-Tourette and J. L. Roberds, 1978).

Recent advances in micromachined electromechanical systems (MEMS) have demonstrated that this technology may be suitable for handset filters. For example, micromechanical resonators with Q 's of 7450 at 100 MHz have been demonstrated (Nguyen, 2000). MEMS switches have also been used for tuning the values of lumped components within filters (Peroulis et al., 2001). The use of tunable filters may be useful in handsets for future systems operating at many different frequencies. An alternative technology for tuning of filter resonators is to use ferroelectric materials with tuning accomplished by an applied electric field (Lancaster et al., 1998; Vendik et al., 2000).

- **Satellite systems**

The satellite communications industry created demand for low-mass narrow-band low-loss filters with severe specifications on amplitude selectivity and phase linearity. These requirements resulted in the development of dual-mode waveguide and dielectric-resonator filters, and advances in the design of contiguous multiplexers. High performance waveguide filters were used to avoid problems caused by the devices used when channelized architecture was first implemented in Intelsat IV series launched in 1971. The first major electrical innovation was the use of dual-mode filters, where size reduction is obtained by exciting two orthogonal degenerate modes in the same physical cavity. This was first reported by Lin (1951). The first practical devices were developed by Comsat Laboratories, Canada (Atia and Williams, 1971; Atia et al., 1974). Dual-mode filters were first launched on

Intelsat IV A in 1976, after which they became the satellite industry standard. Indeed, new types of dual-mode filter are still being reported, (Guglielmi et al., 2001). Surface acoustic wave (SAW) filters also have applications in the satellite industry. Several satellites use dielectric resonators constructed from low-loss high-permittivity (20–100) temperature stable ceramics having high- Q (up to 100 000) for filters to be realized in a fraction of the volume and weight of air-filled waveguide devices (Fiedziuszko et al., 2002). Probably the most significant development in this area was the dual-mode in-line device reported by Fiedziuszko (1982).

The sub-banded American systems require selective filters with percentage bandwidths as low as 0.25%. These filters require higher Q resonators with much better temperature stability than achievable with coaxial resonator filters. Dielectric resonator filters have been proven useful in this respect. The most commonly used designs use a cylindrical puck of ceramic suspended on a support within a metallic housing. The fundamental mode of resonance is the $TE_{01\delta}$ originally reported in (Cohn, 1968). The most commonly used material is calcium titanate–neodymium aluminate (Wersing, 1996), which has a relative permittivity of 45, a Q of greater than 20 000 at 2 GHz, and a temperature coefficient of resonant frequency of less than 1 ppm/°C for the $TE_{01\delta}$ mode.

Superconducting base-station filters are of interest because of their high Q realizable in a very small physical size. For example, a microstrip realization of a fifth-degree Chebyshev bandpass filter with 890-MHz center frequency and 0.3% bandwidth, occupied a surface area of approximately 5 cm and exhibited 1-dB passband insertion loss (Zhang et al., 1995). A complete receiver front-end including 5-MHz bandwidth filters and integrated LNAs in the PCS band at 1.9 GHz is described in (Soares et al., 2001).

The transmit/receive diplexer can be replaced by a switch and a receive filter. The purpose of the receive filter is to protect the LNA and the mixer in the down-converter from being overdriven by extraneous signals.

Recent advances in SAW filter design have enabled them to compete in this market. Their main advantage is very small size (typically 3x 3 x1 mm) and low cost. Typically, they have 3-dB insertion loss and 2-W power handling. The most significant advance in SAW technology has been the replacement of the conventional transversal designs by SAW resonators, which are formed between acoustically reflective gratings on the surface of a SAW crystal (Tagami et al., 1997). Although these remarkable devices offer small size and low cost, their power handling and temperature stability is poor when compared with ceramic filters. Thus, they may not be suitable for third-generation systems where the transmitter and receiver operate simultaneously. However, recent developments in film bulk acoustic resonator (FBAR) devices show very impressive performance (Larson et al., 2000; Weigel et al., 2002).

All the miniature handset filter technologies thus far discussed use passive resonators. Alternatively, several workers are investigating the use of active filters. One design approach is to compensate for the losses in physically small resonators by cancelling them with negative resistance. The negative resistance can be achieved by two distinct methods. In the first method (Brucher et al., 1994), the negative resistance is achieved by connecting a series *LC* resonator to the drain of a single common-source transistor, with a shunt *LC* resonator connected to the source. Alternatively, two transistors may be connected in a feedback configuration (Fort, 1994). This method has been demonstrated in the 3.8–4.2G Hz band. A spiral monolithic microwave integrated circuit (MMIC) inductor is then cascaded with this negative impedance converter to obtain a high *Q* inductor. This active inductance is then used to design bandpass filters. Although microwave filters are often described as a mature technology, it can be seen that this is not the case, and, hopefully, future applications will stimulate further advances in this exciting field.

1.3 Resonators for Microwave Communication

The main frequency bands assigned to the wireless communication are spread throughout a wide range, from several tens of MHz to several tens of GHz. A wide variety of resonators and filters can be applied to these frequency bands. A resonator is any structure that is able to contain at least one oscillating electromagnetic field. The resonating frequency of a resonator determines the frequency response of the corresponding filter. Resonators finding its use in microwave applications are further classified as follows.

1.3.1 Bulk wave, Surface Acoustic Wave and Helical resonator

For frequencies below 1 GHz, the most commonly used resonators are bulk wave, SAW and helical resonators. Bulk wave, SAW resonators/filters are used where there is strong demand for miniaturization and low loss characteristics; and helical resonators/filters are often utilized when a high level of power handling is necessary. In addition, bulk wave and SAW resonators show outstanding temperature characteristics, thus satisfying conditions for applications to narrow band filters.

1.3.2 Coaxial, dielectric, waveguide and stripline resonators

For a frequency range from RF to microwave, various kinds of resonators including the coaxial, dielectric, waveguide and strip line exist. Coaxial resonators have many attractive features including an electromagnetic shielding structure, low loss characteristics and small size but their minute physical dimensions for applications above 10GHz make it difficult to achieve manufacturing accuracy.

Dielectric resonators also possess a number of advantages such as low loss characteristics, acceptable temperature stability and small size. However, high cost and present-day processing technology restriction limits dielectric resonator utilization to applications below 50GHz.

Waveguide resonators have long been used in this frequency range, possessing two main advantages: low loss application and practical application feasibility up to 100GHz. However, the greatest drawback of the waveguide resonator is its size, which is significantly larger than other resonators available in the microwave region. The rectangular waveguide filter consists of a uniform section of rectangular guide with post (or other) discontinuities placed across the broad walls of the guide at approximately half-guide-wavelength intervals. Usually, the waveguide is operated in its fundamental mode (TE_{10}) mode of operation.

Presently, the most common choice for RF and microwave circuits remains the planar resonator or stripline resonator. Due to practical features including small size, easy processing by photolithography, and good affinity with active circuit elements, many circuits utilize the stripline resonator. Another advantage of the planar resonator is a wide applicable frequency range which can be obtained by employing various kinds of substrate materials. However, the major drawback to the use of stripline resonators is a drastic increase in the insertion loss compared to other types of resonators, making it difficult to use them for narrow band filters. Still such resonators yield high expectations for application to ultra low loss superconducting filters, which are now under development and require fabrication methods using planar circuits such as stripline configuration.

1.3.3 Planar resonators

In microwave applications keeping filter structures to a minimum size and weight is very important. Hence, planar filter structures which can be fabricated using printed-circuit technologies would be preferred whenever they are available because of smaller size and lighter weight. As is known, microwave frequency-selective devices occupy a substantial volume in communications, radar, and radio-navigation facilities. As a rule, these devices, designed as systems of coupled resonators, often determine overall dimensions of individual modules and, sometimes, the entire setup. Moreover, the quality and the ultimate characteristics of

radio equipment depend directly on the frequency-selective properties of filtering devices. Hence, the search for new solutions for the design of miniature filters and studies aimed at miniaturization and improvement of frequency-selective properties of known designs are very topical and among the most important problems of modern radio engineering. It is well known that the most miniature “electromagnetic” filters are microstrip filters (MSFs), which are widely used in microwave devices because of the advantages of such electronic components. These filters have small dimensions and are reliable and easy-to manufacture. The results of their high-speed quasi static analysis of various and complex design versions agree well with experimental data. This fact allows the development of efficient program systems for the computer-aided design of MSFs. The overall dimensions of micro strip filters can be reduced using several well-known approaches, such as the use of folded strip line conductors in resonators, formation of smooth and stepwise irregularities in these conductors and application of substrates with a high value of permittivity. Evidently, the maximum effect can be attained by combining several methods for reduction of the MSF dimensions.

In order to improve frequency-selective properties of filters, the slopes of the amplitude–frequency response (AFR), should be more and the attenuation levels in the filter stopbands should be large. These characteristics depend on both the number of the filter resonators and many other design parameters of the device. Therefore, the study of selective properties of particular design versions with different numbers of resonators as functions of the frequency band, fractional bandwidth, permittivity of the substrate, and other design parameters is important. Such studies allow (1) determination of the limits of applicability of the chosen design and (2) creation of optimized MSFs that satisfy particular specifications and contain the minimum number of sections. Stripline resonators are further classified as stepped impedance resonators and transmission line resonators.

○ **Stepped impedance resonators**

Stripline resonators having non uniform impedance characteristics are generally classified under stepped impedance resonators. Despite its simple structure, the SIRs possess numerous features and possibilities for practical applications. SIRs finds its applications in filters, oscillators and mixers as a basic resonator in frequency band from RF to millimeter.

○ **Transmission line resonators**

The most typical transmission line resonators utilizing transverse electromagnetic modes (TEM) or quasi-TEM modes are coaxial and stripline resonators. These resonators possess a wide application frequency range from several 100 MHz range to several 100GHz and presently remain the most common choice for the filters in wireless communication. These resonators do not possess low loss properties. They do not have high Q values compared to waveguide or dielectric resonators. However, they do have valuable features as small size, simple structure and capability of wide application to various devices. Moreover, the most attractive feature of the microstrip line, stripline or coplanar line resonators is that they can be easily integrated with active circuits such as MMICs, because they are manufactured by photo lithography of metallic film on a thin dielectric substrate. There are numerous forms of microstrip resonators. In general, microstrip resonators for filter design may be classified as lumped element or quasi-lumped element resonators and distributed line or patch resonators.

Microstripline resonators are the distributed elements such as quarter wavelength and half wavelength line resonators. The choice of individual components may depend mainly on the types of filters, the fabrication techniques, the acceptable losses or Q factors, the power handling and the operating frequency.

Distributed line resonators shown in Fig.1.2 are termed as quarter wavelength resonators since they are $\lambda_{g0}/4$ long, where λ_{g0} is the guided wavelength at the

fundamental resonant frequency f_0 . They can also resonate at other higher frequencies when $f = (2n - 1)f_0$ for $n=2, 3, \dots$

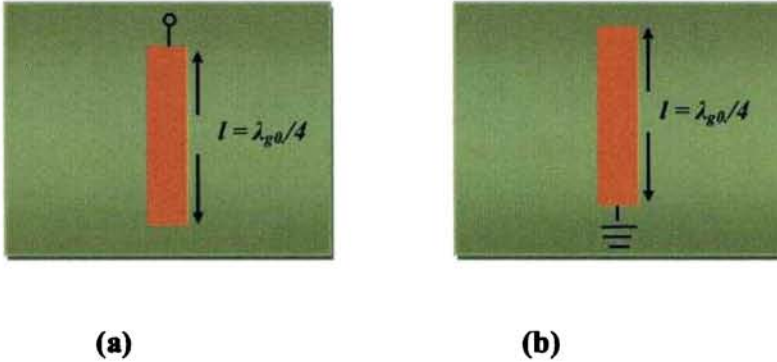


Fig.1.2 Some typical microstrip resonators (a) $\lambda_{g0}/4$ line resonator(Shunt series resonance) (b) $\lambda_{g0}/4$ line resonator(shunt parallel resonance)

Another typical distributed line resonator is the half wavelength resonator as shown in Fig. 1.3 which is $\lambda_{g0}/2$ long at its fundamental resonant frequency and can also resonate at $f = n f_0$ for $n=2, 3, \dots$.

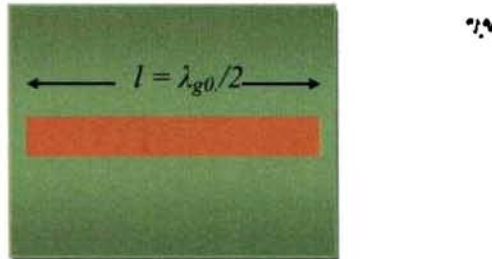


Fig. 1.3 $\lambda_{g0}/2$ line resonator

This type of line resonator can be shaped into many different configurations for filter implementations such as closed or open loop resonators. These are simpler to design and easier to fabricate. Closed ring resonator is merely a transmission line formed in a closed loop (Fig. 1.4). The circular ring will resonate at its fundamental

frequency f_0 where its median circumference $2\pi r = \lambda_{g0}$, where r is the mean radius of the ring. The higher resonant modes occur at $f = n f_0$ for $n=2, 3, \dots$



Fig. 1.4 Circular and square closed ring resonator

Figure 1.5 shows the open loop resonators with a fundamental resonant frequency half that of the closed ring resonators. In the case of rectangular ring resonators the fundamental frequency is determined by the average perimeter.



Fig. 1.5 Circular and square $\lambda_{g0}/2$ open loop resonators

The ring resonators shown in Fig. 1.6 is another type of distributed line resonators called split ring resonators (SRR), formed by two coupled conducting open loop resonators printed on a dielectric slab.

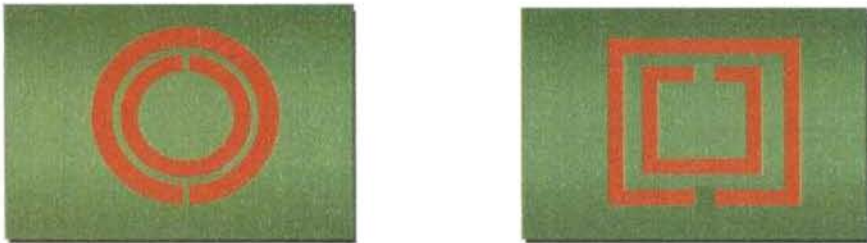


Fig. 1.6 Circular and square split ring resonator

They are considered as electronically small resonators with very high Q and very useful structure in constructing filters requiring sharp notch or pass a certain frequency band. It is possible to construct this type of line resonator into different configurations such as folded and meander loop resonators to reduce the size.

The above portrayal has inspired the investigation of planar loop resonators and their behavioral flexibility in miniaturizing filter structures for present day applications

1.4 Outline of Present Work

Study of the characteristics of planar loop resonators and their use in the construction of filters at microwave frequencies are presented in this thesis. A detailed investigation of parameters affecting the strength of coupling and the resonant frequency are also carried out. Techniques for size reduction in band stop and bandpass filters are using planar loop resonators are developed. Different configurations of compact bandstop and bandpass filters using loop resonator are simulated and experimental results on optimal filter configuration are presented.

1.5 Organisation of the Thesis

Chapter 1 Introduction

This chapter starts with a brief outline regarding relevance of microwave filters, evolution and their uses in communication technology. A brief introduction of planar filters has also been presented.

Chapter 2 Review of Literature

This chapter presents a thorough review of literature on the development in the field of microwave filters giving special attention to planar bandstop and bandpass filters. Attempts have been made to cover all the important development in

microstrip filter theory and experiment. Various types of loop resonator filters based on their specific geometries with their gradual development have been studied to arrive at the motivation of the present thesis.

Chapter 3 Methodology

In this chapter, the methodology adopted for characterizing the filter is described. It deals with the various techniques employed for the design, fabrication and measurement of filters. Simulation and parametric analysis using commercial EM simulation packages Ansoft-HFSS and IE3D are also outlined.

Chapter 4 Planar loop resonator filters

This chapter provides the details of the studies undertaken for the design and development of microstrip planar filters using novel coupling techniques on microstrip loop resonators and finding its utility in compact bandstop and bandpass filters. Parameters affecting the strength of coupling and the resonant frequency are investigated. Techniques for size reduction in bandstop and bandpass filters are developed and empirical formula for the resonant frequency for different types of resonators are deduced.

Chapter 5 SRR based microstrip bandstop filter

In this chapter the propagation characteristics of a microstrip line loaded with an array of SRR as superstrate is investigated. The response of different types of loop resonators is also portrayed.

Chapter 6 SRR based waveguide filter

This chapter presents the behavior of SRR in waveguide for the development of bandstop and bandpass filters. A detailed investigation of band rejection at the second resonance is carried out and exploited to develop a variable bandwidth bandstop filter. Also the frequency response of the waveguide below cut-off with

bandstop filter. Also the frequency response of the waveguide below cut-off with SRR insert is explored for the development of bandpass filter. This study leads to the phenomenon of waveguide miniaturization.

Chapter 7 Conclusions

This chapter serves the conclusions drawn from the study with directions for future work. It describes the important findings of the thesis and salient features of the proposed microstrip filters.

References

Atia A. E and Williams A. E. "New types of waveguide bandpass filters for satellite transponders." *Comsat Tech. Rev.*, vol. 1, pp. 21–43, 1971.

Atia A. E. Williams A. E, and Newcom R.W. "Synthesis of dual-mode filters," *IEEE Trans. Circuits Syst.*, vol. CAS-21, pp. 649–655, 1974.

Brucher A, Cenac C, Delmond M, Meunier P, Billonet L, Jarry B, Guillon P, and Sussman-Fort S. E. "Improvement of microwave planar active filters with MMIC technology," in *Proc. Eur. GAAS'94 Related III–IV Compounds Applicat. Symp.*, pp. 315–318, 1994.

Cohn S. B. "Microwave bandpass filters containing high-Q dielectric resonators," *IEEE Trans. Microwave Theory Tech.*, vol. MTT-16, pp. 218–227, 1968.

Cohn S. B. "Parallel-coupled transmission-line resonator filters," *IRE Trans. Microwave Theory Tech.*, vol. MTT-6, VD, pp. 223–231, 1958.

Cohn S. B. "Parallel-coupled transmission-line resonator filters," *IRE Trans. Microwave Theory Tech.*, vol. MTT-10, pp. 223–231, 1958.

Darlington S. "Synthesis of reactance 4-poles," *J. Math. Phys.*, vol. 18, pp. 257–353, 1939.

Fano R. M and Lawson A. W, "Microwave Transmission Circuits," ser. M.I.T. Rad. Lab. New York: McGraw-Hill, 1948, vol. 9, ch. 9, 10.

Fiedziuszko S. J. "Dual-mode dielectric resonator loaded cavity filters," *IEEE Trans. Microwave Theory Tech.*, vol. MTT-30, pp. 1311–1316, 1982.

Fiedziuszko S. J, Hunter I. C, Itoh T, Kobayashi Y, Nishikawa T, Stitzer S. N, and Wakino K, "Dielectric materials, devices, and circuits." *IEEE Trans. Microwave Theory Tech.*, vol. 50, pp. 706–720, 2002.

Glover I. A and Grant P. M, *Digital Communications*. Englewood Cliffs, NJ: Prentice-Hall, 1997, pp. 146–149.

Guglielmi M. Roquebrun O, Jarry P, Kerherve E, Capurso M, and Piloni M, "Low-cost dual-mode asymmetric filters in rectangular waveguide," in *IEEE MTT-S Int. Microwave Symp. Dig.*, Phoenix, AZ, 2001, pp. 1787–1790.

Hunter I C.. "Microwave Filters—Applications and Technology" *IEEE Trans. Microwave Theory Tech.* vol. 50, pp. 794-805, 2002.

Hunter I. C and Rhodes J. D, "Electronically tunable microwave bandpass filters." *IEEE Trans. Microwave Theory Tech.*, vol. MTT-30, pp. 1354–1360, 1982.

Lancaster M. J, Powell J, and Porch A, "Thin-film ferroelectric microwave devices." *Superconduct. Sci. Technol.*, pp. 1323–1334, 1998.

Larson J. D. Ruby R. C, Bradley P, Wen J, Kok S, and Chien A, "Power handling and temperature coefficient studies in FBAR duplexers for 1900 MHz PCS band," in *IEEE Ultrason. Symp. Dig.*, pp. 869–874, 2000.

La-Tourette P. M and Roberds J. L, "Extended-junction combline multiplexers," in *IEEE MTT-S Int. Microwave Symp. Dig.*, , IEEE cat. 78CH1355-7 MTT, pp. 214–216, 1978.

La-Tourette P. M. "Multi-octave combline-filter multiplexers," in *IEEE MTT-S Int. Microwave Symp. Dig.*, IEEE cat. 77CH1219-5 MTT, pp. 298–301, 1977.

Lin W. G. "Microwave filters employing a single cavity excited in more than one mode." *J. Appl. Phys.*, vol. 22, pp. 989–1001, 1951.

Mason W. P and Sykes R. A, "The use of coaxial and balanced transmission lines in filters and wide band transformers for high radio frequencies." *Bell Syst. Tech. J.*, vol. 16, pp. 275-302, 1937.

Masse D. J and Pucel R. A, "A temperature-stable bandpass filter using dielectric resonators." *Proc. IEEE*, vol. 60, pp. 730–731, 1972.

Matthaei G. L. "Comb-line band-pass filters of narrow or moderate bandwidth," *Microwave J.*, vol. 6, pp. 82–91, 1963.

Matthaei G. L. "Comb-line filters of narrow or moderate bandwidth," *Microwave J.*, vol. 6, pp. 82–91, 1963.

Matthaei G. L, "Interdigital band-pass filters," IRE Trans. Microwave Theory Tech., vol. MTT-10, pp. 479–491, 1962.

Matthaei G. L, "Interdigital band-pass filters: IRE Trans. Microwave Theory Tech., vol. MTT-10, pp. 479–491, Nov. 1962.

Matthaei G. L, Young L, and Jones E. M. T Microwave Filters, Impedance-Matching Networks and Coupling Structures. New York; McGraw Hill, 1964.

Nguyen C. T.-C, "Transceiver front-end architectures using high-Q micromechanical resonators." presented at the IEEE Eur. MIDAS MEMS for High-Q Filters Workshop, Surrey, U.K., 2000.

Ozaki H and Ishii J, "Synthesis of a class of stripline filters," IRE Trans. Circuit Theory, vol. CT-5, pp. 104-109. 1958.

Peroulis D, Pacheco S, Sarabandi K, and Katchi L. P. B, "Tunable lumped components with applications to reconfigurable MEMS filters." in IEEE MTT-S Int. Microwave Symp. Dig., Phoenix, AZ, 2001, pp. 341–344.

Plourde J. K and Linn D. F, "Microwave dielectric resonator filters using Ba₂Ti₉O₂₀ ceramics," in 1977 IEEE MTT-S Int. Microwave Symp. Dig., cat. no. 77CH1219-5 MTT, pp. 290–293.

Ren C. L, " Waveguide bandstop filter utilizing Ba₂Ti₉O₂₀ resonators," in IEEE MTT-S Int. Microwave Symp. Dig., IEEE cat. no. 78CH-1375-7 MTT, pp. 227–229, 1978.

Richards P. I, "Resistor-transmission-line circuits," Proc. IRE. vol. 36, pp. 217-220, 1948.

Schumacher H. L, "Coax multiplexers: Key to EW signal sorting," Microwave Syst. News, pp. 89–93, 1976.

Soares E, Raihn K. F, and Fuller J. D, "Dual 5 MHz PCS receiver front-end." in IEEE MTT-S Int. Microwave Symp. Dig., Phoenix, AZ, pp. 1981–1984, 2001.

Sussman-Fort S. E, "An NIC-based negative resistance circuit for microwave active filters." Int. J. Microwave Millimeter-Wave Computer- Aided Eng., vol. 4, pp. 130–139, 1994.

Tagami T, Ehera H, Noguchi K, and Komaski T, "Resonator type SAW filter," Oki Tech. Rev., vol. 63, p. 59, 1997.

Tsui J. B. *Microwave Receivers with Electronic Warfare Applications*. New York: Wiley, 1992.

Vendik I, Vendik O, Sherman V, Svishchev A, Pleskachev V, and Kurbanov A, "Performance limitation of a tunable resonator with a ferroelectric capacitor," in *IEEE MTT-S Int. Microwave Symp. Dig.*, Boston, MA, , pp. 1371–1374, 2000.

Weigel R., D. P. Morgan, J. M. Owens, A. Ballato, K. M. Lakin, K. Hashimoto, and C. C. W. Ruppel. "Microwave acoustic materials, devices, and applications," *IEEE Trans. Microwave Theory Tech.*, vol. 50, pp. 738–749, 2002.

Wenzel R. J, "Synthesis of combline and capacitively-coupled interdigital filters of arbitrary bandwidth," *IEEE Trans. Microwave Theory Tech.*, vol. MTT-19, pp. 678–686, 1971.

Wersing W. "Microwave ceramics for resonators and filters," *Current Opinion Solid State Phys. Mater. Sci.*, vol. 1, pp. 715–729, 1996.

Zhang D, Liang G.-C, Shih C. F, Johansson M. E and Withers R. S, "Narrow-band lumped-element microstrip filters using capacitively loaded inductors," *IEEE Trans. Microwave Theory Tech.*, vol. 42, pp. 3030–3036, 1995.

REVIEW OF LITERATURE

This chapter serves to review the important developments in conventional and advanced resonators used for the design of planar bandstop and bandpass filters. Filter structures with different types of resonators for bandstop and bandpass characteristics are reviewed with illustrations. Recent findings in filter miniaturization are also presented.

2.1 Microwave Filters

Microwave communication links are an important practical application of microwave technology and are used to carry voice, data over distances ranging from intercity links to deep-space spacecraft. They find applications in virtually any type of microwave communication, radar, or test and measurement system. In some applications such as communication satellite and mobile communication devices, it is critical that filters be devised with small size, light weight, and lower cost along with stringent electrical characteristics. Planar filter geometries are well suited for meeting these requirements.

The recent advances in novel materials and fabrication technologies, including monolithic microwave integrated circuit (MMIC), microelectromechanic system (MEMS), micromachining, high-temperature superconductor (HTS), and low-temperature co-fired ceramics (LTCC) have stimulated the development of new types of filters.

2.2 Microstrip Bandstop Filters

Spurious passband rejection in microwave filters is key aspect in certain applications that require huge stopband extending above the first and even higher order harmonics of the target frequency. Lumped circuit elements like inductors and capacitors are commonly employed as resonant circuits at lower frequencies but at microwave frequencies, planar circuits are preferred as they are of low cost, light weight and can be easily fabricated using printed circuit technology. Band rejection in microstrip transmission line is the phenomenon which occurs when a main transmission line is electrically or magnetically coupled to half wavelength resonators spaced quarter wavelength apart. The resonators used may be open circuited stub, short circuited stub,

hair-pin resonators (Hong and Lancaster, 2001), closed ring resonators, open loop resonators and split ring resonators (Garcia et al., 2004).

Bandstop filters particularly notch filters are an important noise reduction device commonly used in cable televisions, satellite location systems, mobile phones, and numerous other applications. Conventional notch filters suffer from various technical limitations, mostly related to the use of discrete inductors, including: large size, difficulty in integrating onto a single integrated circuit, high power consumption, and susceptibility to parasitic effects in the gigahertz range. A filter with an optimum frequency response curve and reduced size is very essential to a microwave system. Planar filters are popular and have low cost and light weight; particularly, such filters are easily fabricated using printed circuit technology. Since size reduction is always important, the planar filter frequently requires a change in geometry for circuit miniaturization (Gorur et al., 2001, Fig. 2.1; Matthaei et al., 1964; Nguyen and Chang, 1985; Bates, 1977).

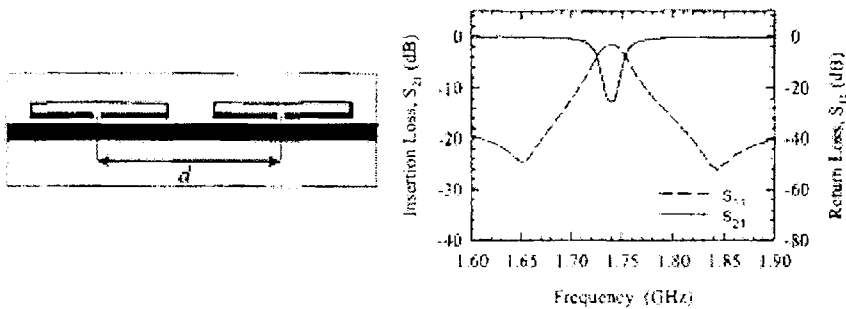


Fig. 2.1 Layout of the bandstop filter and its frequency response

Various types of microstrip notch filters are common but modifications are still being reported, employing resonators of different shapes like triangular resonators (Chen et al., 2004), spurline (Nguyen and Chang, 1985), stubs or some combinations (Tu and Chang, 2005). The level of rejection depends on the coupling between feed line

and resonator. Harikrishna et al., (2007, Fig. 2.2) employed electromagnetic coupling between the transmission line and the resonator to achieve better rejection.

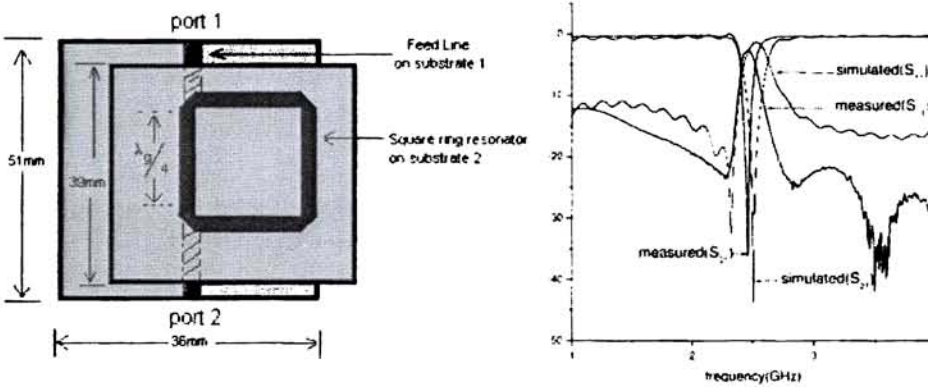


Fig. 2.2 Configuration of EM coupled square ring resonator notch filter and its frequency response.

This method has the additional advantage of flexibility of easy coupling gap adjustment and resonator/circuit replacement or modifications. Added advantage of this type of flexible EM coupling is that resonating circuits can be replaced or additional notch resonators can be added easily without affecting the underlying feed line and port connections, thus giving multifrequency operation.

Traditional techniques based on half wavelength short circuit stubs, chip capacitors or cascaded rejection band filters, are either narrow band, have increased device area or include significant insertion loss. As an alternative, it has been recently demonstrated that electromagnetic band gap (EBG) can be efficiently used to achieve harmonic suppression in microwave circuits. Among several approaches, remarkable findings are uniplanar EBG structure proposed by Itoh et al., (1999) and the Wiggly line concept recently introduced by Lopetegi et al., (2004) to achieve multi-spurious rejection in coupled line bandpass filters. The main advantage of EBG over traditional technique is the possibility to introduce the rejecting structure within the active device

region, thus avoiding the need to cascade the additional stages. However in EBGs the frequency selectivity is based on their periodicity and several stages are required to obtain significant rejection levels. Since the EBG period scales with signal wavelength, the required dimension of the structure may be too big at moderate or low frequencies, or its efficiency very poor in certain applications where miniaturization is mandatory.

Recently, split-ring resonators (SRRs) (Pendry et al., 1999) and complementary split-ring resonators (CSRRs) (Falcone et al., 2004) have been used in planar circuit technology for the design of novel printed microwave components, in particular, bandpass and bandstop filters (Safwat et al., 2007 and Bengin et al., 2007). Pendry et al., (1999) demonstrated that an array of SRRs exhibits negative permeability near its resonant frequency and successfully applied to the fabrication of left-handed metamaterial (LHM). Marques et al., (2002) reported that SRRs should be excited with time varying magnetic field with a significant component parallel to the ring axes. SRRs etched at the top metal level in the close proximity to the central strip guaranteed efficient magnetic coupling as reported by Garcia et al., (2004).

It has been shown that when loaded with SRRs, both microstrip lines (Garcia et al., 2005a; Burokur et al., 2005; Garcia et al., 2005b) and coplanar waveguides (Falcone et al 2004; Baena et al., 2005) behave as compact, high-Q, bandstop filters with deep stopbands in the vicinity of their resonant frequencies. This phenomenon is due to the presence of SRRs in close proximity to the transmission line generating an effective single-negative (SNG) medium with negative effective permeability, μ_{eff} , around their resonant frequencies, and previously propagating waves (in the absence of SRRs) become evanescent waves. As a result, the signal propagation is inhibited. Having a strongly anisotropic electromagnetic nature, the SRR is able to inhibit signal propagation in a narrow band in the vicinity of its resonant frequency, provided that it is illuminated by a time-varying magnetic field with an appreciable component in its axial

direction. If two arrays of SRRs exist closely at both sides of the host microstrip line, a significant portion of the magnetic fields induced by the line is expected to cross the SRRs with the desired polarization which constitute an effective SNG medium with negative μ_{eff} , consequently inhibiting the signal propagation. Based on this explanation, an SRR-based bandstop microstrip filter has been designed and fabricated by Oznazli and Erturk (2007 Fig. 2.3). A total of six square shaped SRRs replacing the conventional circular SRRs have been implemented to improve the coupling between the transmission line and the SRR array.

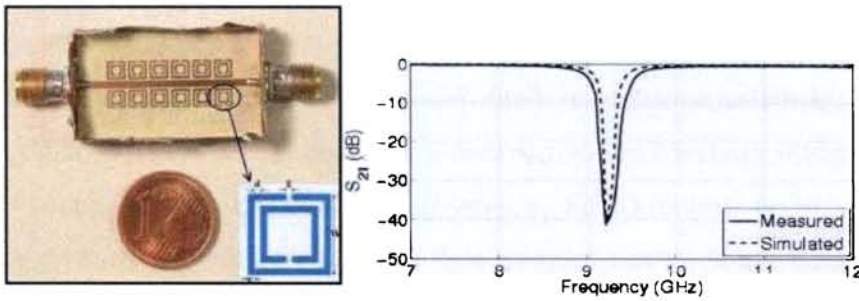


Fig. 2.3 Fabricated SRR-based microstrip bandstop filter and its frequency response.

A novel compact stopband filter consisting of a coplanar waveguide (CPW) with split ring resonators (SRRs) etched in the back side of the substrate has been presented by Martín et al., (2003). By aligning SRRs with the slots, a high inductive coupling between line and rings is achieved, resulting in a sharp and narrow rejection band in the vicinity of the resonant frequency of the rings. In order to widen the stopband of the filter, several ring pairs tuned at equally spaced frequencies within the desired gap are cascaded.

In a similar fashion, when loaded with CSRRs (which is the negative image of SRR), microstrip lines also behave as high-Q bandstop filters with deep stopbands

around their resonant frequencies (Falcone et al 2004; Ying and Alphones, 2005). Since CSRRs are dual counterparts of SRRs, etching CSRRs in the ground plane just beneath a microstrip line (simplest and most standard configuration) yields an effective SNG medium with negative ϵ_{eff} . It has been demonstrated that CSRR etched in the ground plane or in the conductor strip of planar transmission media (microstrip or CPW) provide a negative effective permittivity to the structure. Being the dual counterpart of the conventional SRR, the CSRR requires the excitation of a time-varying electric field having a strong component parallel to its axis so that it can resonate at some frequencies. A microstrip transmission line induces electric field lines that originate from the central strip and terminate perpendicularly on the ground plane. Owing to the presence of the dielectric substrate, field lines are concentrated just below the central conductor, and the electric flux density reaches its maximum value in the vicinity of this region. Hence, if an array of CSRRs is etched on the ground plane just aligned with the microstrip line, a strong electric coupling with the desired polarization is expected. As a result, a linear array of CSRRs constitutes an SNG medium with a negative ϵ_{eff} . Based on this explanation, CSRR-based bandstop microstrip filter was fabricated by Oznazli and Erturk (2007, Fig. 2.4).

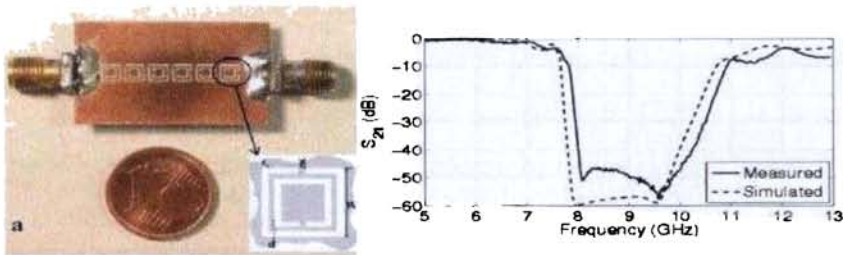


Fig. 2.4 CSRR-based microstrip bandstop filter and its frequency response.

Since SRR /CSRR dimensions are much smaller than signal wavelength, the proposed filters are extremely compact and can be used to reject frequency parasitic in CPW structures by simply patterning properly tuned SRRs in the back side metal. Easy

fabrication and compatibility with MMIC or PCB technology are additional advantages. These resonators were also been used for the design of frequency selective structure in planar circuit technology (Marques et al., 2003). The relevant characteristic of all these resonators which are inspired on the canonical topology proposed by Pendry et al., (1999) is the electrical length. This can be made very small due to the edge capacitance between concentric rings. Hence these resonators can be considered as planar lumped elements which opened the door to new design strategies where design miniaturization is of major concern. The limitations of the EBG periodic structure could be overcome by SRRs properly coupled to the host transmission media, either in the active device region or in the input/output accessing ports. CSRR has been successfully applied to the narrow band filters and diplexer with compact dimensions (Bonache et al., 2005, 2006). Since propagating waves in the absence of etched CSRRs become evanescent waves, the signal propagation is again inhibited. Finally, as in the case of SRRs, these structures can be converted to bandpass filters with small modifications (Wu et al., 2006, 2007; Gil et al., 2006; Bengin et al., 2007).

The defected ground structure was first proposed by Park et al., (1999) based on the idea of photonic band-gap (PBG) structure, and had found its application in the design of planar circuits and low-pass filters (Yablonovitch et al., 1991; Park et al., 1999; Lim et al., 2002). Defected ground structure is realized by etching a defective pattern in the ground plane, which disturbs the shield current distribution in the ground plane. This disturbance can change the characteristics of a transmission line such as equivalent capacitance and inductance to obtain the slow-wave effect resulting bandstop property. A square split-ring resonator (SRR) defected ground structure (DGS) was studied by Wu et al., (2006, Fig. 2.5). This DGS structure has a flat low-pass characteristic and a sharp bandstop property compared to the conventional dumbbell DGS. In order to enhance the out-band suppression, an improved SRR DGS cell with open stubs loaded on the conductor line was proposed.

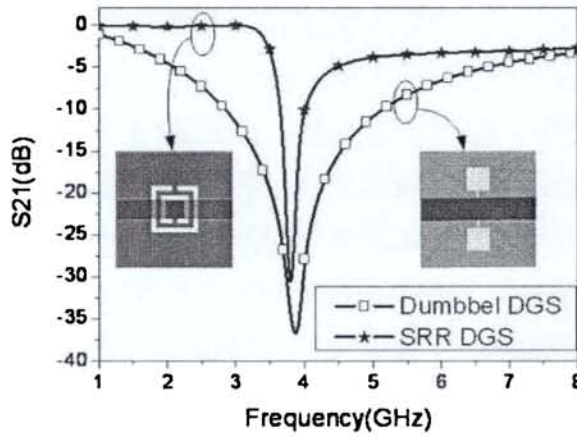


Fig. 2.5 Comparison of bandstop property between SRR DGS and dumbbell DGS.

The frequency response measured in the fabricated prototype device exhibited pronounced slopes at either side of the stopband and near 0 dB insertion loss outside that band.

2.3 Microstrip Bandpass Filters

With the advent of advanced materials and new fabrication techniques, microstrip filters have become very attractive for microwave applications because of their small size, low cost and good performance. There are various topologies to implement microstrip bandpass filters such as end-coupled, parallel coupled, hairpin, interdigital and combline filters.

The microstrip parallel-coupled half-wavelength resonator filter, proposed by Cohn (1958) has been one of the most commonly used filters. A parallel-coupled microstrip bandpass filter structure consists of open circuited coupled microstrip lines. This parallel arrangement of resonators gives relatively large coupling and therefore this configuration is suitable for implementing printed-circuit microstrip filters for

bandwidths from 5% up to 35%. Fringing effects at the ends of the resonators are taken into account and therefore there is no need of additional tuning or adjustments. Filter length can be considerably reduced by using substrate with high dielectric constant. Insertion loss of the filter can be reduced by using low loss substrates. This type of filter has many advantages such as easy design procedures, a wide bandwidth range and a planar structure. They can be easily fabricated and it exhibits reasonably good performance compared to other planar circuit filters.

Recently Chang and Itoh introduced a modified parallel-coupled filter structure to improve the upper stopband rejection and the response symmetry (Chang and Itoh, 1991). Matthaei and Hey-Shipton proposed an aligned microstrip parallel-coupled resonator array filter for design of compact narrow-band filters (Matthaei and Hey-Shipton, 1994). Superconducting filters of this type have been developed by Zhang and his colleagues for cellular communication (Zhang et.al., 1995). In order to reduce the size of half-wavelength resonator filters, Hong and Lancaster have proposed the so-called ladder microstrip line structures (Hong and Lancaster 1995a, Fig.2.6).

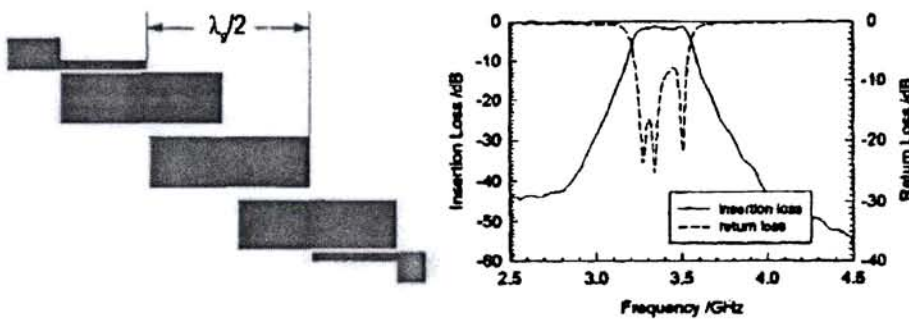


Fig.2.6 Conventional microstrip parallel coupled filter and its frequency response

There are several disadvantages of the traditional parallel coupled filters. One of the disadvantages is that the first spurious passband appears at twice the basic passband

frequency. This is due to the inequality of the even-and odd-mode velocities of the coupled microstrip line. This phenomenon greatly limits the applications of the parallel coupled filters. Also, the filter shows a steeper roll-off on the lower frequency side than on the higher frequency side. The asymmetry in the frequency response is apparent when looking on to the passband group delay. The frequency response symmetry is also important in applications involving pulsed signals.

Several designs have been reported to overcome the inherent disadvantages of the parallel coupled resonators by modifying their structure. Riddle, (1988) showed that an over-coupled resonator extends the phase length for the odd mode to compensate difference in the phase velocities. In 1991, Chang and Itoh (1991) proposed a new filter modifying the traditional parallel coupled filter which fitted in a quite narrow channel resulting in an improvement in the upper stopband rejection by at least 15 dB with symmetric frequency response. The corrugated coupled microstrips were designed for equalization of modal phase velocities in parallel coupled filter for eliminating the spurious response at twice the passband frequencies (Kuo, 2002). Kuo and co-workers (2003) applied over-coupling to the end stages and thus increasing the image impedance of the filter. Coupled microstrip stage with higher image impedance is shown to have smaller difference in the even and the odd mode relative permittivities and parallel-coupled microstrip filters with higher image impedances also showed an improved rejection at double the resonant frequency.

The spurious frequency of the conventional planar filters with half-wavelength resonators is two or three times the fundamental frequency. For efficient harmonic suppression, several unique structures have been designed. Stepped-impedance resonators (SIR) have been found advantageous in designing microstrip bandpass filters (Makimoto and Yamashita, 1980; Lee and Tsai, 2000; Zhu and Wu, 2000; Denis et al., 1988; Makimoto and S. Yamashita, 2001) with good stop band performance. One of the

key features of an SIR is that its resonant frequencies can be tuned by adjusting its structural parameters, such as the impedance ratio of the high- and low- segments. As a result, the first spurious harmonic can be much higher than $2f_0$. The design in (Zhu and Wu, 2000) completely suppresses the resonance with an inductive effect, and the first parasitic response is observed at frequencies close to $3f_0$. A combination of different SIR structures can also be adopted for a bandpass filter with wide stopband (Denis et al., 1988; Makimoto and S. Yamashita, 2001). Nonconventional SIRs can be used to construct high-performance bandpass filters with the control of spurious responses outside of a selected bandwidth over a very large frequency range. A bandpass filter based on parallel coupled structure using SIR unit cells to control the higher harmonics is demonstrated by Kuo et al., (2003, Fig. 2.7) where he applied tapped couplings to both the first and last resonators to fully control the positions of the two extra zeros.

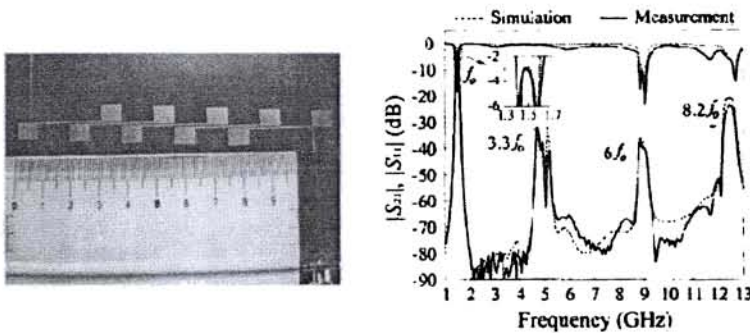


Fig. 2.7 Photograph of the SIR based bandpass filter and its frequency response.

This is a very useful feature for practical receivers in rejecting image frequencies and enhancing the rejection level in the stopband of a bandpass filter. Currently, filters with compact size which suppress spurious sidebands having wider upper stopbands are required for several wireless communication systems. However, most of the planar bandpass filters built on microstrip structures are large in size and their first spurious resonance frequencies appear at $2f_0$ and $3f_0$, which may be close to the desired frequencies. The half-wavelength resonators inherently have a spurious

passband at $2f_0$, while quarter-wavelength resonator filters have the first spurious passband at $3f_0$, but they require short-circuit connections with via holes, which are not quite compatible with planar fabrication techniques.

One of the typical folded-line resonator filters is a hairpin line filter, introduced by Cristal and Frankel (1972). Further miniaturised hairpin resonator filters were reported by Sagawa et al.,(1989) for application to receiver front-end microwave-integrated circuits. Matthaei et al.,(1996, Fig. 2.8) developed narrow-band hairpin-comb filters using hairpin resonators in such a way that their filtering properties are similar to those of comb-line filters.

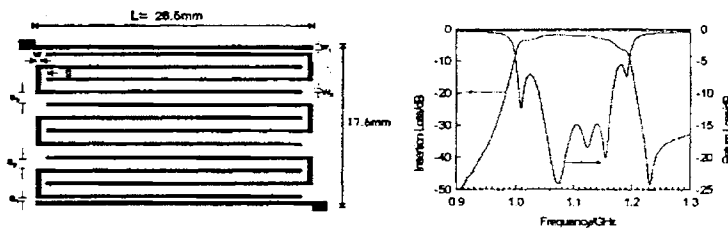


Fig. 2.8 Six-pole microstrip pseudo-interdigital bandpass filter and its frequency response.

This type of filter may be conceptualised from the conventional interdigital bandpass filter whose resonator element is quarter-wavelength long at the midband frequency and is short-circuited at one end and open-circuited at the other end.

The microstrip ring resonator is finding wide use in many bandpass filters (Chang, 1996). In the microwave communication systems, efficient bandpass filters with compact size are required. Many conventional microstrip bandpass filters having high selectivity, use hairpin resonators or ring resonators (Hong and Lancaster, 1998; Yang and Chang, 1999; Yabuki, 1996). However, the conventional end-to-line coupling structure of the ring resonator suffers from high insertion loss (Gopalakrishnan and

Chang, 1994). The coupling gaps between the feed lines and resonator also affect the resonant frequencies of the resonator. To reduce the high insertion loss, filters using an enhanced coupling structure or lumped capacitors were proposed (Hsieh and Chang, 2000; Jung et al., 1999; Zhu and Wu, 1999; Matsuo et al., 2001; Hsieh and Chang, 2002). However, the filters using this enhanced coupling structure still have coupling gaps. In addition, the filters using lumped capacitors are not easy to fabricate. Ring resonators using a high temperature superconductor (HTS) to obtain a very low insertion loss have been reported (Hong et al., 1999). This approach has the advantage of very low conductor loss, but requires a complex fabrication process.

It has been proven that square ring filter elements edge coupled to tapped input/output lines provide narrow bandwidth in the passband and good rejection in the stopband (Yu and K. Chang, 1998). However the corresponding insertion losses are rather high. Increasing the coupling between the ring resonator and the input/output lines will promote a decrease in the insertion losses. Therefore rectangular ring resonator can provide better performance when compared with square ones as per the investigation of Peixeiro (2000).

Saveedra, (2001, Fig. 2.9) proposed a bandpass filter with a ring resonator that uses quarter-wave ($\lambda/4$) edge-coupled lines as the coupling mechanism. Special attention is devoted to the physical structure of the ring to eliminate dual modes, which manifest themselves as a double-resonance in the frequency response of the ring.

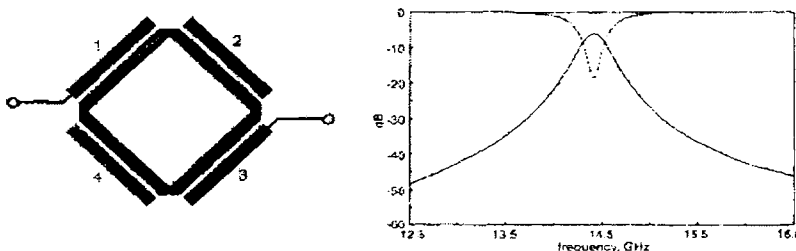


Fig. 2.9 Symmetric square ring resonator and its frequency response

When the ring is loaded with coupled lines on all sides, the structure becomes essentially symmetric and the double-resonance disappears since the impedance is uniform throughout the structure.

Filtering at 3G operating frequencies is inherently a problem. Waveguide and, more generally, 3D approaches which are widely used in 2G base stations for their performance, are not affordable any further in nano- and pico-cellular networks. These applications need more compact solutions such as planar ones that are not commonly used in 2G systems because of their relatively high losses, tuning difficulties and low power handling. In this field of application, microstrip dual-mode filtering (Curtis and Fiedziuszko, 1991; Mansour, 1994) is an interesting technique. For dual-mode operation, a perturbation is introduced in the resonator in order to couple its two degenerate modes. Depending on the position and size of the perturbation, different filter responses can be obtained. Transmission zeros at finite frequencies can also be generated and controlled by the same mechanism.

The first demonstration of dual-mode operation in a microstrip ring has been presented by Wolf who used a circular ring (Wolf, 1972). The circular ring is, unfortunately, not practical for the design of higher order filters because of the difficulty in coupling the modes of two different rings. Only second order dual-mode filters based on a circular ring have been reported in the literature. Later work on this structure mainly focused on the control of the characteristics of the response of second order filters such as the generation and control of transmission zeros at finite frequencies (Karacaoglu et al., 1994; Kundu and Awai, 2001). A partial solution to the limitations of the circular ring is given by the square ring which allows simpler and stronger coupling between two different resonators. The investigation of a new dual-mode microstrip square loop resonator for the design of compact microwave bandpass filters was presented by Hong and Lancaster, (1995b). New filters were developed from the bandstop filter to achieve a wide passband and two sharp stopbands. Hsieh et al., (2003,

Fig. 2.10) developed a new compact, low insertion-loss, sharp-rejection, and wide-band microstrip bandpass filter from a bandstop filter using a ring resonator with direct-connected orthogonal feeders.

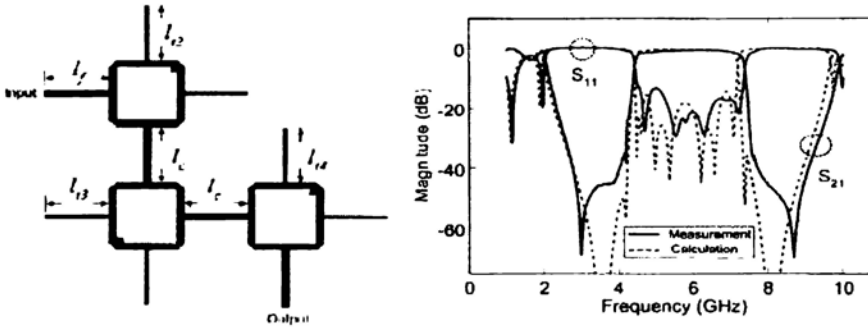


Fig. 2.10 Configuration of the cascaded dual-mode ring resonator and its transmission characteristics.

The new filters were designed for mitigating the interference in full duplex systems in satellite communications.

Microstrip bandpass filters using distributed element components are quite popular in modern communication systems. The design approach associated with coupled-resonator microstrip filters provided in (Hong and Lancaster, 1996) makes the filter simulation procedure simple and routine. Half-wavelength resonators (Cohn, 1958) and Open-loop coupled-resonators (Hong and Lancaster, 2001, Fig. 2.11) are widely used in designing filters. Since the lengths of these resonators are to be at least a half-wavelength, these filters are too large to be used in mobile communication systems where size is a significant parameter. Therefore, some novel open-loop resonators are required for filters' miniaturizations, and the electromagnetic fullwave analysis tools are used to simulate the electromagnetic properties. Hong and Lancaster(1997), introduced a new class of microstrip bandpass filters based on coupled slow-wave open-loop resonators. They showed that the use of slow-wave open loop resonators enable various

filters including those of elliptic or quasi-elliptic function response to be designed, that are not only of compact size, but also have a wide upper stopband.

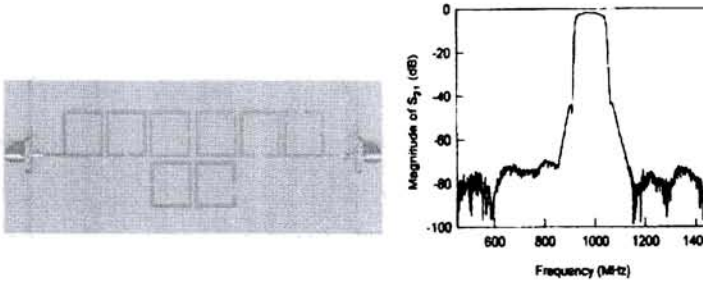


Fig. 2.11 Microstrip open-loop coupled-resonator bandpass filter and its frequency response.

Several designs have been developed in order to increase the filter selectivity. Hong and M. J. Lancaster, (2000a) reported a printed filter composed of square open-loop resonators. In this structure, the transmission zeros were obtained by classical cross-coupling interactions between nonadjacent resonators. This work is based on previous results by (Hong and Lancaster, 1996, Yu and Chang, 1998), in which elliptic transfer functions were implemented by using similar square open-loop resonators combined with cross couplings between nonadjacent resonators. Another example of a printed filter which uses side cross-coupling interactions can be found in Hong and M. J. Lancaster, (1998), where hair pin resonators were placed in a square matrix in order to achieve an elliptic-transfer function for a 2nd-order filter.

Asymmetric trisection bandpass filters with diagonal cross-coupling using open-loop resonators have also been proposed (Hong and Lancaster, 1999). Cross-coupled bandpass filters have attracted much attention because they have one or more transmission zeros in the stopband to reject possible interferences. A previous study by Prayoot and Jaruek (2006) presented a new class of microstrip slow-wave open-loop

resonator filters with reduced size and improved stopband characteristics. A comprehensive treatment of both ends loaded with either triangular or rectangular ends is described, leading to the invention of a microstrip slow-wave open-loop resonator. The filters are not only compact in size due to the slow wave effect, but also have a wider upper stopband resulting from a dispersion effect.

A low loss dual-band microstrip filters using folded open-loop ring resonators (OLRRs) is proposed by Chen and Cheng, (2006, Fig. 2.12).

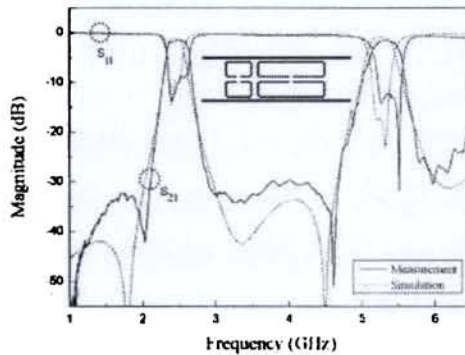


Fig. 2.12 Frequency response of folded open loop resonator dual-band filter.

The first and second passbands of the designed dual-band filter can be easily and accurately shifted to a desired frequency by adjusting the physical dimensions of OLRRs.

In order to suppress spurious response, a number of technologies have been investigated. Electromagnetic periodic structure (EPS) was first introduced to control light wave propagation in the optical frequency bands. It can provide stopband and slow-wave characteristics by etching cells in shapes such as rectangles and circles on the ground plane (Her et al., 2003; Radisic et al., 1998). For a properly designed EPS, the propagation of electromagnetic waves can be forbidden in some specific frequency bands. Most of the EPS concepts have been widely utilized in several microwave and millimeter-wave circuits, such as lowpass filters and patch antennas (Coccioli et al.,

1998; Kim et al., 2000), but few applications for bandpass filters have been developed. Her et al., (2004) proposed an EPS bandpass filter (EPS-BPF) unit cell realized by open-ended stub with EPS patterns on the ground plane. In order to improve the performance, four EPS-BPF unit cells were periodically loaded which not only improved the rolling skirt, but also increased the overall stopband rejection. Wu et al., (2006) constructed a PBG based bandpass filter with square perforations of different dimensions in the ground plane of a microstrip transmission line to achieve a double band stop PBG structure. Thus, the transmission ability of the microstrip line was blocked at different frequency ranges to create a bandpass filter.

DGS (defected ground structure) (Fu and Yuan, 2005; Alfano et al., 2005), complementary split ring resonators (CSRRs) (Burokur et al., 2005; Xu et al., 2006) are widely used in band pass filter design. The CSRR, which is the negative image of an SRR (Falcone et al., 2004), when etched in the ground plane or in the conductor strip of planar transmission media (microstrip or coplanar wave guide-CPW) provided a negative effective permittivity to the structure and signal propagation is inhibited (stopband behavior) in the vicinity of their resonant frequency. Bonache et al., (2006) focused on the application of CSSRs for the design of planar microwave filters in microstrip technology. A new design methodology to achieve the desired frequency responses based on the use of filter cells consisting of the combination of CSRRs with series gaps and shunt stubs was implemented. This is the first time that CSRRs were used for the design of practical planar filters at microwave frequencies. Using CSRR, a new technique is proposed by Mondal et al., (2006, Fig.2.13) to design a compact BPF having wide fractional bandwidth (FBW) variation. Bandpass filtering is obtained by cascading a LPF and a HPF section. The BPF has a number of advantages: compactness, sharp rejection, low insertion loss and low cost. A single section BPF provides skirt attenuation rate at least 50 dB/GHz on both sides of the passband.

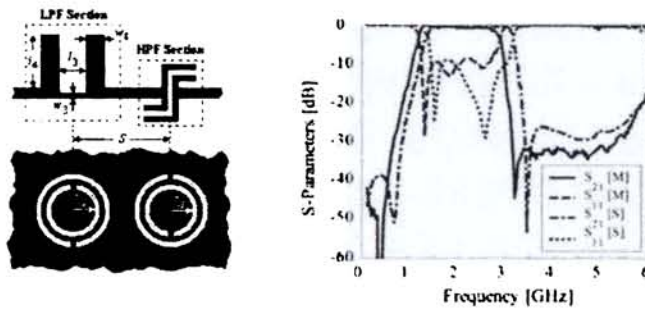


Fig. 2.13(a) Bottom and top views of CSRR BPF **(b)** Frequency response.

A new concept “Substrate Integrated Waveguide (SIW)” has already attracted much interest in the design of microwave and millimeter-wave integrated circuits. Zhang et al., (2007) introduced a bandpass SIW filter based on CSRRs for the first time. The SIW was synthesized by placing two rows of metallic via-holes in a substrate. The field distribution in an SIW is similar to that in a conventional rectangular waveguide. Hence, it takes the advantages of low cost, high Q-factor and can easily be integrated into microwave and millimeter wave integrated circuits. The filter consisted of the input and output coupling line with the CSRRs loaded SIW. Using the high-pass characteristic of SIW and bandstop characteristic of CSSRs, a bandpass SIW filter was designed and fabricated.

For lower frequency bands of mobile communications systems such as for GSM 900 MHz band, the size reduction is a major requirement, and therefore filters with more compact resonators are needed. Banciu (2002) proposed new resonator which occupies less than 51% of the surface area of the square open loop resonator designed for 900 MHz. Advances in high temperature superconducting (HTS) circuits and microwave monolithic integrated circuits (MMIC) have additionally stimulated the development of various planar filters, especially narrow-band bandpass filters which play an important role in modern communication systems (Ma et al., 2005; Zhang et al., 2005; Tsuzuki et al., 2000; Hong et al., 2000a; Liang et al., 1995). A more compact open

loop dual mode filter is developed by Athukorala et al., (2009) but with a second spurious at $3f_0$. To overcome this problem, some approaches endeavor to achieve harmonic rejection without degrading the in-band performance. The harmonics can be removed by equalizing the odd- and even-mode phase velocities of the coupled lines. The phase velocities compensation can be performed by utilizing substrate suspension (Kuo et al., 2004). Another method is to employ stepped-impedance resonators (SIRs). A combination of different SIR structures with the same fundamental resonant frequency but various high-order frequencies can be adopted for spurious-free BPFs with wide stopband (Chen et al., 2005). The spurious responses can also be suppressed by introducing transmission zeros around the harmonic frequencies (Sun and Zhu, 2005; Tu and Chang, 2006). All the above methods try to reflect the harmonic signals at the filter ports. The second harmonics of coupled-line BPFs are rejected without requiring any extra circuit and degrading in-band performance (Zhang and Xue, 2009, Fig 2.14). It is based on discriminated coupling, that is, the coupling region blocks unwanted signals of certain frequencies and allows the transmission of signals of other frequencies.

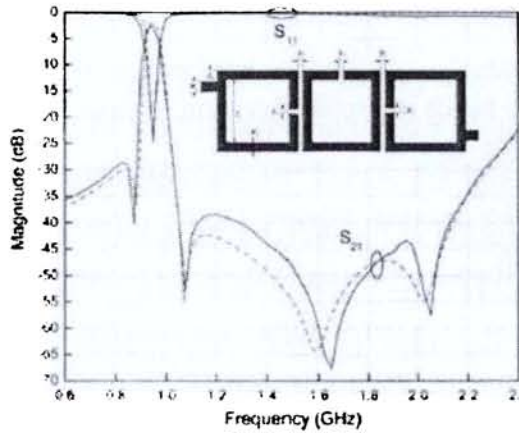


Fig. 2.14 Layout of designed filter and simulated frequency response

The HTSC (high temperature superconductor) films have very low microwave surface resistance, which is 2-3 orders lower than that of normal conductor in the L and S bands, and they are widely used in microwave devices. The use of the HTSC films will drastically improve the system performance and hence, HTSC filters are widely used in mobile communications and satellite communications for their high-selectivity, low loss, small volume, light weight and the property to easily integrate with other microwave circuits Liang et al., (2008) developed a sixth-order miniature HTSC wide-band filter with improved novel open-loop resonators on a 14.8×9.6 mm² YBCO/LaAlO₃/YBCO substrate.

2.4 Waveguide Filter Using Planar Loop Resonator Insert

Rectangular waveguides have been a sustainable solution over the past few decades to design robust, low loss and high power circuits at microwave and millimeter-wave frequencies. Metal inserts placed in the E-plane of a rectangular waveguide along the waveguide axis offer the potential of realizing low cost, mass producible and low-loss millimeter-wave filters (Arndt et al., 1988; Gololobov and Yu., 1987). The classical rectangular waveguide theory is still usable to build various filter structures, which are viable to meet requirements of the modern technology (Postoyalko and Budimir, 1994). However, reduction of the physical size of such structures has become one of the primary goals. The concept of left-handed medium (LHM) have become the subject of extensive investigations owing to their capability to provide unconventional properties to different propagation media (Veselago, 1968; Pendry et. al., 1999; Smith et.al., 2000). This approach makes use of the left-handed medium created by novel type of resonance element, split ring resonator (SRR) in combination with thin metal wire line (Smith et.al., 2000). These are printed on the dielectric slab, which is then inserted into the plane of symmetry of the rectangular waveguide.

The SRR-loaded waveguide bandstop filter is realized as a cascade of the resonator unit cells by Shelkovnikov et. al.,(2006, Fig. 2.15). The transmission line is loaded with the slab of a composite material, which conveniently facilitates both split ring resonators with the metal septa on the top plane, and a thin wire line stretched throughout the full length of the dielectric on its bottom plane.

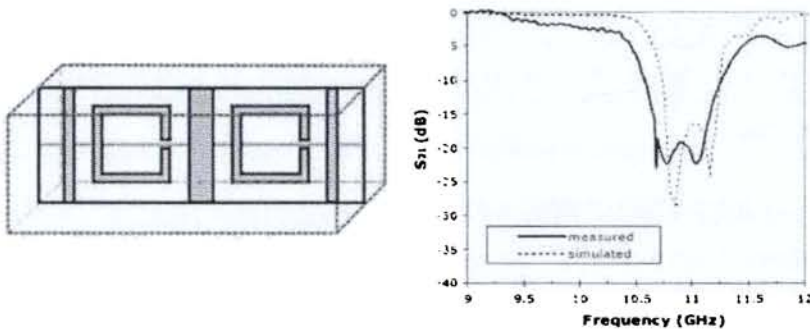


Fig. 2.15 Configuration of an SRR-loaded waveguide bandstop filter and its frequency response

The left-handed properties imposed by double ring and SRRs is made use in rectangular waveguide filters in order to achieve miniaturization (Hrabar et al., 2005, Fig 2.16). The capability of rectangular CSRR elements to design waveguide bandpass filters and its miniaturization method have been demonstrated by Bahrami and Hakkak(2008).

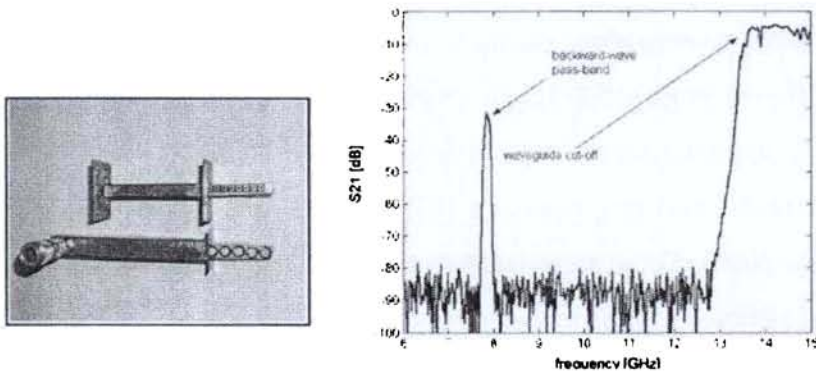


Fig 2.16 SRR based bandpass filter and its frequency response

These structures are able to alter the electromagnetic boundary conditions of the structure and inhibit propagation of signal in a certain frequency band. Thus, the traditional miniaturization techniques, which commonly employ dielectric-filled waveguides with standard dimensions bound to the wavelength (λ), may be enhanced to achieve more compact high performance waveguide components.

References

Akkaraekthalin P and Jantree J, "Microstrip Slow-Wave Open-Loop Resonator Filters with Reduced Size and Improved Stopband Characteristics." *ETRI Journal*, vol. 28, pp. 607-614, 2006.

Alfano L, D'Orazio A, Sario M. D, Petruzzelli V, and Prudenzano F, "A continuous varying impedance passband microstrip filter exploiting a butterfly wing shape." *Journal of Electromagnetic Waves and Applications*, vol. 19, pp. 1145-1156, 2005.

Arndt F, "The status of rigorous design of millimeter wave low insertion loss fin-line and metallic E-plane filters." *J. Inst. Electro. Telecom. Eng.*, vol. 34, pp. 107-119, 1988.

Athukorala L, and Budimir D, "Compact Dual-Mode Open Loop Microstrip Resonators and Filters." *IEEE Microwave and Wireless Components Letters*", vol. 19, pp. 698-700, 2009.

Baena J. D, Bonache J, Martin F, Sillero R.M, Falcone F, Lopetegi T, Laso M.A.G, Garcia-Garcia J, Gil I, Portillo M.F, and Sorolla M. "Equivalent-circuit models for split-ring resonators and complementary split-ring resonators coupled to planar transmission lines," *IEEE Trans Microwave Theory Tech.*, vol. 53, pp. 1451-1461, 2005.

Bahrami H and Hakkak M. "Analysis and design of highly compact Bandpass waveguide filter utilizing Complementary split ring resonators (CSRR)". *Progress In Electromagnetics Research, PIER 80*, pp.107-122, 2008.

Banciu M.G, Ramer R and Ioachim A. "Microstrip filters using new compact resonators." *Electron. Lett.*, vol. 38, pp. 228-229, 2002.

Bates R. N., "Design of microstrip spurline band-stop filters," *IEEE J. Microwaves, Opt. Acoust.*, vol.1, pp. 209–214, 1977.

Bengin V. C. Radonic V, and Jokanovic B.. "Left-handed microstrip lines with multiple complementary split-ring and spiral resonators." *Microwave Opt Technol Lett.*, vol. 49, pp. 1391-1395, 2007.

Bonache J, Gil I, García-García J. and Martín F, "Novel Microstrip Bandpass Filters Based on Complementary Split-Ring Resonators." *IEEE Trans Microwave Theory Tech*, vol. 54, pp. 265-271, 2006.

Bonache J, Martin F, Falcone F, Baena J.D, Lopetegi T, Garcia- Garcia J., Laso M.A.G, Gil I, Marcotegui A, Marques R, and Sorolla M. "Application of complementary split-ring resonators to the design of compact narrow band-pass structures in microstrip technology," *Microwave Opt Technol Lett.*, vol. 46, pp 508-512, 2005.

Bonache J, Martin F, Gil I, Garcia-Garcia J, Marques R, and Sorolla M, "Microstrip bandpass filters with wide bandwidth and compact dimensions," *Microwave Opt Technol Lett.*, vol. 46, pp. 343-346, 2005.

Boutejdar A, Nadim G, Omar A. S, "Compact Bandpass Filter Structure Using an Open Stub Quarter-Wavelength Microstrip Line Corrections," *European microwave week Symposium 2005*, vol. 2, ISBN: 2-9600551-2-8, 2005.

Burokur S. N , Latrach M, and Toutain S, "Study of the effect of dielectric split-ring resonators on microstrip-line transmission," *Microwave Opt Technol Lett.*, vol. 44, pp. 445-448, 2005.

Burokur S. N. Latrach M, and Toutain S, "Analysis and design of waveguides loaded with split-ring resonators," *Journal of Electromagnetic Waves and Applications*, vol. 19, pp. 1407– 1421, 2005.

Chambers D. and Rhodes J. D., "Asymmetric synthesis of microwave filters." *Proc 11th Euro Microwave Conf (EuMC)*, The Netherlands, pp. 105–110, 1981.

Chang C. Y and Itoh T, "A modified parallel coupled filter structure that improves the upper stop band rejection and response symmetry." *IEEE Trans. Microwave Theory Tech.*, vol. 39, pp. 310-314, 1991.

Chang K. "Microwave Ring Circuits and Antennas,"New York: Wiley. 1996.

Chen C. F, Huang T. Y, and Wu R. B. "A miniaturized net-type microstrip band pass filter Using $\lambda/8$ Resonators". *IEEE Microwave and Wireless Components Letters*", vol. 15, pp. 481-483, 2005.

Chen C.-F, Huang T.-Y, and Wu R.-B, "Design of microstrip bandpass filters with multiorder spurious-mode suppression." *IEEE Trans. Microw. Theory Tech.*, vol. 53, no. 12, pp. 3788–3793, Dec. 2005.

Chen C.Y and Hsu C.Y, "A Simple and Effective Method for Microstrip Dual-Band Filters Design ," *IEEE Microwave and Wireless Components Letters*, vol. 16, pp. 246-248, 2006.

Chen W. N, Weng M. H. Tang I. T, Hung C. Y, Cheng T. C, and Houng M. P, "Notch filters with novel microstrip, triangle-type resonators." *IEEE Trans Ultrasonics Ferroelectrics Frequency Control.*, vol. 51, pp. 1018 – 1021, 2004.

Chen Wu-N, Weng M-H, Tang I-T, Hung C-Y, Cheng T-C, and Houng M-P. "Notch Filters with Novel Microstrip, Triangle-Type Resonators." *IEEE Transactions on Ultrasonics, Ferroelectrics, and frequency control*, vol. 51, pp.1018-1021, 2004.

Coccioli R, Yang F.R, Ma K.P, Qian Y, and Itoh T, An aperture coupled patch antenna on UC-PBG substrate, *IEEE Trans Microwave Theory Tech.*, vol. 47, pp. 2123–2130, 1999.

Cohn S. B. "Parallel-coupled transmission-line-resonator filters," *IEEE Trans. Microw. Theory Tech.*, vol. 6, pp. 223–231, 1958.

Cristal E. G. and Frankel S.. "Hairpin-line and hybrid hairpin-line half-wave parallel-coupled-line filters". *IEEE Trans. MIT-20*, pp.719- 728, vol., 1972.

Curtis J. A and Fiedziuszko S. J, "Miniature dual mode microstrip filters." in *IEEE International Microwave Symposium*, vol. 2, pp. 443–446, 1991.

Denis S. Person C. Toutain S. Vigneron S, and Theron B, "Improvement of global performances of band-pass filters using nonconventional stepped impedance resonators." in *28th Eur. Microwave Conf. Dig.*, 1998, pp. 323–328.

Falcone F, Lopetegui T. Baena J.D. Marques R, Martin F, and Sorolla M. "Effective negative- ϵ stopband microstrip lines based on complementary split-ring resonators," *IEEE Microwave Wireless Compon Lett.*, vol. 14, pp. 280-282, 2004.

Falcone F, Martin F, Bonache J, Marques R, and M. Sorolla. "Coplanar waveguide structures loaded with split-ring resonators," *Microwave Opt Technol Lett.*, vol 40, pp. 3-6, 2004.

Fu Y. Q. and Yuan N. C. "Reflection phase and frequency bandgap characteristics of EBG structures with anisotropic periodicity," *Journal of Electromagnetic Waves and Applications*, vol. 19, pp. 1897–1905, 2005.

Garcia-Garcia J, Bonache J, Gil I, Martin F, Marques R, Falcone F, Lopetegi T, Laso M.A.G, and Sorolla M. "Comparison of electromagnetic band gap and split-ring resonator microstrip lines as stop band structures," *Microwave Opt Technol Lett.*, vol. 44, pp. 376-379, 2005.

Garcia-Garcia J, Martin F, Falcone F, Bonache J, Baena J.D, Gil I, Amat E, Lopetegi T, Laso M.A.G, Iturmendi J.A.M, Sorolla M, and Marques R, "Microwave filters with improved stopband based on sub-wavelength resonators," *IEEE Trans Microwave Theory Tech.*, vol. 53, pp. 1997-2006, 2005.

Gil I, Bonache J, Gil M, Garcia-Garcia J, and Martin F, "Left-handed and right-handed transmission properties of microstrip lines loaded with complementary split rings resonators," *Microwave Opt Technol Lett.*, vol. 48, pp. 2508-2511, 2006.

Gololobov V. P and Omel'yanenko M. Yu, "Bandpass filters based on planar metal-dielectric structures in the E-plane of a rectangular waveguide - A Review," *Radio-Electron.* vol. 30, pp. 1–15, 1987.

Gopalakrishnan G. K and Chang K. "Novel excitation schemes for the microstrip ring resonator with lower insertion loss," *Electron. Lett.*, vol. 30, pp. 148–149, 1994.

Gorur A, Karpuz C, Yalcin K, and Gorur H, "Bandstop filter with a wider upper passband using microstrip open-loop resonator," in *IEEE Microwave Conf., APMC-2001*, vol. 2 pp. 527– 530, 2001.

Harikrishna J. V. S, Karekar R. N, and Aiyer R. C, "Improved high rejection for notch filter using square ring resonator with flexible electromagnetic coupling," *Microwave Opt Technol Lett.*, vol. 49, pp. 1201-1203, 2007.

Her M. L., Chang C. M., Wang Y. Z., Kung F. S. and Chiou Y.C, "Improved coplanar waveguide (CPW) bandstop filter with photonic bandgap (PBG) structure," *Microwave Opt Technol Lett.*, vol. 38, pp. 274–277, 2003.

Her M. L., Chiou Y. C., Wang Y. Z., and Lin K. Y., "Electromagnetic Periodic Structure Bandpass Filter (Eps-Bpf) With Two Transmission Zeros," *Microwave Opt Technol Lett.*, vol. 42, pp. 265–267, 2004.

Hong J. S and Lancaster M. J., "Couplings of microstrip square openloop resonators for cross-coupled planar microwave filters," *IEEE Trans.Microw. Theory Tech.*, vol. 44, pp. 2099–2109, 1996.

Hong J. S and Lancaster M. J. "Microstrip Slow-Wave Open-Loop Resonator Filters," *IEEE M'IT-S Digest*, pp. 713–716, 1997.

Hong J. S and Lancaster M. J., "Bandpass characteristics of new dual-mode microstrip square loop resonators," *Electron. Lett.*, vol. 31, pp. 891–892, 1995b.

Hong J. S and Lancaster M. J., "Couplings of microstrip square openloop resonators for cross-coupled planar microwave filters," *IEEE Trans Microwave Theory Tech.*, vol. 44, pp. 2099–2109, 1996.

Hong J. S and Lancaster M. J. "Cross-coupled microstrip hairpin-resonator filters," *IEEE Trans. Microwave Theory Tech.*, vol. 46, pp. 118–122, 1998.

Hong J. S and Lancaster M. J., "Cross-coupled microstrip hairpin-resonator filters," *IEEE Trans Microwave Theory Tech.*, vol 46, pp 118–122, 1998.

Hong J. S and Lancaster M. J. "Design of highly selective microstrip bandpass filters with a single pair of attenuation poles at finite frequencies," *IEEE Trans. Microwave Theory Tech.*, vol. 48, pp. 1098–1106, 2000a.

Hong J. S and Lancaster M. J., "Design of highly selective microstrip bandpass filters with a single pair of attenuation poles at finite frequencies." *IEEE Trans Microwave Theory Tech.*, vol. 48, pp. 1098–1107, 2000.

Hong J. S and Lancaster M. J., "Microstrip cross-coupled trisection bandpass filters with asymmetric frequency characteristics." *Proc. Inst. Elect. Eng.*, vol. 146, pp. 84–90, 1999.

Hong J. S and Lancaster M. J, "Realisation of quasielliptic function filter using dual-mode microstrip square loop resonators." *Electron. Lett.*, vol. 31, pp. 2085–2086, 1995d.

Hong J. S, Lancaster M, Jedamzik D, and Greed R. B, "On the development of superconducting microstrip filters for mobile communications applications." *IEEE Trans. Microwave Theory Tech.*, vol. 47, pp. 1656–1663, 1999.

Hong J. S, Lancaster M. J, Jedamzik D, Greed R.B, and Mage J.C, "On the Performance of HTS Microstrip Quasi-elliptic Function Filters for Mobile Communications Application." *IEEE Trans. Microwave Theory Tech.*, vol. 48, pp. 1240-1246, 2000.

Hong J. S. and Lancaster M. J, "A novel microwave periodic structure- the ladder microstrip line", *Microwave and Optical Technology Letters*, vol.9, pp.207-210, 1995a.

Hrabar S, Bartolic J, and Sipus Z, "Waveguide Miniaturization Using Uniaxial Negative Permeability Metamaterial," *IEEE Trans on Antennas and Propag.*, vol. 53, no. 1, pp. 110-119, 2005.

Hsieh L. H, and Chang K, "Compact dual-mode elliptic-function bandpass filter using a single ring resonator with one coupling gap," *Electron. Lett.*, vol. 36, pp. 1626–1627, 2000.

Hsieh L. H and Chang K, "Dual-mode quasi-elliptic-function bandpass filters using ring resonators with enhanced-coupling tuning stubs," *IEEE Trans. Microwave Theory Tech.*, vol. 50, pp. 1340–1345, 2002.

Hsieh L. H and Chang K, " Compact, Low Insertion-Loss, Sharp-Rejection, and Wide-Band Microstrip Bandpass Filters," *IEEE transactions on microwave theory and techniques*, vol. 51, pp. 1241-1246, 2003.

Jung W. C, Park H. J, and Lee J. C, "Microstrip ring bandpass filters with new interdigital side-coupling structure," in *Asia-Pacific Microwave Conf.*, vol. 3, pp. 678–681, 1999.

Karacaoglu U, Robertson I. D and Guglielmi M, "An improved dual-mode microstrip ring resonator filter with simple geometry", in *Proc. European Microwave Conf.*, vol.1 pp. 472-477, 1994.

- Kim C. S, Park J.S, Ahn D, and Lim J.B, "A novel 1D periodic defected ground structure for planar circuits," *IEEE Microwave Guided Wave Lett.*, vol. 10, pp. 131–133, 2000.
- Kundu A. C and Awai I, "Control of the attenuation pole frequency of a dual-mode microstrip ring resonator bandpass filter". *IEEE Trans. Microwave Theory Tech.*, vol. 49, pp. 1113-1117, 2001.
- Kuo J. T, and Shih E, "Microstrip Stepped Impedance Resonator Bandpass Filter With an Extended Optimal Rejection Bandwidth," *IEEE Trans. Microwave Theory Tech.*, vol. 51, pp. 1554–1559, 2003.
- Kuo J. T, Chen S. P. and Jiang M, "Parallel-coupled microstrip filters with over-coupled end stages for suppression of spurious responses," *IEEE Microw. Wireless Compon. Lett.*, vol. 13, pp. 440–442, 2003.
- Kuo J. T, Hsu W. H, and Huang W.T, "Parallel-coupled microstrip filters suppression of harmonic responses," *IEEE Microw. Wireless Compon. Lett.*, vol. 12, pp. 383–385, 2002.
- Kuo J.-T, Hsu W. H, and Huang W. T, "Parallel coupled microstrip filters with suppression of harmonic response," *IEEE Microw. Wireless Compon. Lett.*, vol. 12, no. 10, pp. 383–385, Oct. 2002.
- Kuo J.-T, Jiang M, and Chang H.-J, "Design of parallel-coupled microstrip filters with suppression of spurious resonances using substrate suspension." *IEEE Trans. Microw. Theory Tech.*, vol. 52, pp. 83–89, Jan. 2004.
- Lee S.-Y and Tsai C.-M, "New cross-coupled filter design using improved hairpin resonator." *IEEE Trans. Microwave Theory Tech.*, vol. 48, pp. 2482–2490, 2000.
- Liang G. C, Zhang D, Shih C.F, Johansson M.E, Withers R.S, Oates D.E, Anderson A.C. Polakos P, Mankiewich P, Obaldia E.D, and Miller R.E, "High-Power HTS m\Microstrip Filters for Wireless Communication." *IEEE Trans. Microwave Theory Tech.*, vol. 43, pp. 3020-3029, 1995.
- Liang Z. T, Kai Y, JunSong N, ShiRong B, JuanXiu L and Xiang L. Z, "Development of miniature HTSC wide-band filter with open-loop resonators," *Chinese Science Bulletin*, vol. 53, pp. 1300-1303, 2008.

Lim J. S. Kim C. S, Lee Y. T, Ahn D. and Nam. S. "Design of lowpass filters using defected ground structure and compensated microstrip line". *Electronics Letters*, vol. 38, pp. 1357–1358, 2002.

Lopetegi T., Laso M. A. G, Falcone F, Martin F, Bonache J, Garcia J, Cuevas L P, Sorolla M, Guglielmi M, "Microstrips Wiggli line bandpass filters with multi-spurious rejections," *IEEE Microwave Wireless Comp. Lett.*, vol. 14, pp.531-533, 2004.

Ma Z. Kawaguchi T, and Kobayashi Y, "Miniaturized High- Temperature Superconductor Bandpass Filters Using Microstrip S-Type Spiral Resonators," *IEICE Trans. Electron.*, vol. E88-C, pp. 57-61, 2005.

Makimoto M and Yamashita S, "Bandpass filters using parallel-coupled stripline stepped impedance resonators," *IEEE Trans. Microwave Theory Tech.*, vol. MTT- 28, pp. 1413–1417, 1980.

Makimoto M and Yamashita S, *Microwave Resonators and Filters for Wireless Communication—Theory and Design*. Berlin, Germany: Springer, 2001, pp. 79–83.

Mansour R. R, "Design of superconductive multiplexers using single-mode and dual-mode filters," *IEEE Trans. Microwave Theory Tech.*, vol. 42, pp. 1411–1418, 1994.

Marques R, Medina F and Rafii-El-Idrissi R, "Role of Bianisotropy in negative permeability and left handed metamaterials," *Physics Rev. B*, vol. 65, pp. 144441-144446, 2002.

Marques R., Baena J. D, Martel J, Medina F, Falcon F, Sorolla M. Martin S. "Novel small resonant electromagnetic particles for metamaterial and filter design." *Proc. ICEAA, '03* Torino, Italy, pp. 439-422, 2003.

Martin F, Falcone F, Bonache J, Lopetegi T, Marquez R and Sorolla M, "Miniaturized CPW stop band filters based on multiple tuned split ring resonators," *IEEE Microwave Wireless Comp. Lett.*, vol. 13, pp. 511-513, 2003.

Matsuo M, Yabuki H. and Makimoto M, "Dual-mode stepped impedance ring resonator for bandpass filter applications," *IEEE Trans. Microwave Theory Tech.*, vol. 49, pp. 1235–1240, 2001.

Matthaei G. L. and Shipton H.G.L., "Concerning the use of high-temperature superconductivity in planar microwave filters", IEEE Trans., MTT-42, pp. 1287-1294, 1994.

Matthaei G. L., Oung L. and Jones E. M. T., "Microwave Filters, Impedance Matching Networks and Coupling Structures," New York: McGraw-Hill, 1964.

Matthaei G.L., Frenzi N. O., Forse R. and Rohlifing S., "Narrow-band hairpin-comb filters for HTS and other applications", 1996 IEEE MTT-S Digest, pp. 457-460.

Mondal P, Mandal M. K, Chaktabarty A, and Sanyal S, "Compact Bandpass Filters With Wide Controllable Fractional Bandwidth," IEEE Microw. Wireless Compon. Lett., vol. 16, pp. 540-542, 2006.

Nguyen C and Chang K, "Analysis and design of spurline bandstop filters," IEEE MTT-S Digest, pp. 445-448, 1985.

Oznazlı V and Erturk V. B, "A comparative investigation of SRR- and CSRR-based bandreject Filters: simulations, Experiments, and discussions," Microwave and Optical Technology Letters. vol. 50, pp. 519-523, 2008.

Park J. I, Kim C. S, Kim J, Park J-S, Qian Y, Ahn D, Itoh, "Modeling of a photonic bandgap and its application for the low-pass filter design," Singapore: Asia Pacific Microwave Conference, 1999, pp. 331-334, 1999.

Park J. S, Yun J. S, Ahn D, "A Design of the Novel Coupled-Line Bandpass Filter Using Defected Ground Structure With Wide Stopband Performance," IEEE Transactions on Microwave Theory and Techniques, vol. 50, pp. 2037 - 2043, 2002.

Peixeiro C, "Microstrip rectangular ring bandpass filter elements for GSM," APMC2000, pp. 1273-1276, 2000.

Pendry J. B, Holden A. J, Robbins D. J. and Stewart W. J, "Magnetism from conductors and enhanced nonlinear phenomena," IEEE Trans. Microwave Theory & Tech., vol. 47, pp. 2075-2084, 1999.

Pendry J.B, Holden A.J, Robbins D.J. and Stewart W.J, "Magnetism from conductors and enhanced nonlinear phenomena," IEEE Trans. Microwave Theory & Tech., vol. 47, pp. 2075-2084, November 1999.

Postoyalko V and Budimir D, "Design of waveguide E-plane filters with all-metal inserts by equal-ripple optimization," *IEEE Trans. Microwave Theory Tech.*, vol. 42, pp. 217–222, 1994.

Postoyalko V, and Budimir D, "Design of Waveguide E-plane Filters with All-Metal Inserts by Equal-Ripple Optimization," *IEEE Trans. Microwave Theory & Tech.*, vol. MTT-42, pp. 217-222, 1994.

Radisic V, Qian Y, Coccioli R, and Itoh T, Novel 2D photonic bandgap structure for microstrip lines, *IEEE Microwave Guided Wave Lett.*, vol. 8 pp. 69–71 1998.

Riddle A. "High performance parallel coupled microstrip filters," *IEE, MTTS Int. Microwave sym. Dig.*, pp. 427-430, 1998.

Saavedra C. E, "Microstrip ring resonator using quarterwave couplers" *Electron. Lett.*, vol. 37, pp. 694-695, 2001.

Safwat A. M. E, Tretyakov S and Raisanen A, "Dual bandstop resonator using combined split ring resonator and defected ground structure," *Microwave Opt Technol Lett.*, vol 49, pp. 1249-1253, 2007.

Sagawa M. Takahashi K., and Makimoto M., "Miniaturized hairpin resonator filters and their application to receiver frontend MIC's", *IEEE Trans. MTT-37*, vol 37, pp.1991-1997, 1989.

Shelkovnikov A, Suntheralingam N, and Budimir D, "Novel SRR Loaded Waveguide Bandstop Filters," *IEEE AP-S/URSI Int. Symp.*, Albuquerque, USA, pp. 4523-4526 , 2006.

Smith D. R, Padilla W. J, Vier D. C. Nasser N.S.C, and Schultz S, "Composite medium with simultaneously negative permeability and permittivity." *Phys. Rev. Lett.*, vol. 84, pp. 4184-4187, 2000.

Smith D. R, Padilla W. J, Vier D. C, Nemat-Nasser S. C. and Schultz S, "Composite medium with simultaneously negative permeability and permittivity." *Phys. Rev. Lett.*, vol. 84, pp. 4184-4187, May 2000.

Sun S and Zhu L, "Periodically nonuniform coupled microstrip-line filters with harmonic suppression using transmission zero reallocation." *IEEE Trans. Microw. Theory Tech.*, vol. 53, pp. 1817–1822, May 2005.

Tsuzuki G, Suzuki M, and Sakakibara N, "Superconducting Filter for IMT-2000 Band," *IEEE Trans. Microwave Theory Tech.*, vol. 48, pp. 2519-2525, 2000.

Tu W. H and Chang K, "Compact microstrip bandstop filter using open stub and spurline," *IEEE Microwave Wireless Components Lett.*, vol. 15, pp. 268-270, 2005.

Tu W.-H and Chang K. "Compact second harmonic-suppressed bandstop and bandpass filters using open stubs," *IEEE Trans. Microw. Theory Tech.*, vol. 54, no. 6, pp. 2497-2502, Jun. 2006.

Veselago V. G. "The electrodynamics of substances with simultaneously negative values of ϵ and μ ," *Soviet Phys. Uspekhi*, vol. 10, pp. 509-514, 1968.

Veselago V.G. "The electrodynamics of substances with simultaneously negative values of ϵ and μ ," *Soviet Phys. Uspekhi*, vol. 10, pp. 509-514, 1968.

Wolf I. "Microstrip bandpass filter using degenerate modes of a microstrip ring resonator", *Electron. Lett.*, vol. 8, pp. 302-303, 1972.

Wu H. W, Su Y. K, Weng M. H, and Hung C. Y, "A compact narrow-band microstrip bandpass filter with a complementary split ring resonator," *Microwave Opt Technol Lett.*, vol. 48, pp. 2103-2106, 2006.

Wu H.W, Weng M.H, Su Y.K, Yang R.Y, and Hung C.Y, "Propagation characteristics of complementary split-ring resonator for wide bandgap enhancement in microstrip bandpass filter," *Microwave Opt Technol Lett.*, vol 49, pp. 292-295, 2007.

Wu J. H , Shih I, Qiu S. N and Qiu C. X, "Characterization of microwave photonic band-gap structures with bandpass filter applications," *J. Vac. Sci. Technol.. A*, vol. 24, pp. 827-830, 2006.

Xu W, Li L. W, Yao H. Y, Yeo T. S. and Wu Q, "Extraction of constitutive relation tensor parameters of SRR structures using transmission line theory," *Journal of Electromagnetic Waves and Applications*, vol. 20, pp. 13-25, 2006.

Yablonovitch E, Gmitter T. J, and Leung K. M. "Photonic band structure: The face centered cubic case employing nonspherical atoms." *Physical Review Letters*, vol. 67, pp. 2295-2298, 1991.

Yabuki H, Sagawa M, Matsuo M, and Makimoto M, "Stripline dualmode ring resonators and their application to microwave devices." IEEE Trans. Microwave Theory Tech., vol. 44, pp. 723–728, 1996.

Yang C. C and Chang C. Y, "Microstrip cascade trisection filter." IEEE Microw. Guided Wave Lett., vol. 9, pp. 271–273, 1999.

Yang F. R., Ma K. P, Qian Y, and Itoh T, "A uniplanar compact photonic-bandgap (UC-PBG) structure and its applications for microwave circuits," IEEE Trans. Microwave theory tech., vol. 47, pp. 1509-1514, 1999.

Ying X and Alphones A. "Propagation characteristics of complimentary split ring resonator (CSRR) based EBG structure," Microwave Opt Technol Lett., vol. 47, pp. 409-412, 2005.

Yu C. C and Chang K, "Novel compact elliptic-function narrow-band bandpass filters using microstrip open-loop resonators with coupled and crossing lines," IEEE Trans Microwave Theory Tech., vol. 46, pp. 952–958, 1998.

Yu C.C and Chang K, "Novel compact elliptic-function narrowband bandpass filters using microstrip open-loop resonators with coupled and crossing lines." IEEE Trans. Microwave Theory Tech., vol. 46, pp. 952–958, 1998.

Zhang D, Liang G. C, Shih C.F, Withers R.S, Johansson M.E and Cruz A.D, "Compact forward-coupled superconducting microstrip filters for cellular communication". IEEE Trans., AS4 (2), vol. 5, pp. 2656-2659, 1995.

Zhang G, Huang F, and Lancaster M.J. "Superconducting Spiral Filters with Quasi-elliptic Characteristic for Radio Astronomy." IEEE Trans. Microwave Theory Tech., vol. 53, pp. 947-951, 2005.

Zhang X Y and Xue Q. "Harmonic-Suppressed Bandpass Filter Based on Discriminating Coupling." IEEE Microwave Wireless Components Lett., vol. 19, pp. 695-697, 2009.

Zhang X. C. Yu Z. Y, and Xu J. "Novel band-pass substrate integrated Waveguide (SIW) filter based on Complementary split ring resonators". Progress In Electromagnetics Research, PIER, vol. 72, pp. 39–46, 2007.

Zhu L and Wu K. "A joint field/circuit model of line-to-ring coupling structures and its application to the design of microstrip dual-mode filters and ring resonator circuits," *IEEE Trans. Microwave Theory Tech*, vol. 47, pp. 1938–1948, 1999.

Zhu L and Wu K. "Accurate circuit model of interdigital capacitor and its application to design of new quasi-lumped miniaturized filters with suppression of harmonic resonance," *IEEE Trans. Microwave Theory Tech.*, vol. 48, pp. 347–356, 2000.

METHODOLOGY

The experimental and simulation methodology utilized for the analysis of the proposed filters are described in this chapter. Photolithographic process is used to fabricate different filter geometries, while the filter characterization is done with the help of Vector Network Analyzer. The FEM based Ansoft HFSS is used to perform the parametric analysis of the filter geometry.

3.1 Techniques for Design and Optimization of Filters

A short description of the softwares used for the simulation and optimization of the filter structures is presented. The fabrication methods and the measurement techniques utilized are also described. The simulation of different filter structures presented in this thesis is performed using the commercial software Ansoft High Frequency Structure Simulator (HFSS) and IE3D.

3.1.1 Ansoft HFSS

Ansoft HFSS is one of the globally accepted electromagnetic solver which utilizes a 3D full-wave Finite Element Method (FEM) to compute the electrical behavior of high-frequency and high-speed components. With HFSS, engineers can extract parasitic parameters (S, Y and Z), visualize 3D electromagnetic fields (near- and far-field), and generate Full-Wave SPICE™ models to effectively evaluate signal quality, including transmission path losses, reflection losses due to impedance mismatches, parasitic coupling, and radiation. It is one of the most popular and powerful applications used for microwave structure design. The optimization tool available with HFSS is very useful for antenna engineers to optimize the antenna parameters very accurately. There are many kinds of boundary schemes available in HFSS. Radiation and PEC boundaries are widely used in this work. The vector as well as scalar representation of E, H and J values of the device simulation gives a good insight in to the problem under simulation.

The first step in simulating a structure in HFSS requires the definition of the geometry of the structure by giving the material properties and boundaries for 3D or 2D elements available in HFSS window. The next step is to draw the intended architecture using the drawing tools available in the software (Fig. 3.1). The designed structure is excited using the suitable port excitation schemes. The next step involves the assigning of the boundary scheme. A radiation boundary filled with air is commonly used for

Chapter 3

radiating structures. The size of air column is taken to be equal to a quarter of the free space wavelength of the lowest frequency of operation.

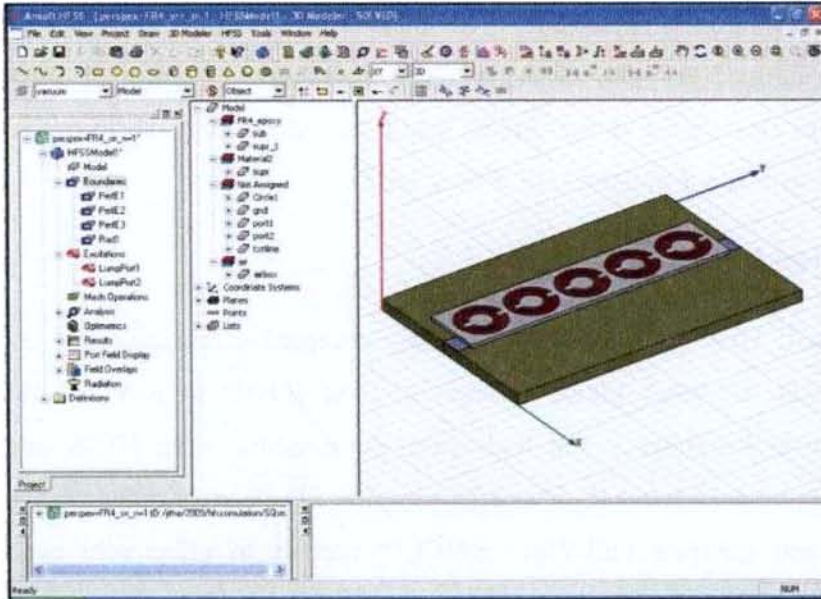


Fig. 3.1 Modelled structure in the HFSS window

Now the simulation engine can be invoked by giving the proper frequency of operation and the number of frequency points. Finally the simulation results such as scattering parameters(Fig. 3.2), port surface characteristic impedance, 3D static and animated field(electric or magnetic) plots(Fig. 3.3) on any surface, radiation pattern, current distributions and vector and magnitude are displayed and visualised in various forms like 2D/3D Cartesian/Polar plots, Smith charts and Data tables. The vector as well as the scalar representation of E, H and J values of the device under simulation gives good insight into the structure under analysis [1].

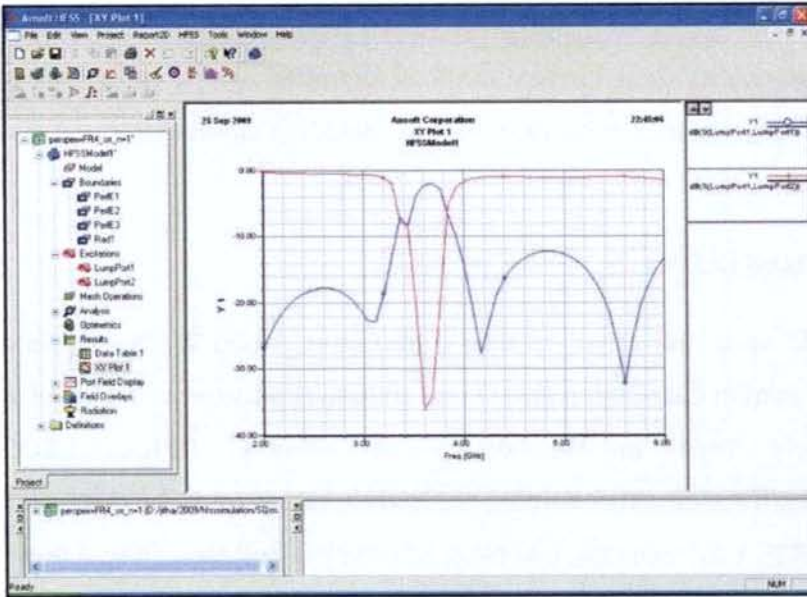


Fig. 3.2 Simulation results showing the Scattering parameters

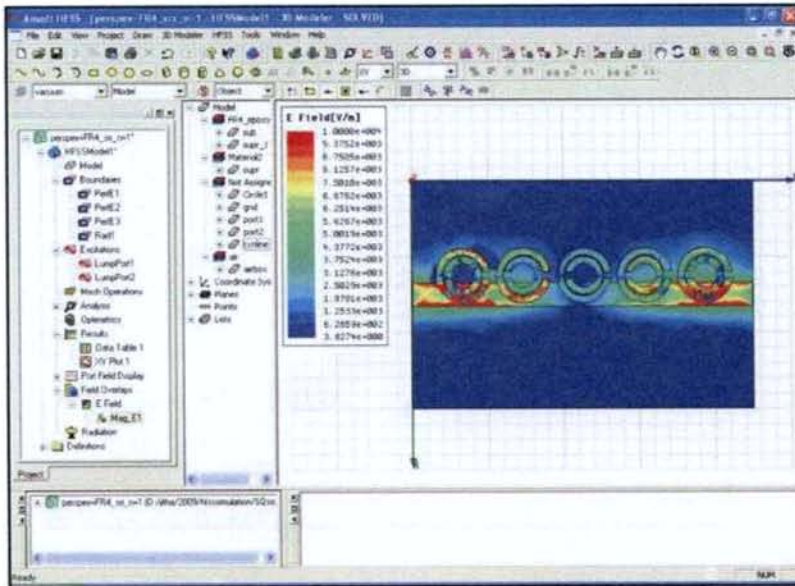


Fig. 3.3 Field distribution plot of the simulated structure

Advanced version, HFSS v11, features new higher-order, hierarchical basis functions combined with an iterative solver that provides accurate fields, smaller

meshes, and more efficient solutions for large, multi-wavelength structures. A new fault tolerant, high-quality finite element meshing algorithm further enhances HFSS's ability to simulate very complex geometric models, including models imported from 3D CAD environments.

3.1.2 Zealand IE3D

IE3D is a full-wave, method-of-moments based electromagnetic simulator solving the current distribution on 3D and multilayer structures of general shape. It has been widely used in the design of MMICs, RFICs, LTCC circuits, microwave/millimeter-wave circuits, IC interconnects and packages, HTS circuits, patch antennas, wire antennas, and other RF/wireless antennas. The designed structure is drawn and the material characteristics for each object are defined, and identified the ports and special surface characteristics (Fig.3.4).

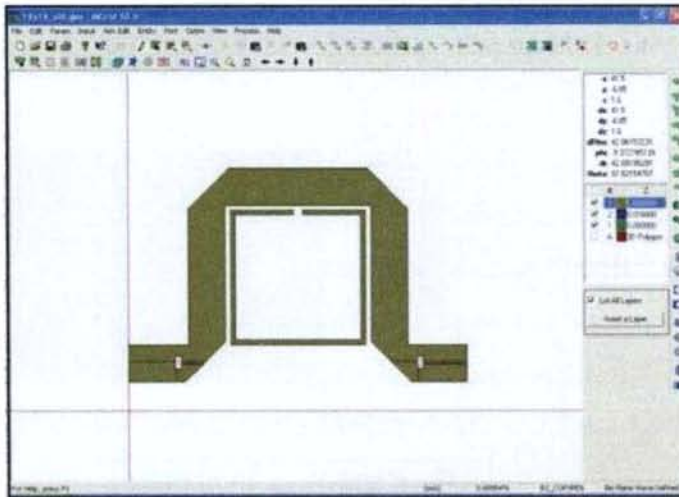


Fig. 3.4 Modelled structure in IE3D window

The system then generates the necessary field solutions and associated port characteristics and S-parameters.

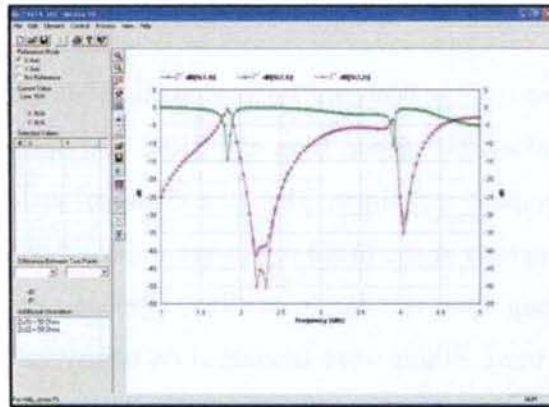
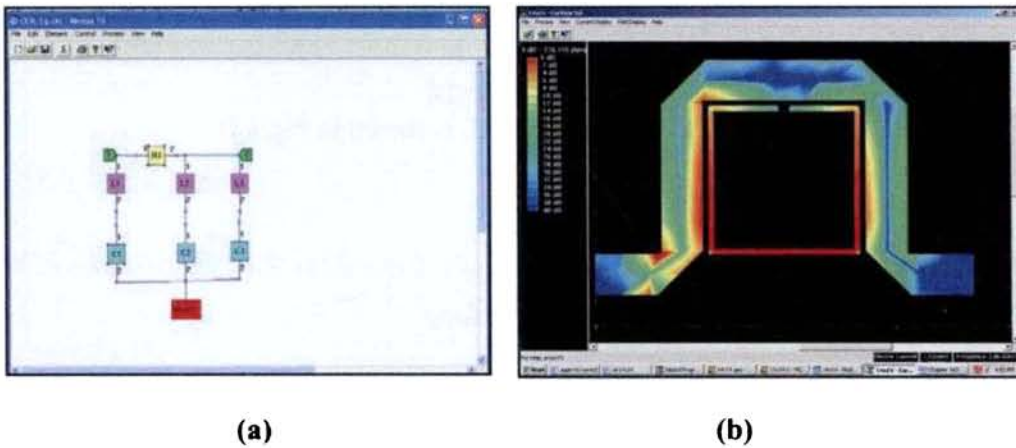


Fig. 3.5 S-parameter plots of the simulated structure

IE3D comes with the MODUA post-processor for display of S (Fig.3.5), Y, and Z-parameters in data list, rectangular graphs and Smith Chart. MODUA is also a circuit simulator (Fig 3.6a). A user can graphically connect different S-parameter modules and lumped elements together and perform a nodal simulation.



(a)

(b)

Fig. 3.6 (a) Circuit simulator MODUA (b) Field distribution of the simulated structure

Current distribution (Fig. 3.6b), both 2D and 3D radiation pattern and field distribution images are also provided [2].

3.2 Filter Fabrication

Different resonators designed for constructing bandpass and bandstop filters are based on OLR, folded U- shaped loop and SRR. The optimized filters are fabricated using photolithographic technique. This is a chemical etching process by which the unwanted metal regions of the metal layers are removed so that the intended design is obtained. Depending upon the design of filter, uniplanar or biplanar, double or single sided substrate is used. Filters were fabricated on two types of substrates, FR4 and RT Duroid. The substrate used to fabricate the SRR and folded U- shaped filter under study is the FR4 epoxy and that of OLR filter is RT Duroid. The FR4 substrate has a dielectric constant of 4.4, and a thickness of 1.6mm and corresponding values for RT Duroid are 3.2 and 1.6mm. RT Duroid which is costlier than FR4 has a low loss tangent of 0.0009 compared to 0.02 for FR4. The geometry of the resonators in the filters under study are given below which are designed to operate in conjunction with 50Ω microstrip transmission line fabricated on the corresponding substrate material.

OLR based bandstop filter

Geometry of the square OLR of size $W \times L$ is shown in Fig.3.7:

s is the slit width

t is the metal width and

p_{av} is the average perimeter of the open loop

Typical dimensions on RT Duroid substrate($\epsilon_r = 3.2$):

$W = L = 14mm,$

$s = 1mm$ and

$t = 0.5mm$

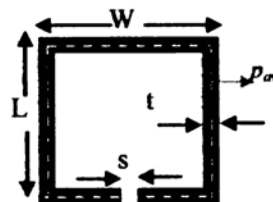


Fig.3.7 Layout of OLR

Folded U- shaped bandpass filter

Geometry of the folded U- shaped resonator is shown in Fig. 3.8:

W is the coupling length

L is the length of the side arm

t is the metal thickness of the metal

d is the gap between the folds and

s is the gap between the two open ends

Typical dimensions on the FR4 substrate ($\epsilon_r = 4.4$):

$L=20mm$,

$w=6mm$,

$t=0.3mm$,

$d=0.2mm$ and

$s = 0.5mm$

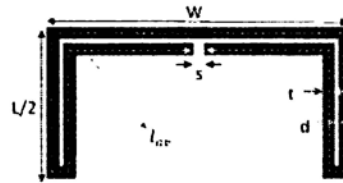


Fig.3.8 Layout of Folded U resonator

SRR based filter

Geometry of the SRR is shown in Fig.3.9:

r_1 is the inner

r_2 is the outer

c is the metal width between the rings

s is the slit width of the rings

d is the gap between two rings

Typical dimensions on the FR4 substrate:

$r_1 = 1.6\text{mm}$,
 $r_2 = 3.6\text{mm}$,
 $c = 0.9\text{mm}$,
 $d = 0.2\text{mm}$ and
 $s = 0.5\text{mm}$



Fig.3.9 Layout of SRR

3.2.1 Photolithographic technique

Photolithography is a process of transferring geometrical shapes from a photolithographic mask to the surface of a substrate which results in optical accuracy. After the proper selection of the substrate, a computer aided design of the structure was made and a negative mask of geometry is generated. The precise fabrication of a prototype falling within the microwave frequency is very essential. With the help of a high resolution laser printer, the computer designed filter geometry was printed on a transparent sheet for the use as the mask.

The copper clad substrate of suitable dimension was cleaned with solvents like acetone to remove any chemical impurities and dried. Thereafter, a thin layer of negative photo resist material was coated over the substrate using a high speed spinner. This substrate was then exposed to U.V. light through the carefully aligned mask. Extreme care was taken to ensure that the region between the copper clad and mask remains dust-free. The U. V. exposure results in the hardening of the photo resist layer. Subsequently, the substrate was immersed in a developer solution and followed by ferric chloride treatment to remove the unwanted copper.

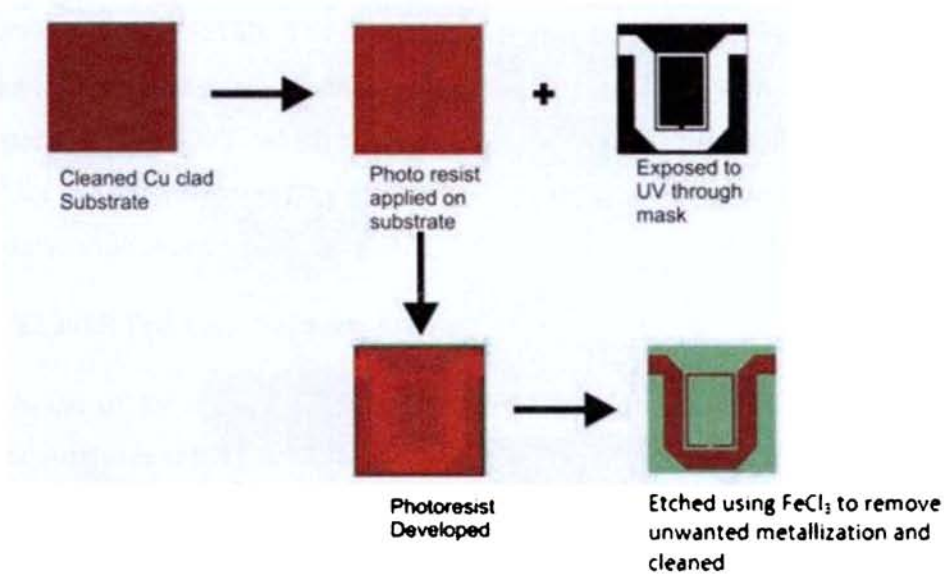


Fig. 3.10 Various steps involved in the photolithographic process

Then the substrate was cleaned to remove the hardened photoresist using acetone solution. Photolithography process is illustrated in Fig. 3.10.

3.3 Filter Characteristics Measurement

A short description of equipments and facilities used for the measurements of filter characteristics is presented in this section.

3.3.1 HP 8510C Vector Network Analyzer

The HP 8510C microwave vector network analyzers provide a complete solution for characterizing the linear behaviour of either active or passive networks over the 45 MHz to 50 GHz frequency range. The network analyzer system consists of a microwave source, S-parameter test set, signal processor and display unit as shown in Fig. 3.11.

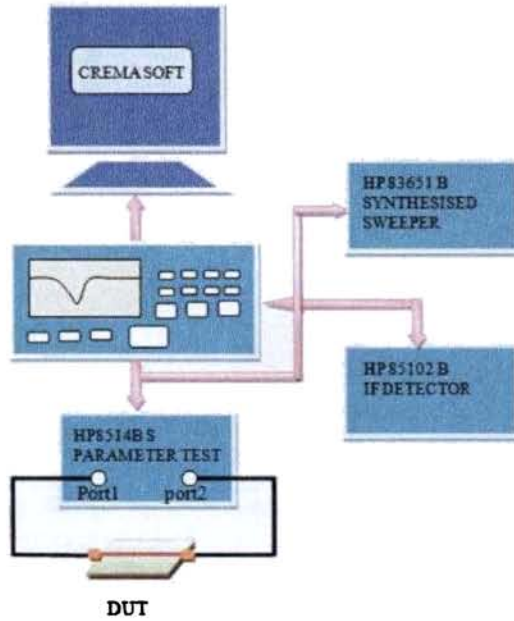


Fig.3.11 Block diagram of HP8510C Vector Network Analyzer

The network analyzer measures the magnitude, phase, and group delay of two-port networks to characterize their linear behaviour. The analyzer is also capable of displaying a network's time domain response to an impulse or a step waveform by computing the inverse Fourier transform of the frequency domain response. The synthesized sweep generator HP 83651B uses an open loop YIG tuned element to generate the RF stimulus.

Frequencies from 10 MHz to 50 GHz can be synthesized either in step mode or ramp mode depending on the required measurement accuracy. The frequency down converter unit separates the forward and reflected power at the measurement point and down converted it to 20MHz. It is again down converted to lower frequency and processed in the HP8510C processing unit with Motorola 68000 processor. All the above systems are interconnected with HP-IB bus and RF cables.

The device under test (DUT) is connected between the two ports of the S-parameter test set HP8514B. The filter characteristics such as insertion loss, return loss in magnitude and phase are measured using the Network Analyzer. The indigenously developed CREMASOFT, which is Matlab based data acquisition software in IBM PC, is used for the automatic measurement of the characteristics using the network analyser. It coordinates the measurements and records the data in csv format [3].

3.3.2 E8362B Precision Network Analyzer (PNA)

Some of the measurements were carried out using PNA E8362B. Precision Network Analyzer (PNA) is the recent series from Agilent Vector Network Analyzer family which provides the combination of speed and precision for the demanding needs of today's high frequency, high-performance component test requirements. The modern measurement system meets these testing challenges by providing the right combination of fast sweep speeds, wide dynamic range, low trace noise and flexible connectivity. The Analyzer is capable for performing measurements from 10 MHz to 20 GHz and it has 16, 001 points per channel with $< 26 \mu\text{sec/point}$ measurement speed. The photograph of the PNA E8362B used for the antenna measurements is shown in Fig. 3.12 below.



Fig. 3.12 PNA E8362B Network Analyzer

3.3.3 Measurement procedure

The experimental procedure followed in determining the filter characteristics is discussed below. Power is fed to the filter from the S parameter test set of the analyzer through the cables and connectors. The connectors and cables tend to be lossy at higher microwave frequencies. Hence the instrument should be calibrated with known standards to get accurate scattering parameters.

3.3.4 S Parameters, Resonant Frequency and Bandwidth

The network analyser is calibrated for full two ports by connecting the standard short, open and thru loads suitably. Proper phase delay is introduced while calibrating to ensure that the reference plane for all measurements in the desired band is actually at zero degree thus taking care of probable cable length variations. The two ports of the filter is then connected to the ports of the S parameter test unit as shown in Fig. 3.11. The magnitude and phase of S_{11} , S_{22} and S_{21} are measured and stored in ASCII format using the CREMASOFT. S_{11} and S_{22} indicate the return loss at the two ports of the filter and S_{21} indicate the insertion loss (transmission characteristics) of the filter from which the resonant frequency and the bandwidth are calculated.

References

- [1] HFSS User's guide, Ver.9.2, Ansoft Corporation, Pittsburgh, 2004.
- [2] IE3D User's manual, Zealand Software Inc., CA, USA, Dec, 1999.
- [3] Hp8510C Network Analyzer, Operating and service manual, Hewlett-Packard company, Santa Rosa, CA,USA.

PLANAR LOOP RESONATOR FILTERS

This chapter presents the application of loop resonators in developing compact bandstop and bandpass filters. The characteristics of planar loop resonators are introduced in the beginning of this chapter with emphasis on the size of the structure. A detailed study of open loop resonator and its application in narrow bandstop filter design is investigated in the first section. The second section deals with the design of compact bandpass filters using parallel coupled folded loop resonators. Parameters affecting the strength of coupling and the resonant frequency are investigated and techniques for size reduction are developed. Empirical formula for the resonant frequency for different types of resonators is deduced. Experimental results on optimal filter configuration are presented.

4.1 Introduction

A filter with an optimum frequency response curve and reduced size is very essential in a microwave system. Planar filters are popular and have low cost and light weight; particularly, such filters are easily fabricated using printed circuit technology. Since size reduction is always important, the planar filter frequently requires a change in geometry for circuit miniaturization. The loop resonators are equivalent to LC tank circuits which resonate at a particular frequency depending on its dimension when properly excited by the electromagnetic fields. When placed in close proximity to the transmission line, it inhibits the propagation of signal from input port to the output port. The same structure can also be used for coupling the power from input to output at a particular frequency band. Reducing the resonant frequency by open loop and folding technique is the theme of present work. Miniaturization is also brought about by altering the coupling technique. The simulation study has been carried out using Ansoft HFSS and Zealand IE3D. The result has been validated by fabrication and measurement.

- **Microstrip transmission line**

Planar filters are synthesized using microstrip transmission line for suitably exciting the resonators. Figure 4.1 shows the fundamental structure of a microstrip transmission line.

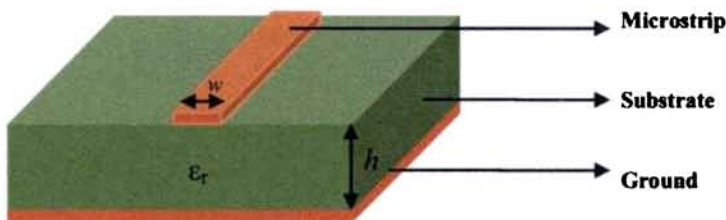


Fig 4.1 Microstrip transmission line

It can also be considered as a half wavelength resonator with two open-circuited ends, illustrated as a typical example of a transmission line resonator most commonly used in the microwave region.

It consists of a strip conductor of uniform width w and an overall length equivalent to half wavelength, formed on a grounded dielectric substrate of relative permittivity ϵ_r and thickness h . The structure can be expressed in electrical parameters as a transmission line possessing uniform characteristic impedance with an electrical length of π radian. Such transmission line resonators are referred to as uniform impedance resonators (UIR). General requirements for the UIR intended dielectric substrate materials include a low loss-tangent, high permittivity, and temperature stability. In practical design, such resonators have a number of intrinsic disadvantages such as limited design parameters, spurious responses at integer multiples of the fundamental resonance frequency.

The microstrip has most of its field lines in the dielectric region, concentrated between the strip conductor and the ground plane, and some fraction in the air region above the substrate as shown in Fig.4.2. For this reason the microstrip line cannot support a pure TEM wave, since the phase velocity of TEM fields in the dielectric region would be $c/\sqrt{\epsilon_r}$, but the phase velocity of TEM fields in the air region would be c . Thus, a phase match at the dielectric- air interface would be impossible to attain for a TEM-type wave.



Fig. 4.2 Electric and magnetic field lines in microstrip transmission line.

The phase velocity and propagation constant can be expressed as

$$v_p = \frac{c}{\sqrt{\epsilon_{eff}}},$$

$$\beta = k_0 \sqrt{\epsilon_{eff}} \quad ; \quad k_0 = c/v_p$$

where ϵ_{eff} is the effective dielectric constant of the microstrip line. Since some of the field lines are in the dielectric region and some are in the air, the effective dielectric constant satisfies the relation,

$$1 < \epsilon_{eff} < \epsilon_r,$$

The effective dielectric constant of a microstrip line is given by

$$\epsilon_{eff} = \frac{\epsilon_r + 1}{2} + \frac{\epsilon_r - 1}{2} \frac{1}{\sqrt{1 + 12h/w}}$$

- **Loop resonators**

Closed loop resonators when compared to the microstrip linear resonators, does not suffer from the open end effects and can be used to give more accurate results. Among the closed loop resonators, ring resonators are distributed line resonator where r is the median radius of the ring. Ring resonator is merely a transmission line formed in a closed loop. The ring will resonate at its fundamental frequency f_0 which is given by

$$f_0 = \frac{nc}{2\pi r \sqrt{\epsilon_{eff}}} \quad (4.1)$$

The higher resonant modes occur at $f = n f_0$ for $n=2, 3, \dots$.

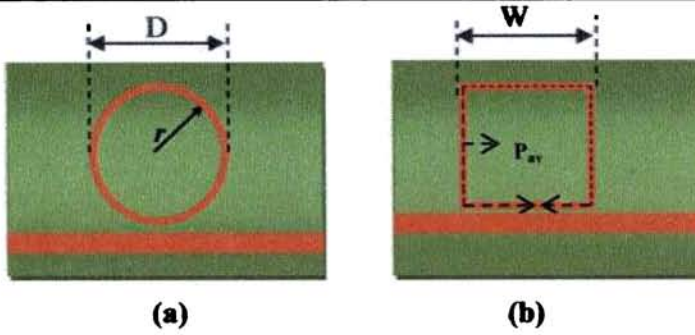


Fig. 4.3 (a) Ring resonator (b) Square resonator

Closed square loop with the same performance that of the circular loop has essentially been used in many of the microstrip filters. The square ring resonates at a fundamental frequency f_0 given by

$$f_0 = \frac{c}{p_{av}\sqrt{\epsilon_{eff}}} \quad (4.2)$$

where p_{av} is the average perimeter of the loop.

The characteristics of these resonating loops are studied by exciting them by placing in close proximity to the transmission line as shown in Fig.4.3.

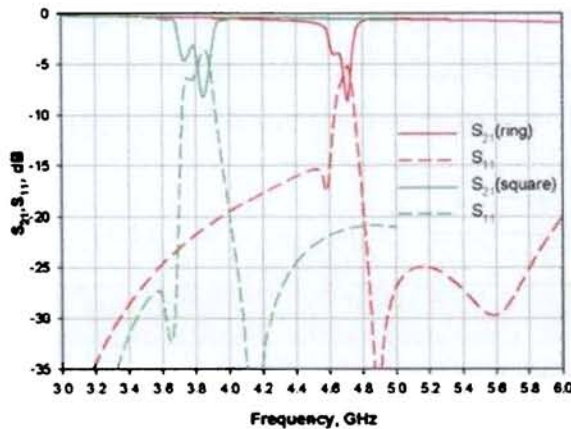


Fig. 4.4 Simulated S-parameter for the closed loop resonators

The simulated S-parameters in Fig.4.4 shows the transmission characteristics the loop resonators occupying the same dimensional area ($D=W$).

The closed loop resonators illustrated above are full wavelength resonators which are larger in dimension and less preferred for compact devices. The size of the resonator can be further reduced by employing open loop resonators (OLR) which resonates at half the frequency as that of the closed resonator with same dimension. Open loop resonators are also considered as a microstrip line loaded with folded open stubs at both ends, are essentially folded half- wavelength resonators. The Fig.4.5 shows the circular and square open loop resonators placed near the microstrip line for excitation.

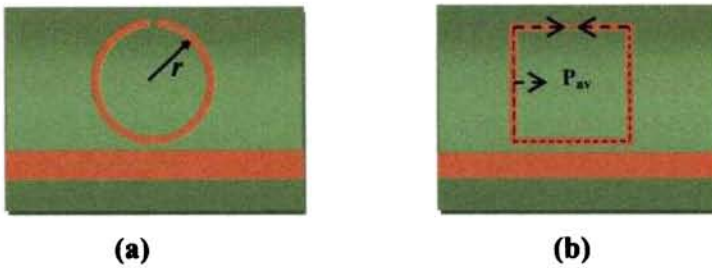


Fig. 4.5 Open loop resonator (a) Circular OLR (b) Square OLR

The resonant frequency f_0 for the open loop ring resonator is given by

$$f_0 = \frac{nc}{4\pi r \sqrt{\epsilon_{eff}}} \quad (4.3)$$

And that of the square open loop resonator with a fundamental resonant frequency f_0 given by

$$f_0 = \frac{c}{2(p_{av} - s) \sqrt{\epsilon_{eff}}} \quad (4.4)$$

where r and p_{av} the mean radius and average perimeter of the loop and s are is the gap between the open ends.

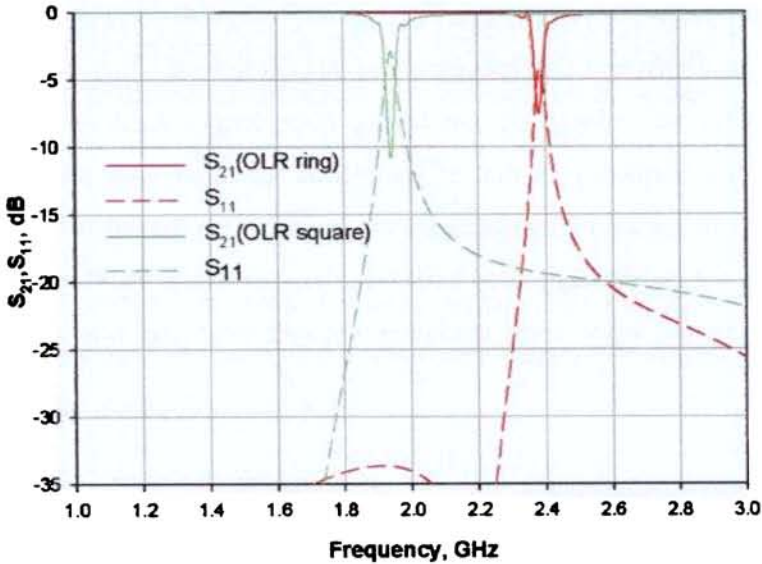


Fig. 4.6 Simulated S-parameter of open loop resonators

From the plots in Fig. 4.6, it is clear that the square loop resonator occupying the same area ($D=W$) as that of the circular loop resonates at a lower frequency with greater attenuation due to larger coupling and interaction with the feed line.

Another type of distributed line resonators called split ring resonators (SRR), formed by two coupled conducting open loop resonators. They are considered as electronically small resonators with very high Q and very useful structure in constructing filters requiring sharp notch or pass a certain frequency band. The band rejection characteristics of the resonator are studied by placing it in close proximity to a transmission line as shown in Fig. 4.7. The signal propagation is inhibited at the resonant frequency of the resonator.

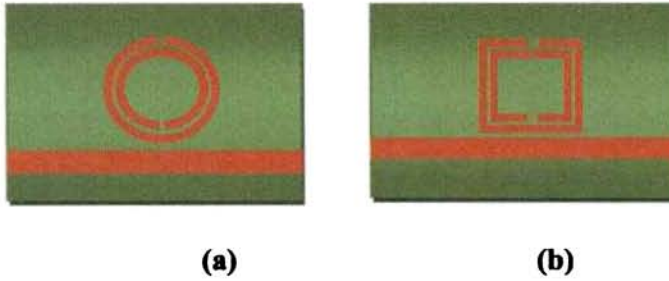


Fig. 4.7 Split Ring Resonators (a) Circular (a) Square

Simulation results of circular and square SRRs having equal parameters ($D=W$) are shown in Fig. 4.8.

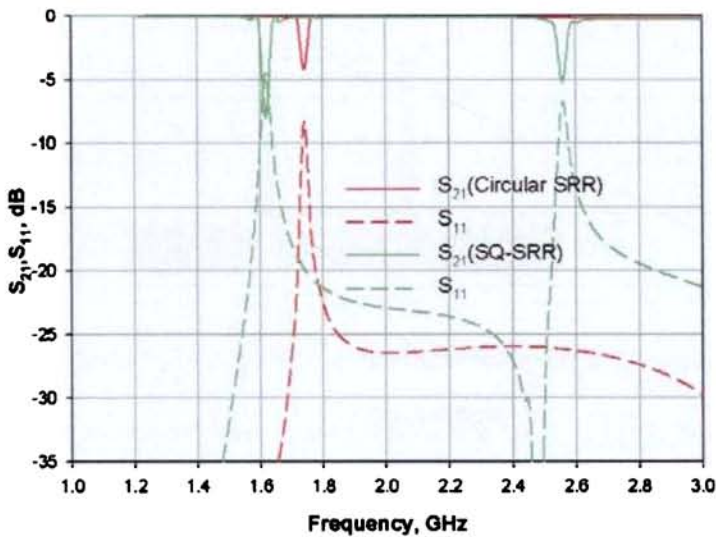


Fig. 4.8 Simulated S-parameter of split ring resonators

The resonators in Fig.4.9 (a&b) are spiral resonators (SRs) side coupled to the transmission line to investigate its band rejection characteristics at the center frequency. SRs allow significant reduction in the electrical size of unit cell when compared to other ring resonators. It is verified that the resonant frequency of SRs are one half that of its SRR counterparts.

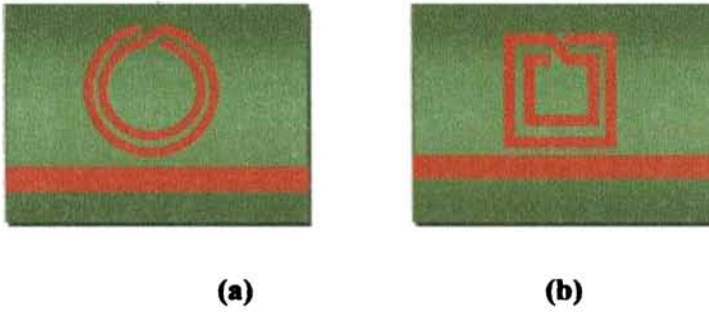


Fig. 4.9 Spiral resonators (a) Circular (b) Square resonators

The simulation results in Fig.4.10 compares the frequency responses of the square and circular SRs with all parameters same as mentioned above for all the cases ($D=W$).

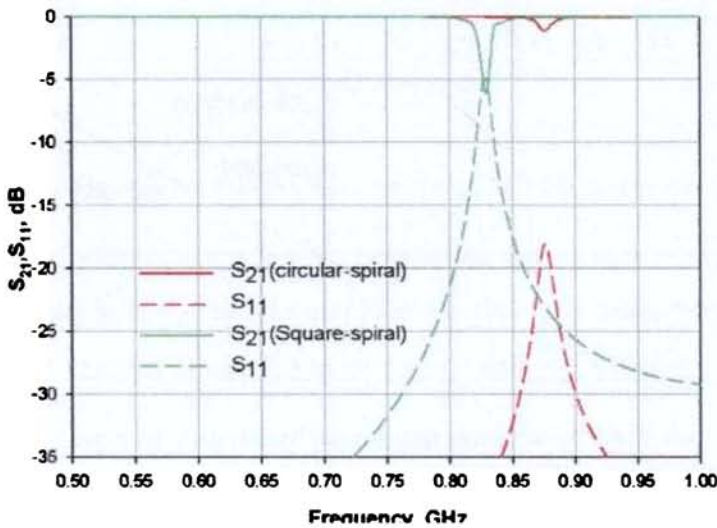


Fig. 4.10 Simulated S-parameter of spiral resonators

From all the above illustrations, the band rejection characteristics of the square resonators propose it as a good candidate for designing filters. In the following section the characteristics of square resonators are studied by coupling it to a microstrip transmission line.

- **Band rejection Characteristics of closed loop resonator**

The characteristics of the square closed loop resonator has already been introduced and compared with that of its circular counterpart. The resonant frequency of the loop is normally determined by its physical dimension. The characteristics are studied by using the basic circuit consisting of the feed line, and the resonator. The feed line is the microstrip line etched on a dielectric material of known dielectric constant. Fig.4.11 shows the circuit arrangement employed where a square loop resonator is placed near the microstrip line with a coupling gap g . Throughout this section, side coupling is used to reduce the insertion loss. The power is coupled into and out of the resonator through feed line and the coupling gap.

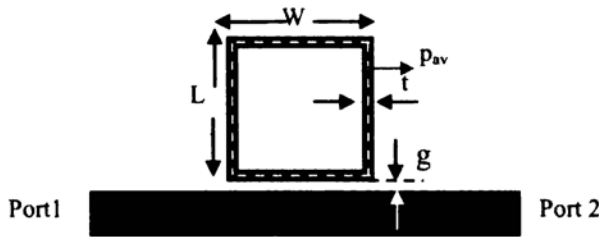


Fig. 4.11 Schematic of square loop resonator coupled to a microstrip line.

A closed loop square resonator of dimension $L \times W = 14 \times 14$, having a resonance at 3.8GHz according to (4.2), is fabricated on a substrate of permittivity $\epsilon_r = 3.2$ and height $h = 1.6\text{mm}$ is simulated for various coupling gap distances. The results depicting the frequency response with the coupling gap is shown in Fig. 4.12. It is evident from the plots that two resonant peaks (f_{p1} and f_{p2}) appear for small values of g due to strong coupling. As coupling gap increases, the attenuation level decreases but frequency selectivity increases and a single resonant peak is obtained at $g = 1\text{mm}$.

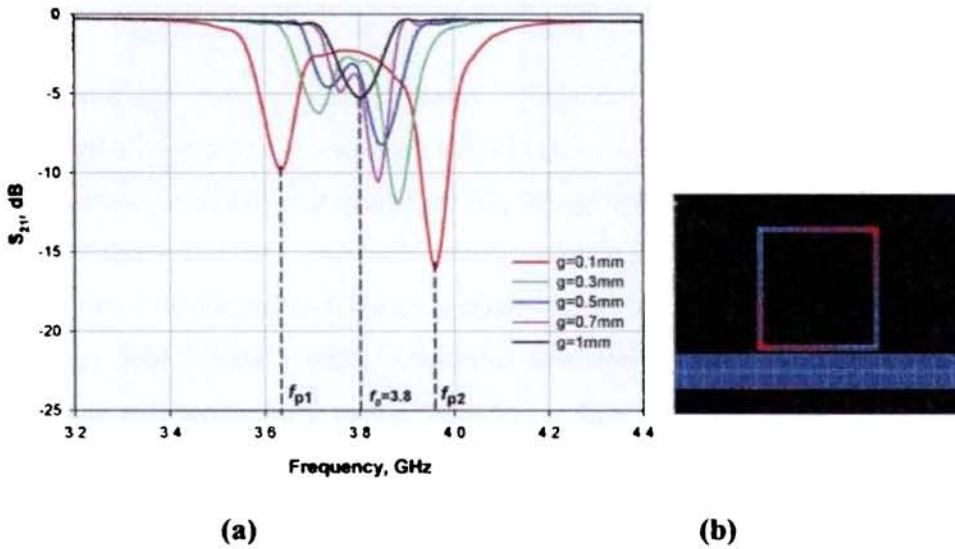


Fig.4.12 Simulation results (a) S_{21} when coupling gap g is varied (b) Vector current density at 3.8GHz

The vector current density plotted for gap $g = 1$ mm at the resonant frequency (3.8GHz) is given in Fig.4.12(b) which shows one full wave variation in the loop. The resonator can be considered as a RLC tank circuit.

- **Field distribution in side coupled closed loop resonator**

The E-field and H-field distribution at a coupling gap $g = 0.1$ mm, for f_{p1} , f_0 and f_{p2} . are obtained for the structure and shown in Fig.4.13. Investigation of the field distribution at these frequencies reveals that at f_{p1} and f_{p2} , the H field distribution is more intense compared to the E field distribution.

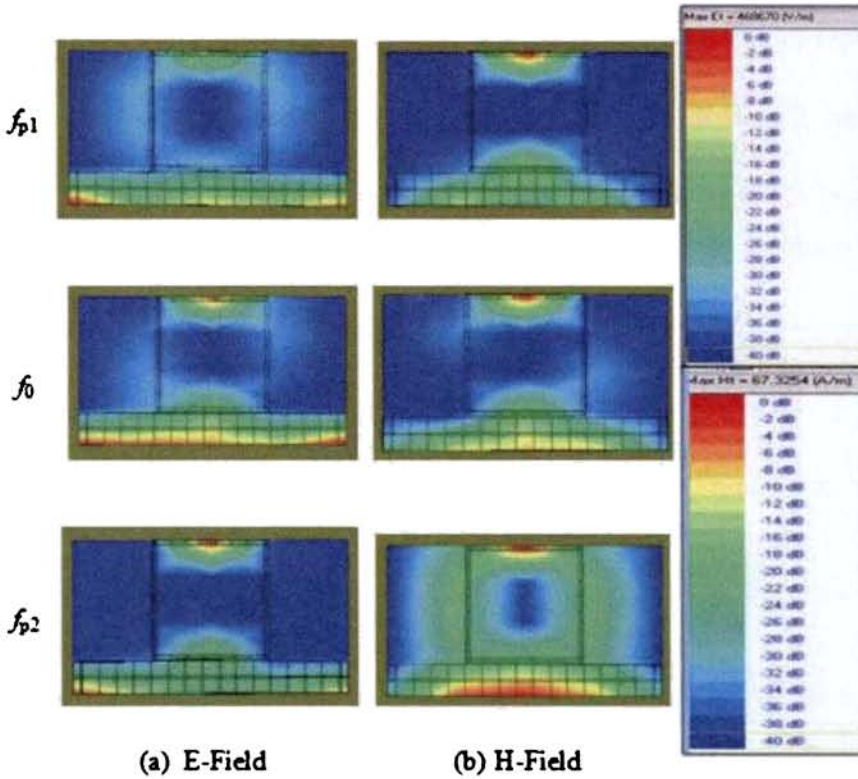


Fig.4.13 Field distribution at $g=0.1\text{mm}$ for f_{p1} , f_0 and f_{p2} (a)E-Field (b) H-field

At f_0 , both E field and H field distributions are almost equal. Since the loop resonator is magnetically coupled to the transmission line, a mutual inductance L_m between the transmission line and the resonator influences the frequency response to have two peaks at f_{p1} and f_{p2} given as

$$f_p = \frac{1}{2\pi\sqrt{(L \pm L_m)C}} \quad (4.5)$$

The magnetic coupling coefficient given by $k_m = L_m/L$ varies with the coupling gap g . The values for k_m can also be found from the simulation results as

$$k_m = \frac{f_{p2}^2 - f_{p1}^2}{f_{p2}^2 + f_{p1}^2} \quad (4.6)$$

where f_{p1} and f_{p2} are the frequencies corresponding to the two resonant peaks.

Coupling coefficient is extracted from simulated results and is shown in Fig.4.14 as a function of coupling gap g .

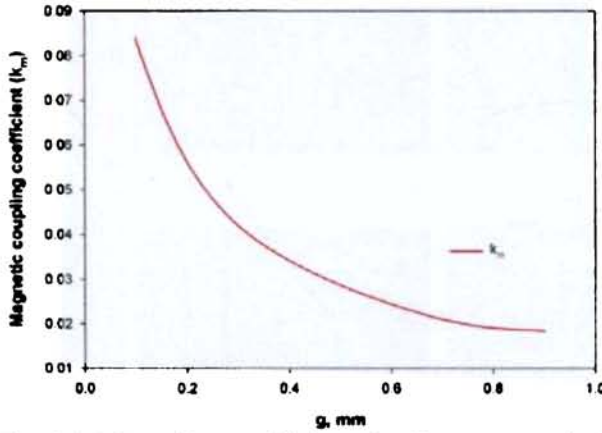


Fig.4.14 Coupling coefficient for the structure in Fig. 4.11.

Even though this configuration exhibits the desired frequency behavior, it presents practical problems like dual resonant peaks due to tight coupling or very low attenuation for weak coupling. Also, the configuration is not suitable for the compact filter designs. In order to alleviate these problems, an open loop resonator is used for the compact filter design. As introduced in Fig 4.6, the simulation characteristics of the OLR demonstrates an improved characteristics at half the resonant frequency compared to its closed loop counterpart.

4.1.1 Open loop resonator

The characteristic of OLR is studied by electromagnetically coupling it to a microstrip transmission line. The wave propagation is rejected in the vicinity of the resonant frequency. Unlike the closed ring resonator the open loop resonator has

electric resonance along with the magnetic resonance. The electric resonance is induced by the slit in the ring. The layout of the OLR with LC equivalent circuit representation is shown in Fig. 4.15.

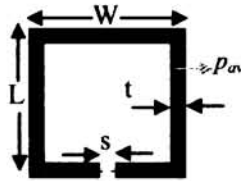


Fig.4.15 Layout of the OLR

Figure 4.16 shows the open loop resonator fabricated on a substrate and placed over the transmission line in three orientations based on the position of the slit. It is obvious that the coupling in these structures is the proximity coupling, which is basically through fringing fields. For optimum excitation the ring is placed close to the transmission line. The nature and the extend of the fringe fields determine the nature and the strength of the coupling.

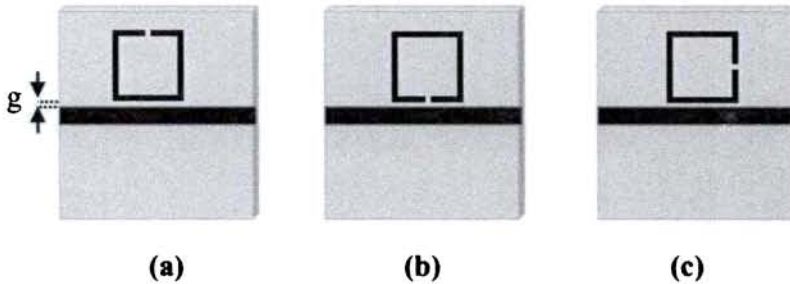


Fig. 4.16 Different configurations of OLR unit cell

The open loop resonator inhibits signal propagation in a narrow band in the vicinity of its resonant frequency. Since the OLR is a half wavelength resonator, the resonant frequency is determined by Equation (4.4) and repeated here:

$$f_0 \cong \frac{nc}{2(p_{av} - s)\sqrt{\epsilon_{eff}}} \quad (4.7)$$

where p_{av} is the average perimeter, s is the gap between the open ends of the resonator, c is the speed of light in free space, n is the mode number and ϵ_{eff} is the effective dielectric constant calculated for the microstrip line. This equation is for the resonant frequency for the intrinsic resonator which does not take the coupling gap into account.

- **Characteristics of open loop resonator**

An OLR of dimension $L \times W = 14 \times 14$ with a slit width $s = 1\text{mm}$ placed at a distance $g = 0.5\text{mm}$ from the transmission line is simulated for the three configurations. Based on the above equation, the calculated resonant frequency is 1.95GHz . The plots in Fig.4.17 depict a slight shift in the frequencies from the designed value.

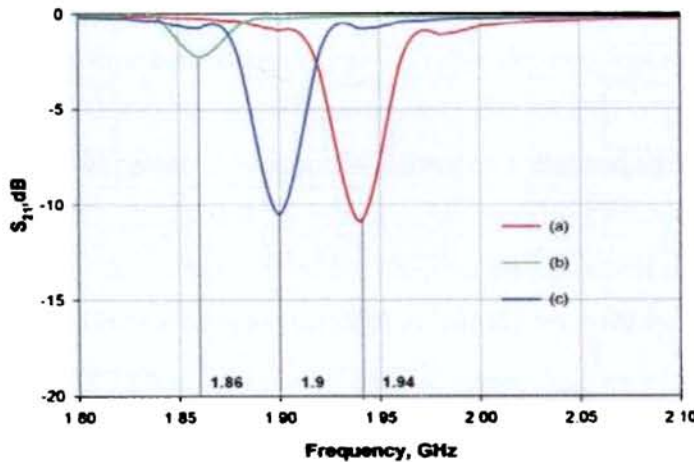


Fig.4.17 S-parameters obtained by simulation for three orientations ($g=0.5\text{mm}$)

- **Field distribution**

The shift in frequency is contributed by the nature of coupling that the resonator experience when the slit comes closer to the transmission line. This is evident from the nature of electric and magnetic field intensity plots obtained from the simulation and shown in Fig.4.18. It can be observed that at resonance of the fundamental mode, each of the open loop resonators has the maximum electric field density at the side with slit, and the maximum magnetic field density at the opposite side. In the configuration in Fig.4.16 (a), the magnetic coupling dominates the electric coupling since the slit is not directly coupled to the transmission line. Whereas the resonator in configuration (Fig.4.16 (b)) is electrically coupled to the transmission line as the slit is in close proximity to the transmission line.

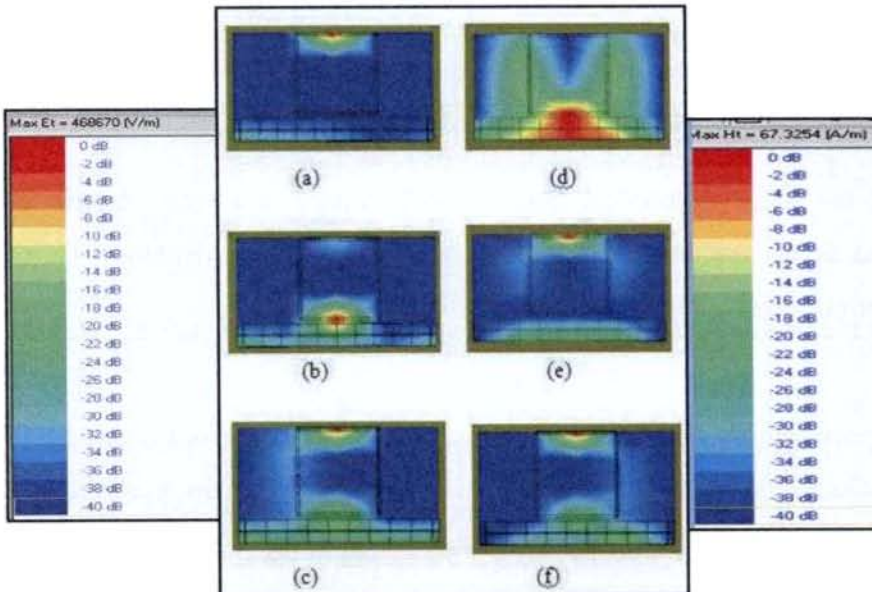


Fig. 4.18 Field distribution for the three configurations (a,b&c) E-Field (d,e&f) H-Field

For the configuration (Fig.4.16c) where the electric and magnetic fringe fields have comparable distributions, electric and magnetic couplings occur equally. In this case the coupling is referred to as mixed coupling as is seen in Fig.4.18 (c) and (f).

- **Effective permittivity**

The shift in resonant frequency can be explained by examining the effective permittivity, ϵ_{eff} . In microstrip, the effective permittivity is a measure of the fields confined in the region beneath the strip. For the configuration in Fig. 4.16(a), the E field distribution (Fig.4.18 (a)) shows a negligible value of field strength beneath the transmission line while a large value for the magnetic field as depicted in 4.18(d). The ϵ_{eff} is given by,

$$\epsilon_{eff1} = \frac{\epsilon_r + 1}{2} \quad (4.8)$$

where ϵ_r is the relative dielectric of the substrate.

For the configuration in Fig. 4.16(b), where a strong electric field is concentrated under the transmission line due to the OLR orientation (4.16c), the effective permittivity is given by,

$$\epsilon_{eff2} = \frac{\epsilon_r + 1}{2} + \frac{\epsilon_r - 1}{2} \left(1 + \frac{12h}{t}\right)^{\frac{1}{2}} \quad (4.9)$$

where t is the width of the resonator and h is the height of the substrate.

For the configuration in Fig.4.16(c), both electric and magnetic field distributions are comparable and thus the resonant frequency is always the average of the other two which implies that ϵ_{eff} is also the average of the values of other two conditions given as

$$\epsilon_{eff3} = \frac{\epsilon_{eff1} + \epsilon_{eff2}}{2} \quad (4.10)$$

The resonant frequencies calculated (4.7) by substituting appropriate value of ϵ_{eff} for an OLR of dimension $L \times W = 14 \times 14$ are compared with simulated results and are shown in Table 4.1.

621.372 85.0.1
JIT




| (t=0.5mm,s=0.1mm and h=1.6mm) | | | | |
|---|------------------|------------------|-------------------|-------------------|
| Lx W=14x14 | f_0 | $\epsilon_r=3.2$ | $\epsilon_r=6.15$ | $\epsilon_r=10.2$ |
|  | f_{eff1} , GHz | 1.96 | 1.50 | 1.19 |
| | f_{sim} , GHz | 1.94 | 1.48 | 1.16 |
|  | f_{eff3} , GHz | 1.87 | 1.417 | 1.12 |
| | f_{sim} , GHz | 1.86 | 1.4166 | 1.126 |
|  | f_{eff2} , GHz | 1.91 | 1.45 | 1.15 |
| | f_{sim} , GHz | 1.90 | 1.44 | 1.14 |

Table 4.1. Calculated and simulated resonant frequencies for different OLR configurations.

Additional resonators are used to get a sharper frequency response with good attenuation levels. A microstrip transmission line that allows propagation of quasi-TEM modes induce field lines that close upon themselves around the line. Figure 4.19(a) shows the typical 3-pole narrow band stop filter fabricated on a RT Duroid substrate of $\epsilon_r = 3.2$, and $h=1.6$ mm. The OLR is designed to resonate at 1.96 GHz, with an outer dimension $L \times W = 14 \times 14 \text{ mm}^2$, $t=0.5$ mm, $s=1$ mm, $g=0.2$ mm and $a=19$ mm.



The plot in Fig 4.19(b) shows the transmission characteristics of the 3-pole narrow bandstop filter simulated with the aid of commercial simulation software Zealand IE3D.

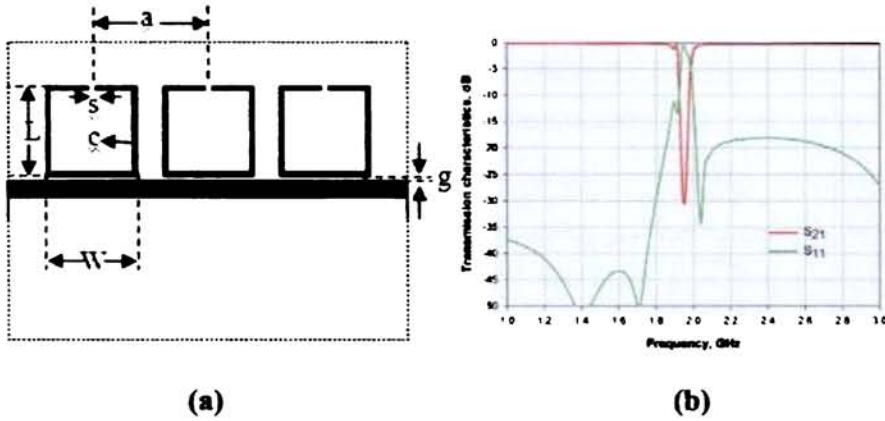


Fig. 4.19 (a) Schematic drawing of the 3-pole OLR filter ($L=W=14\text{mm}$, $s=1\text{mm}$, $c=0.5\text{mm}$, $a=19\text{mm}$, $g=0.2\text{mm}$ and $N=3$) **(b)** Simulated transmission characteristics.

It is evident from the above study that as the number of resonant elements are increased, the rejection level increases but at the cost of structure dimension. The drawback of this implementation is the structure dimension. The compactness of the overall structure can be achieved by side coupling the resonator to the transmission line which is bent to form a U-shaped layout. The resonator is placed in close proximity within the empty U region. This approach produces considerable attenuation level and a narrower bandwidth with a single resonator. This is discussed in the next section.

4.1.2 Compact microstrip bandstop filter

As stated in the previous section, the OLR particles can be employed to synthesize narrow bandstop filter, if adequate number of resonators are used. An alternative approach consists of employing a U-shaped microstrip line that interacts

with the single half wavelength resonator throughout its length, thereby exciting it adequately to produce considerable attenuation level. With this idea in mind, a compact OLR filter is proposed as depicted in the layout in Fig. 4.20.

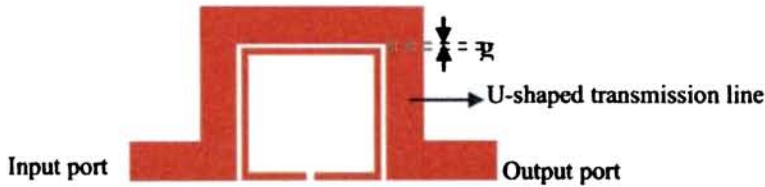
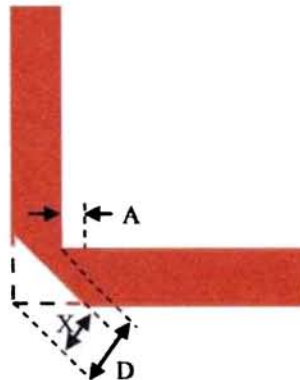


Fig 4.20 Layout of compact OLR based filter

Figure illustrates a U-bend of a microstrip transmission line around the open loop resonator to achieve band rejection which is a fully planar approach. This structure is more compact and the configuration ensures better coupling between the resonator and the transmission line.

- **Mitered transmission line**

An abrupt 90° bend in a microstrip will cause a significant portion of the signal on the strip to be reflected back. The ninety degree bend will also add a small amount of capacitance by changing the line characteristic impedance. But in reality the small capacitance doesn't change the circuit's performance very much. A common technique to build a low reflection bends and one which consumes a smaller area of substrate, is to use a mitered bend. "Mitering" the bend chops off some capacitance, restoring the line back to its original characteristic impedance. The image below shows the important parameters of a mitered bend.



$$D = w\sqrt{2}$$

$$X = D(0.52 + 0.65e^{-1.35\frac{w}{h}}) \quad (4.11)$$

$$A = (X - D/2)\sqrt{2}$$

Notice the result that the miter is not a function of substrate dielectric constant. But the range that the accuracy of this calculation is valid is limited to:

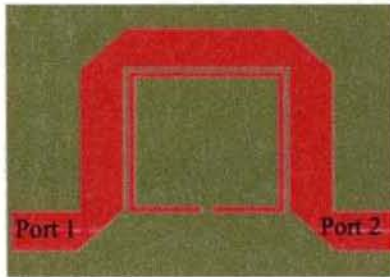
$$0.5 \leq w/h \leq 2.75$$

$$2.5 \leq \epsilon_r \leq 250$$

where, w and h are the width and height of the transmission line respectively.

- **Characteristics of OLR coupled to U-shaped transmission line**

Taking the above fact into account, an OLR filter with a single OLR unit cell coupled to U-shaped mitered transmission line was fabricated on a RT Duroid substrate by photolithographic technique. The layout of the prototype filter is shown in Fig.4.21.



Dimension of the filter:

$L \times W = 14 \times 14 \text{ mm}^2$

$c = 0.5 \text{ mm}$

$s = 1 \text{ mm}$

$g = 0.2 \text{ mm}$

$w = 3.853 \text{ mm}$

Substrate: RT Duroid

$\epsilon_r = 3.2$

$h = 1.6 \text{ mm}$

. **Fig. 4.21** Layout of the compact OLR filter

The resonant frequency is given by the Equation (4.7) where the effective permittivity is that of the magnetic coupling case (4.8), since the slit is not directly

coupled to the U-shaped transmission line. Figure 4.22 shows the simulation results obtained for the proposed filter. A rejected frequency band is present in the vicinity of the resonant frequency (1.96 GHz) but with a very low attenuation level (Fig.4.22(a)).

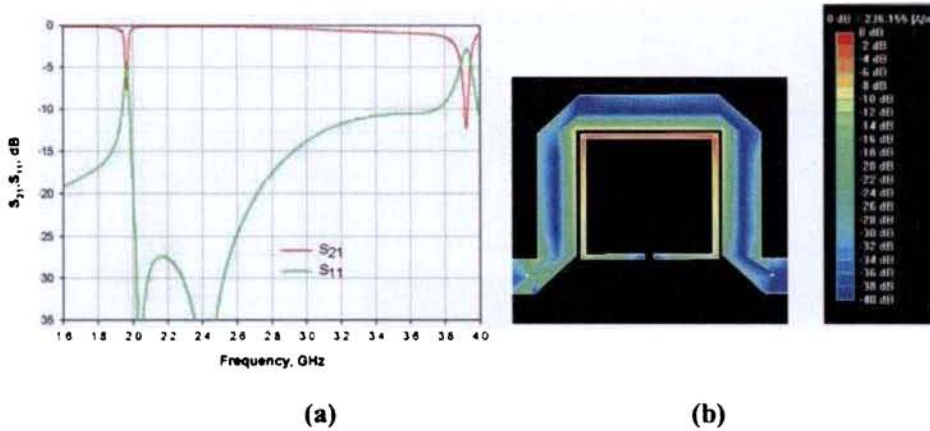


Fig. 4.22 Simulation results for the compact OLR filter **(a)** S parameters **(b)** Surface current density

From the current density plot (Fig.4.22(b)) in the rejected band, it is clear that the OLR is not properly excited by the microstrip line. To get an appreciable attenuation level, the OLR is positioned in the U-shaped transmission line as shown in Fig. 4.23(a). The simulated S-parameters are shown in Fig.4.23 (b). There is a shift in the center frequency from the designed value which is due to the capacitive effect of the slit in the close vicinity of transmission line which is already explained in terms of effective permittivity. From the simulation results it is clear that there is total transmission except at the resonant frequencies.

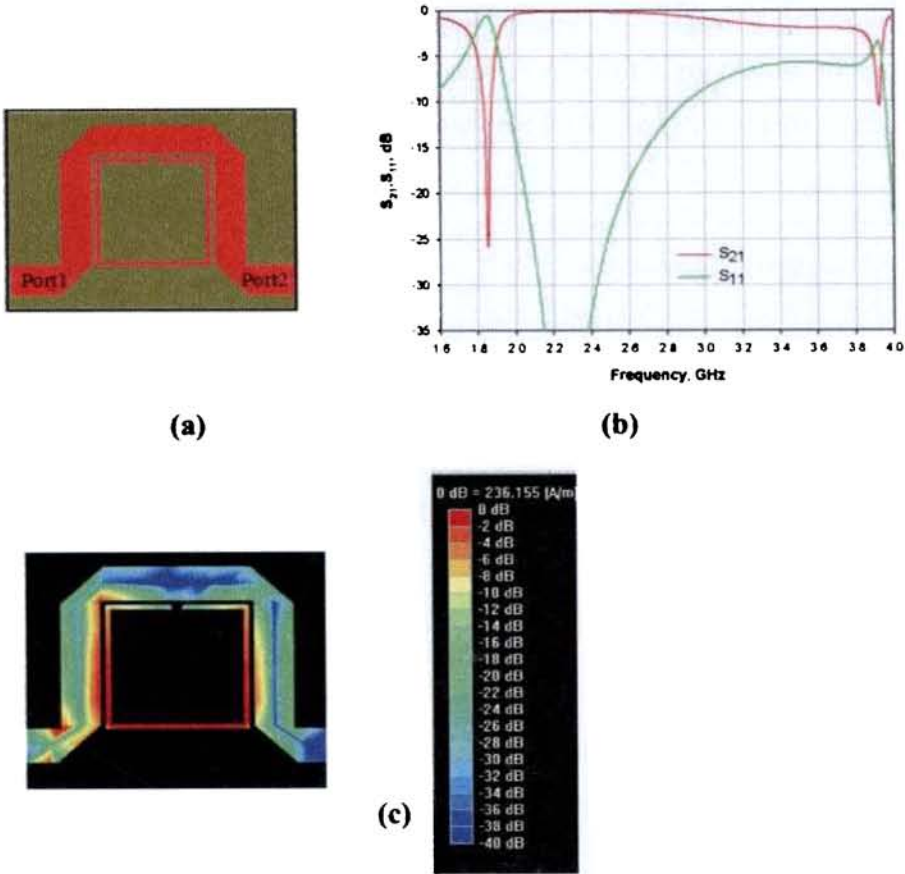


Fig. 4.23 (a) Schematic of the compact OLR filter with slitted side near the transmission line (b) Frequency response (c) Current density at resonance

An appreciable attenuation dip of -25dB is obtained with the single resonator in this configuration. To gain further insight in the behavior of this filter, current density within the rejected band are plotted and shown in Fig. 4.23(c). It is clear from the plots that the OLR particle is effectively excited to inhibit the wave propagation from input port to output port.

- **Effect of coupling length**

The effect of coupling length over the resonant frequency is investigated by modifying the configuration of the resonator keeping the overall perimeter of the loop constant. Figure 4.24(a) shows three configurations: $L < W$, $L = W$ and $L > W$.

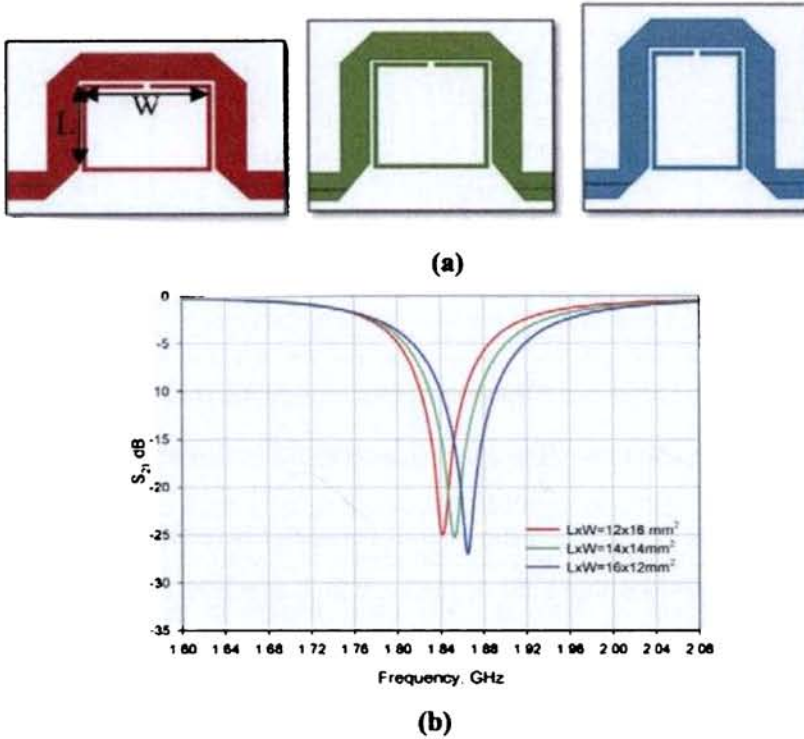


Fig. 4.24 (a) Three configurations: $W > L$, $W = L$ and $W < L$ respectively **(b)** Simulation results showing effect of coupling length

The simulation results in Fig. 4.24(b) show a small shift in the resonant frequency, which is due to the change in coupling length W , which affects the overall capacitance of the structure.

- **Effect of slit width**

As is evident from (4.7), the rejection frequency of the filter depends on the slit width 's'.

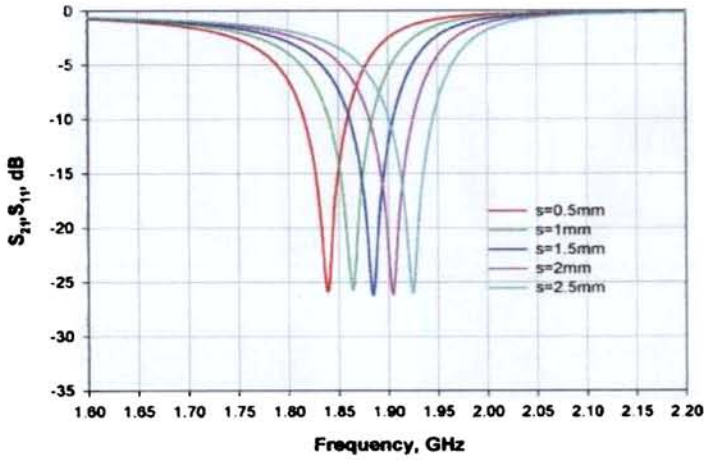


Fig. 4.25 Simulated S parameter values with variation in slit width s

As the slit width is increased the overall perimeter is reduced and the frequency increases (Fig.4.25). Besides this kind of tuning which involves change in the physical dimension, the slit in the loop facilitates integration of RF devices such as varactor or PIN diodes.

- **Experimental Results**

In order to verify the theoretical predictions, a prototype of the OLR filter has been fabricated by means of photomask-etching technique. The performance of the filter was experimentally verified using Agilent E8362B Network analyzer. The photograph of the fabricated structure is shown in Fig.4.26 (a). Simulated and measured results are compared in Fig. 4.26(b). It is worth noting that outside the rejected frequency band, a signal passes with very low insertion loss.

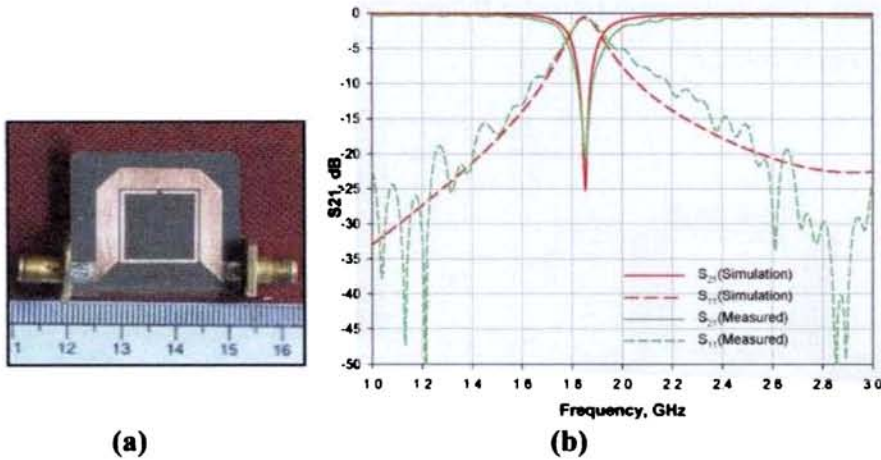


Fig. 4.26 (a) Photograph of the compact OLR filter **(b)** Measurement results compared with the simulation results (both structure and circuit)

A stop bandwidth of about 40MHz (-10dB) is observed for the filter. The advantage of this approach is the possibility of implementing a very compact filter which otherwise would have been large with N number of cells. For example, an array with three resonators to reject a band around 20dB, occupied an overall area of $42 \times 32 \text{ mm}^2$. Instead the U-shaped bend line approach if designed to attain same frequency and attenuation level, occupies a smaller dimensional area of $35 \times 25 \text{ mm}^2$ which is a size reduction of more than 35%.

- **PIN Diode integration for switching**

It is already discussed that open loop resonator obtained by introducing a small slit in the closed loop resonates at half the resonant frequency as that of the closed one resulting in size reduction. Besides size reduction, the slit facilitate device integration. PIN diode can be mounted in the loop for electronic switching. For this purpose, the loop resonator with two slits is selected since it has no resonance at lower frequency region i.e., 1.85GHz. A resonance at the lower frequency appears only if either of the

slits is closed. This design also provides the isolation between the PIN terminals while applying the bias voltage.

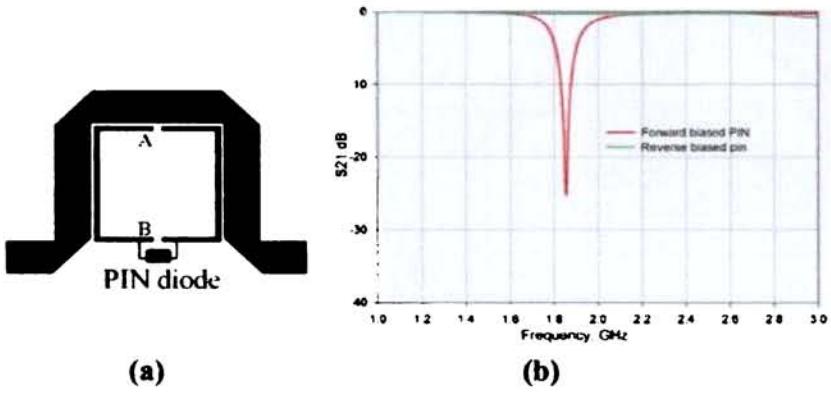


Fig.4.27 (a) Layout showing the PIN integrated OLR filter **(b)** Simulated results for PIN switch/filter

The circuit arrangement is as shown in Fig.4.27 (a).The PIN diode is connected at the slit B, and the slit A is left open. The result is an electronic switch/filter. Like other diodes the PIN diode acts as an open circuit when reverse biased and short circuit when forward biased. The simulation results for the PIN diode connected in forward and reverse biased condition is shown in Fig.4.27 (b). The circuit has a resonance at 1.85GHz when the diode is forward biased and when reverse biased, there is no resonance present.

Pin diode integrated filter is tested using HP8510C network analyzer. The experimental results of the electronic switching achieved by integrating a PIN diode across the slit B is shown in Fig.4.28. When the diode was reverse biased the circuit had no resonance. When the diode was forward biased, the mode is turned on and there appeared a resonance at 1.85GHz.

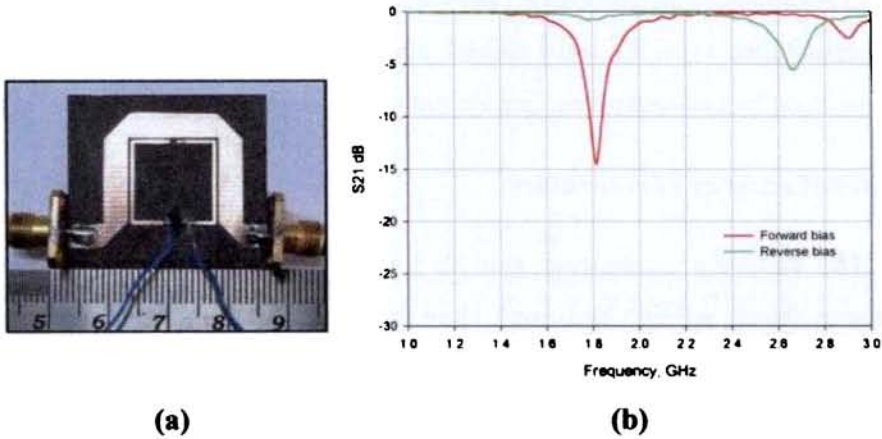


Fig. 4.28(a) Photograph of the PIN diode integrated OLR filter (b) Measured results

- **Effect of variable capacitance at the slit**

The rejection frequency of the OLR filter can be tuned by connecting a variable capacitance across the slit s . This was verified by simulation using different capacitance values across the split and the results are shown in Fig. 4.29(a).

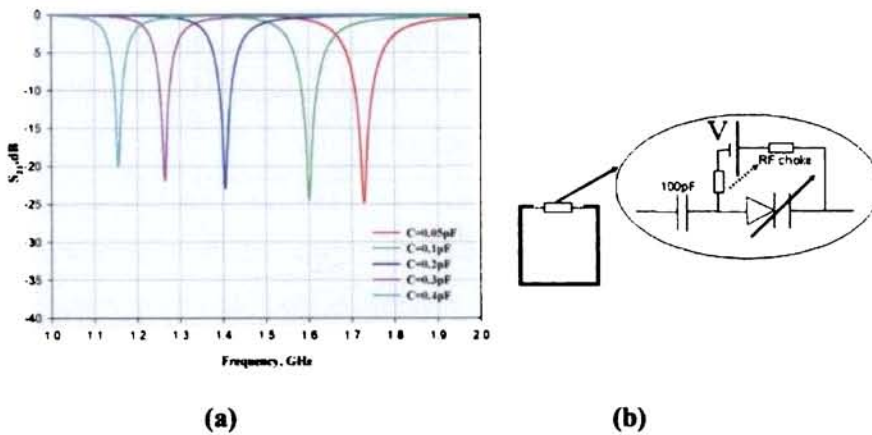


Fig. 4.29 (a) Simulation results illustrating the tunability of the compact OLR filter(b) DC isolation circuit for connecting the varactor.

It was seen that the resonant frequency can be controlled in a wide range by varying the capacitance. Electronic tuning can be achieved by integrating a varactor

diode across the split as shown in Fig. 4.29 (b) with an isolation circuit employing a 100pF capacitance as an RF short and RF chokes for protecting the DC voltage source. This is verified by connecting surface mount capacitors of different values.

- **Effect of number of resonators**

The bandstop attenuation can be further increased by using two resonating elements as shown in Fig.4.30 (inset). Here the distance between the resonator elements is taken as $15\text{mm} (\geq \lambda_g/4)$ to minimize losses in the passband. The simulated response shown in Fig.4.30 indicates a sharp roll-off which is an important consideration in wireless communication system.

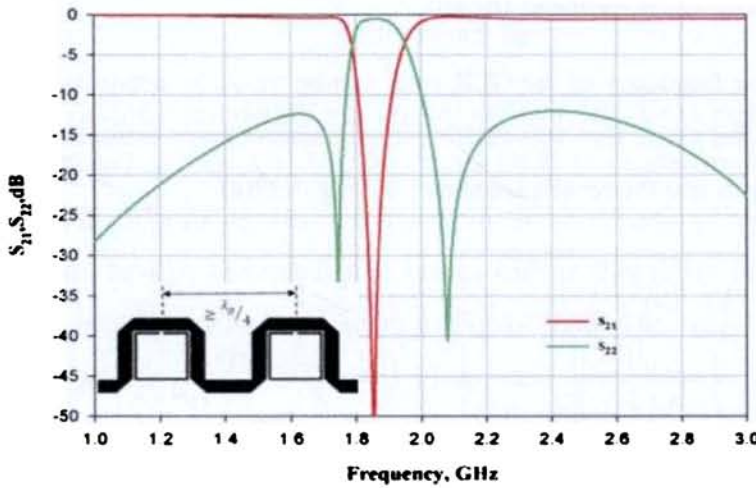


Fig. 4.30 Simulated response of notch filter with two OLSR elements (inset: layout)

- **Other type of resonators**

The characteristics of the square loop resonators introduced in the beginning of the section are implemented in the U- shaped microstrip for efficient coupling and size reduction. They are shown below (Fig.4.31):

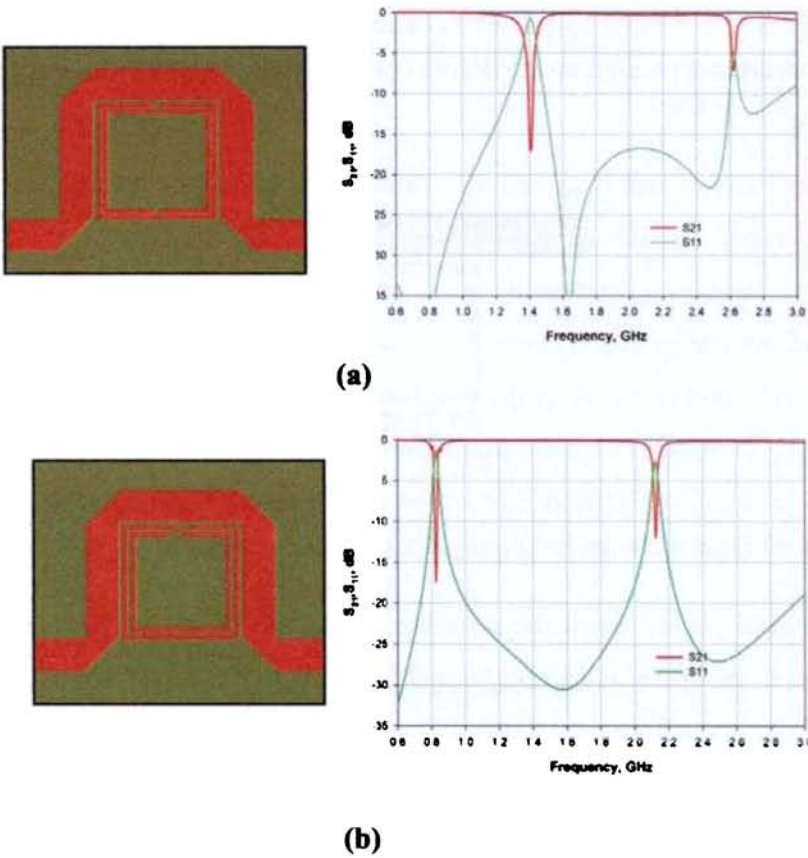


Fig. 4.31 Square loop resonators and their transmission characteristics **(a)** Square SRR
(b) Square SR

The characteristics of the square SRR and SR loop resonators coupled to U-shaped mitred transmission line show an improvement in the attenuation level compared to the one shown in the beginning of this section.

4.2 Bandpass Filters

Loop resonators have the bandpass characteristics when placed between the input and output feed lines. Among the various coupling techniques, the parallel coupling technique is used for analyzing the bandpass characteristics of the loop

resonator throughout the section. Figure 4.32 shows a closed square loop resonator placed in between two parallel coupled 50Ω open circuited transmission lines through a gap distance g .

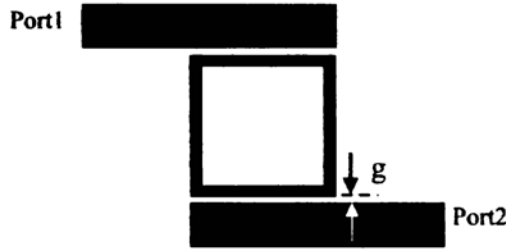


Fig.4.32 Square closed loop resonator coupled to input output feed lines

Resonance occurs when the standing waves are set up in the resonator; this happens when its perimeter is an integral multiple of the guided wavelength.

$$n\lambda_g = p_{av} \quad (4.12)$$

where λ_g is the guided wavelength, n is the mode number and p_{av} is the average perimeter of the closed loop.

For a microstrip loop, λ_g can be related to the frequency by

$$\lambda_g = \frac{\lambda}{\sqrt{\epsilon_{eff}}} = \frac{1}{\sqrt{\epsilon_{eff}}} \frac{c}{f}$$

where c is the speed of light and ϵ_{eff} is the effective dielectric constant. Equation (4.12) becomes

$$f = \frac{nc}{p_{av}\sqrt{\epsilon_{eff}}} \quad (4.13)$$

for $n=1,2,3,\dots$

The resonator in close conjunction with the input and output feed lines gives a very tight coupling due to which two resonant peaks appear around the designed resonant frequency. The coupling gap is an important parameter is the passband behavior of the loop resonator structure. It not only affects the performance of the resonator but also support the selective frequencies. A larger gap results in less field perturbation and greater losses. Here the square loop resonator of outer dimension $L \times W = 19 \times 19 \text{ mm}^2$ with a strip width of $t = 0.5 \text{ mm}$ is designed on a dielectric substrate of relative permittivity 4.4 and thickness $h = 1.6 \text{ mm}$. According to the design equation, the passband should appear at 2.47 GHz which is the calculated resonant frequency.

4.2.1 Bandpass characteristics of closed loop resonator

The structure is simulated in HFSS to study the effect of coupling. The S-parameter plots in Fig.4.33 depict the effect of coupling on the bandwidth and selectivity of the filter.

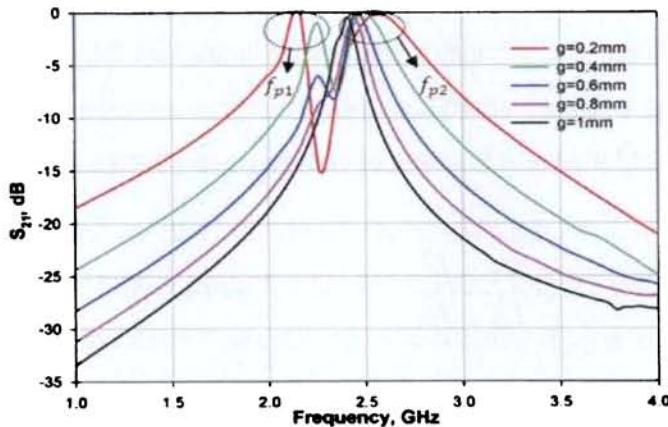


Fig. 4.33 Simulated S-parameters for the loop resonator placed at different coupling gaps.

The loop resonator considered as two half wavelength linear resonators connected in parallel. The current density plots of two resonant peaks f_{p1} and f_{p2} are shown in Fig. 4.34. The occurrence of two resonances can be attributed to the difference in path lengths of the fundamental mode of the closed loop resonator.

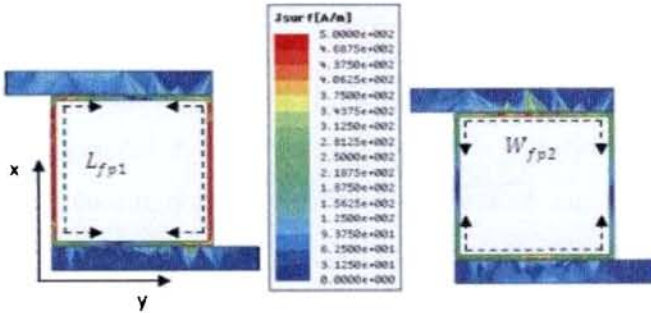


Fig.4.34 Current density plot at (a) $f_{p1} = 2.2GHz$ (b) $f_{p2} = 2.53GHz$

At f_{p1} , the intensity of the current vector is considerably larger on the portion of the resonator between the two feed lines along the side length L . Two symmetric half wavelength resonators are contributed by $L_{f_{p1}}$ about the x -axis. Whereas at f_{p2} , the two half wavelength resonators are formed by $W_{f_{p2}}$, symmetric about the y -axis. As coupling gap is increased, the two peaks get nearer to each other to resonate at the center frequency of the loop resonator, but with a larger loss for the peak at f_{p1} due to weak coupling. The coupling coefficient extracted from simulated results is shown in Fig. 4.35 where it is plotted as a function of coupling gap g by the relation given by,

$$k = \frac{f_{p2}^2 - f_{p1}^2}{f_{p2}^2 + f_{p1}^2} \quad (4.14)$$

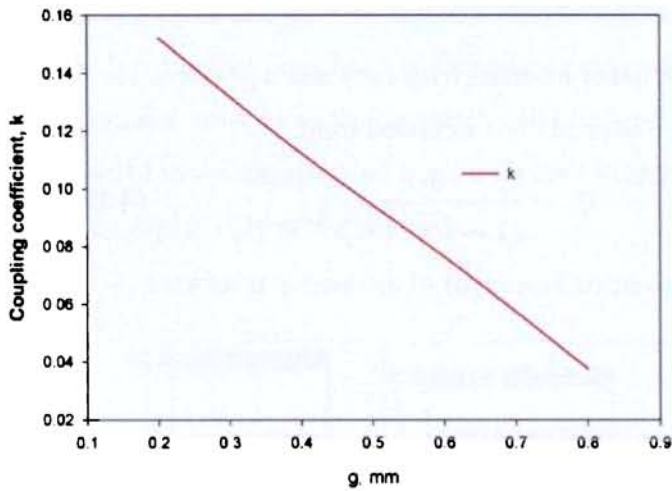


Fig. 4.35 Coupling coefficient for the structure in Fig. 4.34.

A figure of merit for resonator is the circuit Q-factor as defined by expression

$$Q = \frac{\omega_0 U}{P} \quad (4.15)$$

where ω_0 is the angular frequency, U is the stored energy per cycle, and P is the average power lost per cycle. The three main losses associated with the microstrip circuits are conductor losses, dielectric losses, and radiation losses. The total Q factor, Q_0 , can be expressed as

$$\frac{1}{Q_0} = \frac{1}{Q_c} + \frac{1}{Q_d} + \frac{1}{Q_r} \quad (4.16)$$

where Q_c , Q_d , and Q_r are the individual Q-values associated with the conductor, dielectric and radiation losses, respectively.

The unloaded Q, Q_0 , can also be determined by measuring the loaded Q-factor, Q_L , and the insertion loss of the loop at the resonance. The loaded Q of the resonator is

$$Q_L = \frac{\omega_0}{\omega_2 - \omega_1} \quad (4.17)$$

where ω_0 is the angular resonant frequency and $\omega_2 - \omega_1$ is the 3-dB bandwidth.

The unloaded Q- factor can be calculated from

$$Q_0 = \frac{Q_L}{(1 - 10^{-IL/20})} \quad (4.18)$$

where IL is the insertion loss in dB of the loop at resonance .

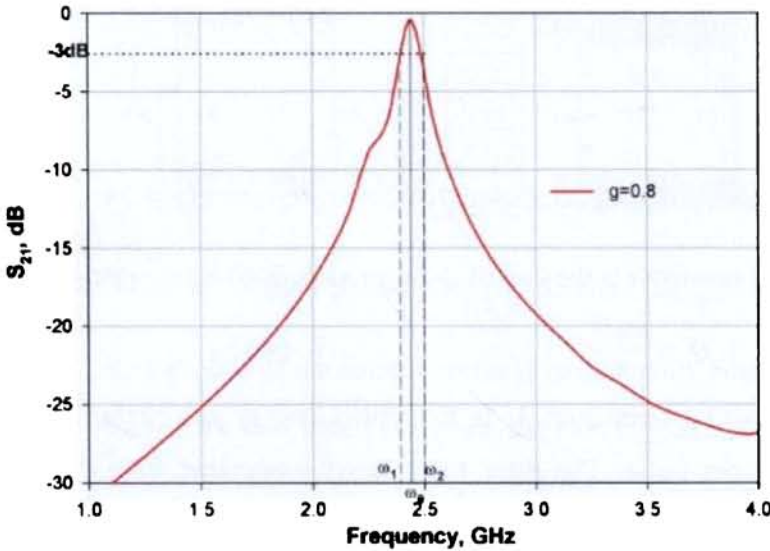


Fig.4.36 Resonator frequency response at $g=0.8\text{mm}$

An unloaded Q-factor of 518.79 is obtained from the frequency response of the square loop resonator parallel coupled to the feed lines when placed at a gap distance of $g=0.8\text{mm}$ shown in Fig. 4.36.

- **Effect of coupling length**

The effect of variation in coupling length of the loop resonator with the transmission line is studied by changing the configuration of the loop resonator maintaining the perimeter constant.

As it is evident from plots in Fig. 4.34 that the loop resonator when placed in close proximity with the input/output lines have two resonant peaks which are found to be due to either of the opposite arms. Here the asymmetry lies in the fact that, two arms along the side W are coupled to the transmission line throughout the length, whereas the arms along the side L are coupled only at the two ends.

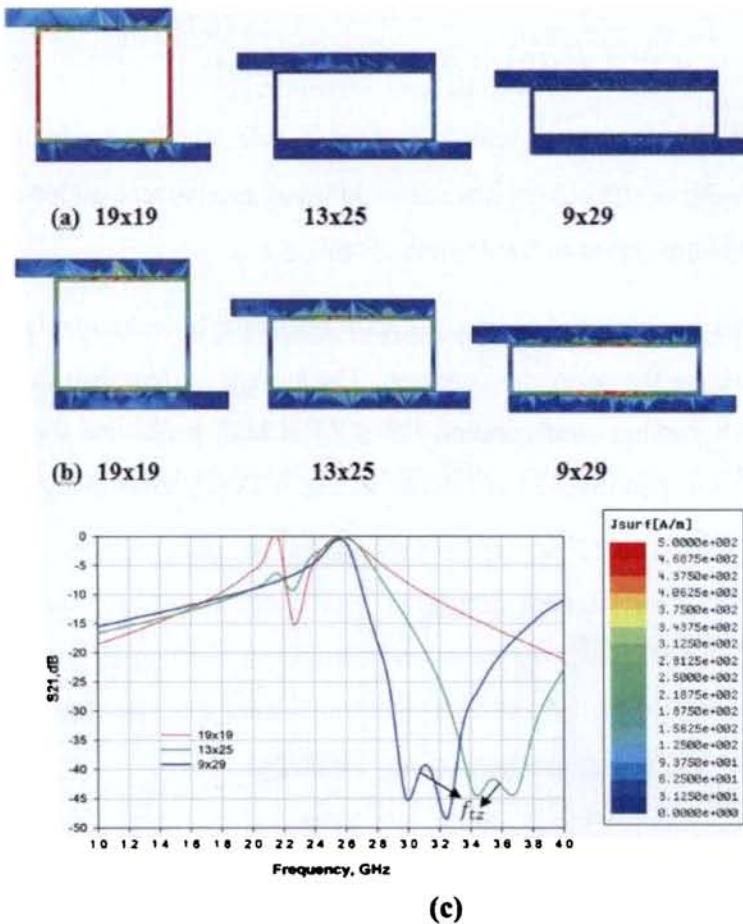


Fig. 4.37 Surface current distribution for varying $L \times W$ (a) at $f_{p1} = 2.17$ GHz (b) at $f_{p2} = 2.5$ GHz (c) corresponding S parameters

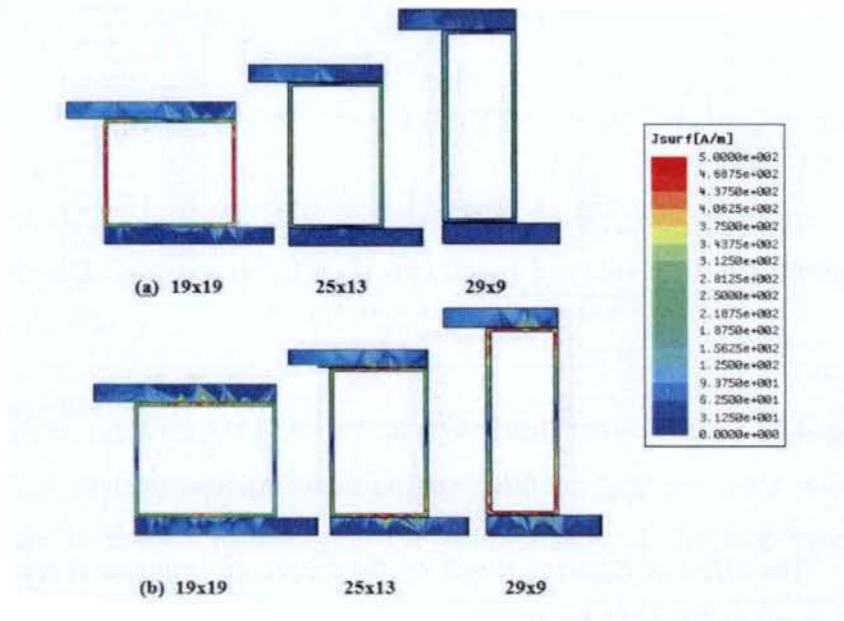
The effect of coupling length on the frequency response is studied for various configurations ($W \geq L$) by plotting the surface current distribution as shown in Fig.

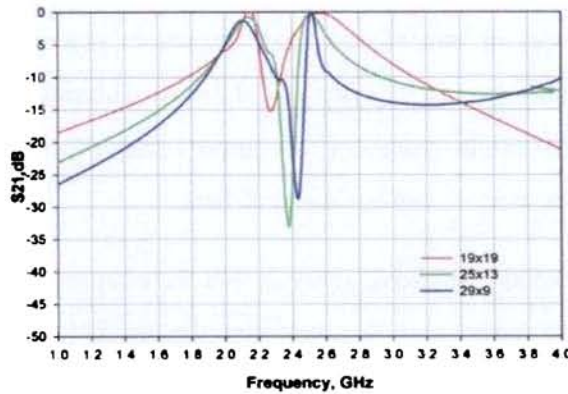
4.37 (a&b) at both peaks and its corresponding S21 are shown in Fig. 4.37 (c) respectively. It is clear from the plots that as the coupling length increases, the passband to stopband transition becomes sharper as the transmission zero at frequency corresponding to the half guided wavelength of the coupling length W shifts to the lower frequency.

$$f_{tz} = \frac{c}{2W\sqrt{\epsilon_{eff}}} \quad (4.19)$$

The peak at f_{p1} disappears with reduction in side length L which causes a decrease in the inductance offered by it and an additional capacitance added parallel to it when the two feed lines draws nearer to each other.

The study has been carried out for the loop resonator by reducing the coupling length W by maintaining the perimeter constant. The surface current distribution of the loop resonators with varying configuration ($W \leq L$) at both peaks are shown in Fig. 4.38 (a&b) and its corresponding S21 are shown in Fig. 4.38 (c) respectively.





(c)

Fig. 4.38 Surface current distribution for varying $L \times W$ (a) at $f_{p1} = 2.17\text{GHz}$ (b) at $f_{p2} = 2.5\text{GHz}$ (c) corresponding S parameters

In this case, the resonances corresponding to the two peaks are strongly coupled to the output feed for all the configurations.

- **Effect of number of closed loop resonators between the parallel coupled lines**

As discussed in the previous section, the closed loop resonator placed in between two parallel coupled lines produces passband with two peaks due to tight coupling and a gradual passband transitions. A conventional and well established approach to obtain steep passband transitions is by increasing the number of resonators.

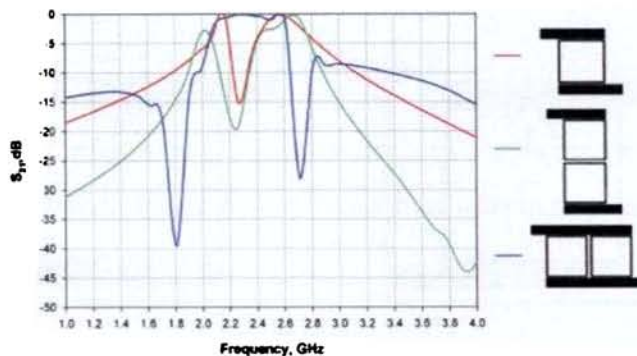


Fig.4.39 S-parameter comparison for parallel coupled closed loop resonators

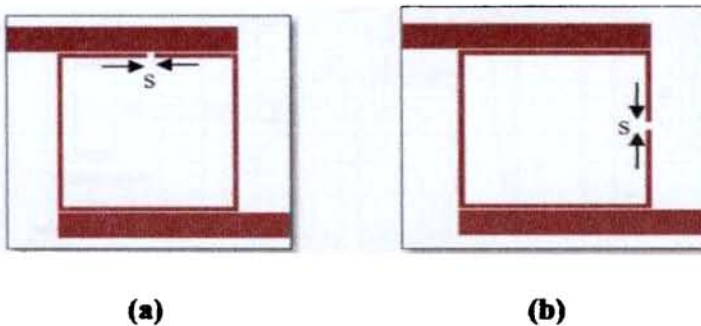
The S-parameters of two closed loop resonators placed between the parallel coupled lines with minimum coupling gap $g = 0.2mm$, is shown in Fig.4.39. Compared to the response of the single resonator, an improvement in passband-stopband and stopband - passband transitions, can be observed here.

It is evident from all the above analysis that the coupling efficiency between the feed lines and the resonator, and that between the resonators affects the passband characteristics and the Q-factor of the circuit. It is concluded from the studies so far, that the behavior of the side coupled closed loop resonator requires further modification for the production of band pass filter with improved transitions and good out of band rejection. Introducing proper breaks in the loop substantially improves the resonance characteristics, which is investigated in the next section.

4.2.2 Bandpass characteristics of open loop resonator

The previous section described a closed loop resonator parallel coupled to the input and output feed lines. In order to remove the dual peak in the passband, slits are introduced in either of the two arms of the closed loop to form two parallel coupled half wavelength open loop resonators.

The Fig. 4.40(a & b), illustrates open loop resonators with slits introduced along the side arms W and L respectively.



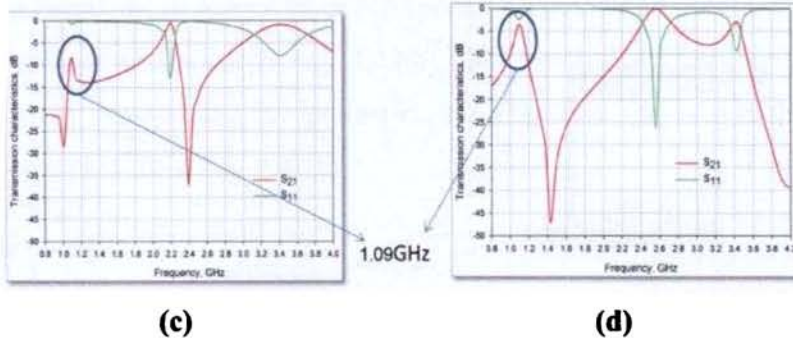


Fig. 4.40 Parallel coupled open loop resonator (a) slit along W (b) slit along L (c&d) Transmission characteristics of (a) & (b) respectively.

The simulation results in Fig. 4.40(c & d) portray the transmission characteristics with the resonance at lower frequency which is nearly half the resonance of the closed loop. These resonances at lower frequencies are inappropriate for the development of a bandpass filter due to its large insertion loss and poor out of band rejection.

- **Bandpass characteristics of parallel coupled hairpin resonators**

In this section investigations are carried out by introducing proper breaks in the maximum field points of the closed loop resonator to suppress the corresponding peak and maintain the required peak.

- ❖ **Slit along W**

The schematic of square loop resonator with two slits($s=0.2\text{mm}$) introduced along the side arm length W to form two parallel coupled hairpin resonators is shown in Fig. 4.41.

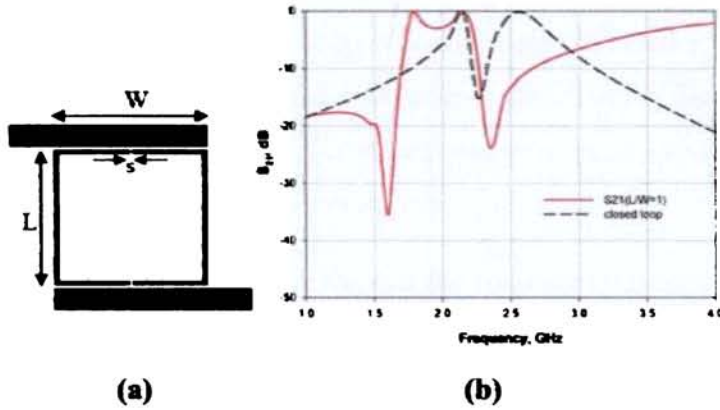


Fig.4.41 (a) Layout of parallel coupled hairpin resonators (slits in W arm of closed loop resonator) **(b)** Corresponding S-parameters

The simulation results are obtained with the aid of Ansoft HFSS and are shown in Fig. 4.41(b). A passband can be seen centered around the frequency f_{p1} . Whereas the peak at f_{p2} disappears due to the break at the maximum field point at f_{p2} . Again a dual band nature is found due to the close coupling between the two half wavelength resonators.

• **Effect of coupling length**

The passband response is studied by varying L/W ratio of the resonator by maintaining the perimeter constant.

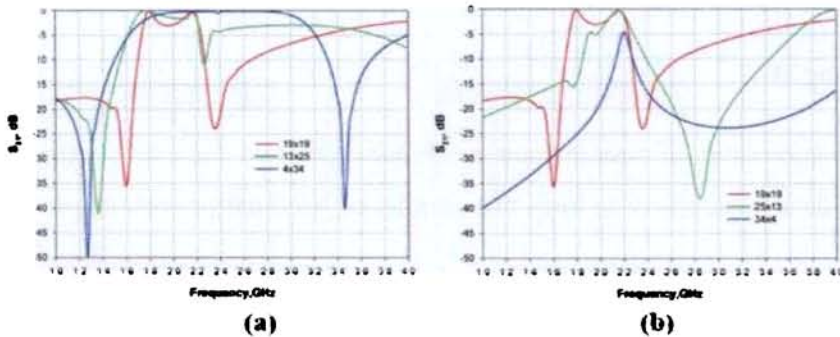


Fig. 4.42 Effect of varying coupling length W (a) increasing W (b) decreasing W

The plots in Fig.4.42 depict the variation in S_{21} for different coupling length. As the coupling length W is increased, the response becomes comparable to that of a wide bandpass filter as shown in Fig. 4.42(a). Whereas, when the coupling length W is decreased by maintaining the perimeter, the response approaches the behavior of a narrow bandpass filter Fig. 4.42(b).

❖ Slits along L

Introducing a pair of slit in the opposite arms i.e., at maximum field points at f_{p1} , as shown in Fig. 4.43(a), produces a passband around f_{p2} suppressing the peak at f_{p1} (Fig. 4.43(b)). This configuration becomes equivalent to two coupled hairpin resonators.

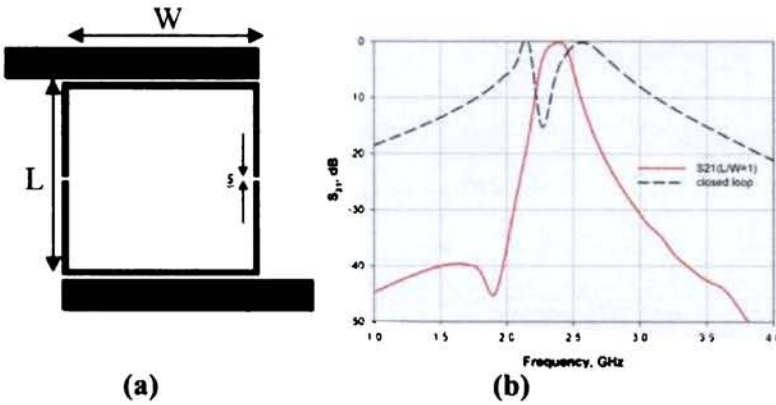


Fig. 4.43 (a) Layout of closed loop resonator with slits along L **(b)** Corresponding S -parameters

Here a single resonance at the resonant frequency of the two parallel coupled half wave length resonators is observed with a transmission zero at the lower frequency due to the introduction of slit, which is an advantage over the closed loop resonator.

• Effect of coupling length

Varying the coupling length of this type of coupled resonators yields single passband with a comparatively narrow bandpass filter response. The behavior of the passband response is studied by varying L/W of the resonator by maintaining the perimeter constant.

The plots in Fig.4.44(a) depicts the comparison of $LxW = 19x19mm^2$ with $LxW = 13x25mm^2$ and $LxW = 4x34mm^2$. From the S parameters plotted in Fig.4.44 for different configurations, it is observed that a single passband with transmission zeros at lower and higher frequencies appear for both increase and decrease of coupling length W by maintaining the perimeter.

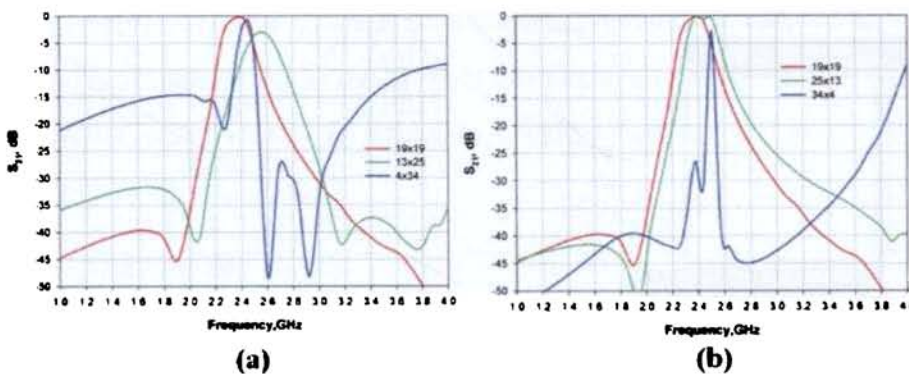


Fig. 4.44 Effect of coupling length (a) Increasing W (b) decreasing W

From the analysis of the above results, it is established that the introduction of discontinuity in the appropriate position in the closed loop resonator can suppress the undesired modes. Also it is clear that coupling length is an important parameter deciding the filter response including the bandwidth, out of band rejection and insertion loss. Hence, this configuration is selected for further study for the design of a moderate band pass filter with good out of band rejection.

4.2.3 Bandpass filter: Slits along L ($L < W$)

As it was found earlier, it is possible to obtain a narrow bandpass filter response with two parallel coupled half wavelength resonators (slits along side arm L) closely coupled to the input and output feedlines. The width of the passband is determined by the occurrence of transmission zeros on either side of the passband. The proposed filter is designed to operate at 2.4 GHz and the parameters of the filter are $p_{av} = 76mm$, $t = 1mm$, $s = 0.2mm$ and $g = 0.2mm$ on an FR4 epoxy substrate of $\epsilon_r = 4.4$ and $h = 1.6mm$. The simulation results comparing the responses of configurations (Fig 4.45(a)) with increase in W maintaining the perimeter is shown in Fig. 4.45(b).

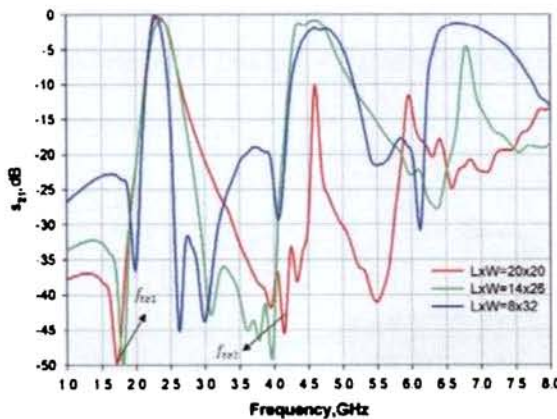
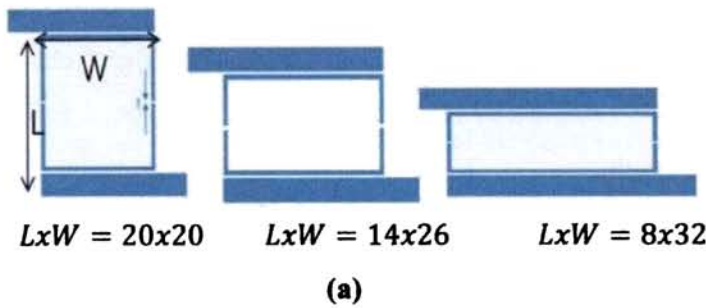


Fig. 4.45 (a) Layouts for different configurations

($LxW = 20x20$, $LxW = 14x26$ and $LxW = 8x32$) (b) corresponding S parameters

It is clearly seen from Fig.4.45 (b) that larger is the value of W , narrower is the bandwidth. The upper transmission zero decreases with the increase in W , which can be computed as a function of coupling length.

$$f_{tz2} = \frac{c}{2W\sqrt{\epsilon_{eff}}} \quad (4.20)$$

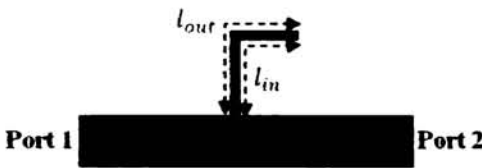
With the improvement in the passband response, the drawback arises in the occurrence of higher harmonics.

- **Higher harmonics suppression**

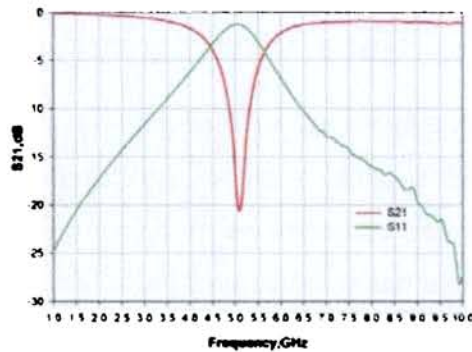
The traditional approach to suppress the harmonics is to integrate lowpass or bandstop filter to the bandpass filter. For this a simple design technique to remove the second harmonics is achieved by integrating the input and output feed lines with quarter wavelength open stub.

- **Quarter wavelength open stub bandstop filter**

The schematic of the quarter wavelength L-stub designed to resonate at 5GHz on a FR4 substrate of permittivity $\epsilon_r = 4.4$ and thickness $h = 1.6mm$ is shown in Fig. 4.46(a).



(a)



(b)

Fig.4.46 Narrow bandstop filter (a) L-shaped resonator (9mm) (b) Simulated transmission characteristics.

The response of the unit cell of the L-type resonator is shown in Fig.4.46 (b) whose resonant frequency is obtained from the relation,

$$l_{av} = \frac{(2n + 1)\lambda_g}{4} \quad (4.21)$$

where, l_{av} is the mean of the inner and outer lengths of the L-resonator, λ_g is the guide wavelength in the microstrip line at the center frequency and n is the mode number.

$$l_{av} = \frac{l_{out} + l_{in}}{2} \quad (4.22)$$

An electromagnetic simulation in Ansoft HFSS is performed to investigate the behavior of the proposed filter. The bandwidth of the filter can be improved by increasing the number of resonators at the expense of the circuit size.

Figure 4.47 (a) shows the layout of the bandstop filter which uses 2 pairs of L-shaped resonators designed to resonate at two nearby frequencies to improve the rejection bandwidth. The dimensions of filter in BRF I are $l_{out} = 8mm, l_{in} = 7mm$ and $D_1 = 2mm$ and that in BRF II are $l_{out} = 9mm, l_{in} = 8mm$ and separation $D_2 = 2mm$.

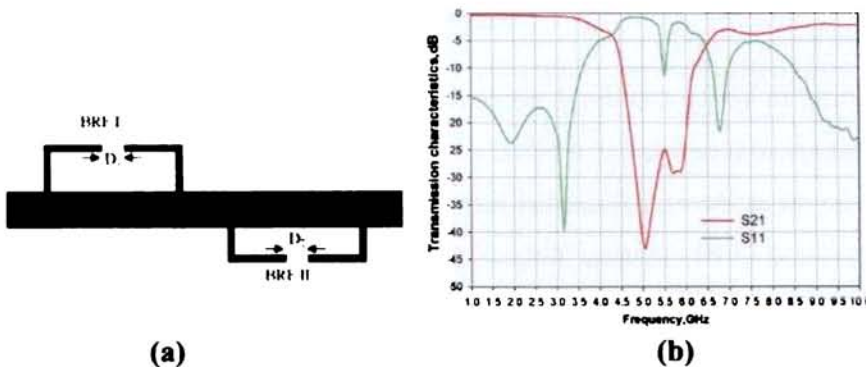


Fig. 4.47 (a) Schematic of the bandstop filter (b) Simulated transmission characteristics

The filter is fabricated on an FR4 substrate of $\epsilon_r = 4.4$ and thickness 1.6mm. It is designed to reject a wide band centred at 5.5 GHz. The response of the band rejection filter optimized to reject the second harmonics of the bandpass filter is shown in Fig.4.47 (b).

- **Bandpass filter with harmonics suppression**

The layout of the bandpass filter with second harmonics removed using above proposed bandstop filter is shown in Fig.4.48(a). The simulated frequency response is shown in Fig. 4.48(b).

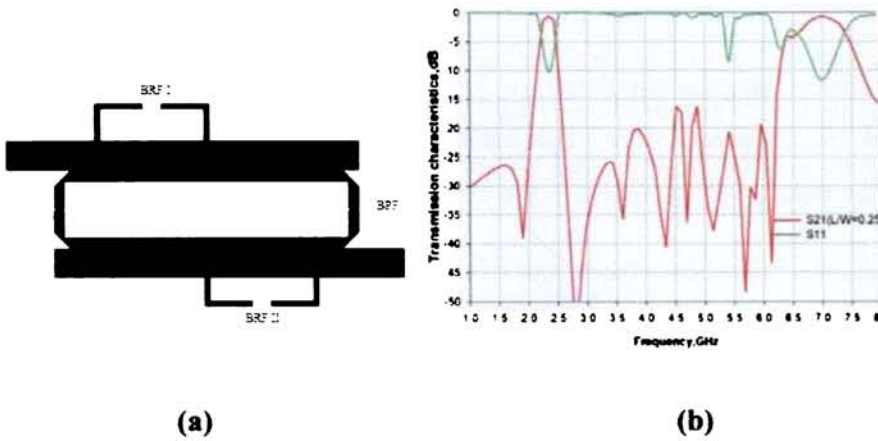
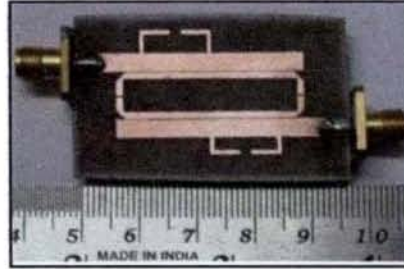


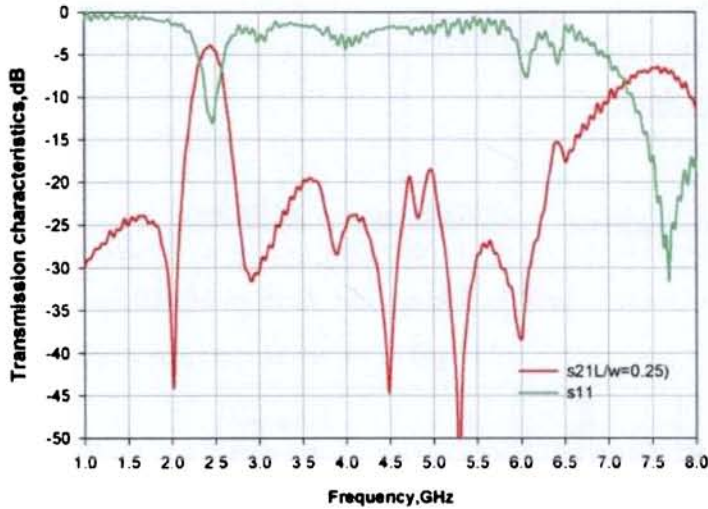
Fig. 4.48 (a) Schematic of the proposed bandpass filter **(b)** Simulated frequency response.

In order to verify the above predictions, a prototype of parallel coupled hairpin resonator bandpass filter has been fabricated on FR4 substrate. The corners of the loop resonators are mitred to minimize the loss due to radiation, and optimized to produce a narrow pass band at its resonant frequency and the L-resonators arranged suitably to produce wide band rejection to suppress the spurious harmonics. Photograph of the fabricated prototype is shown in Fig. 4.49(a). Transmission and reflection

characteristics are measured using Agilent E8362B Precision Network Analyzer and the result is presented in Fig. 4.49(b).



(a)



(b)

Fig. 4.49(a) Photograph (b) Measured transmission coefficient

A -10dB bandwidth of 370MHz and a good out of band suppression is observed for the filter. It is a moderate band filter with a fractional bandwidth of 15%. The insertion loss and the return loss are 3.9dB and 13dB respectively. The suppression of the spurious harmonics is more than 20 dB. The size of the filter is $45 \times 30 \text{mm}^2$.

4.2.4 Bandpass filter: Slits along L ($L > W$)

Based on the design in Fig.4.44 (b) narrow bandpass response can also be achieved by decreasing the coupling length W maintaining the perimeter. The average perimeter of the parallel coupled hairpin resonator is chosen to resonate at 2.7GHz fabricated on a RT Duroid substrate of permittivity 3.2 and thickness 1.6mm. The parameters of the filter are $t = 0.5mm$, $s = 0.5mm$ and $g = 0.2mm$. The simulation results comparing the responses of configurations (Fig 4.50(a)) with different L/W ratios is shown in Fig. 4.50(b).

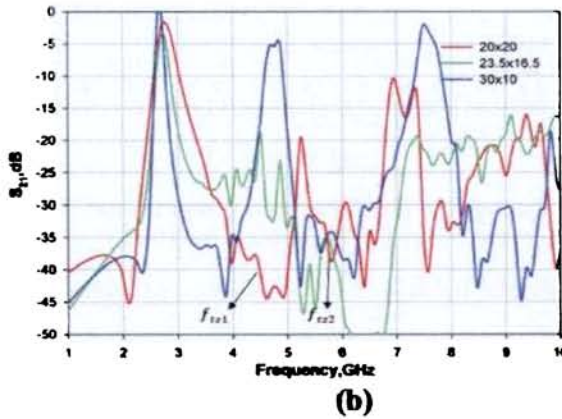
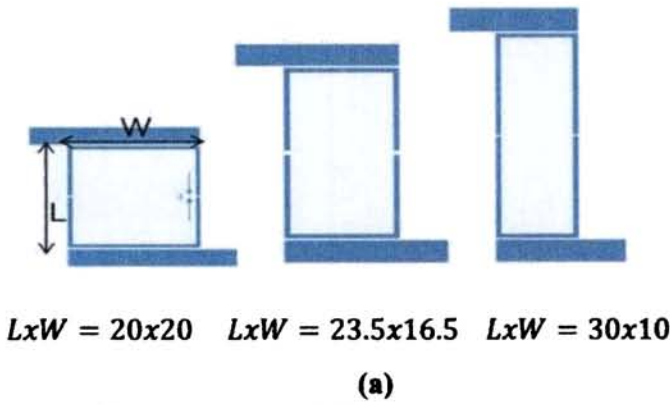


Fig. 4.50 (a) Layout of different configurations ($L \times W = 20 \times 20$, $L \times W = 23.5 \times 16.5$ and $L \times W = 30 \times 10$) **(b)** Simulated frequency response

It is clear from the plot shown in Fig.4.50 that depending on the configuration of the resonant cell, the resonant frequency remains unchanged with a reduction in bandwidth and elimination of higher harmonics.

The reduction in bandwidth is due to the shift of transmission zero t_{z1} towards the lower frequency with increase in L . The analytical expression for the transmission zero, f_{tz1} , can be computed as a function of side arm length L as,

$$f_{tz1} = \frac{c}{2L\sqrt{\epsilon_{eff}}} \quad (4.23)$$

The transmission zero created by the coupling length W , f_{tz2} , is given by

$$f_{tz2} = \frac{c}{2W\sqrt{\epsilon_{eff}}} \quad (4.24)$$

The configuration of the proposed filter is optimized to produce a single passband at its resonant frequency by suppressing the higher spurious harmonics. The simulated frequency response is shown in Fig. 4.51.

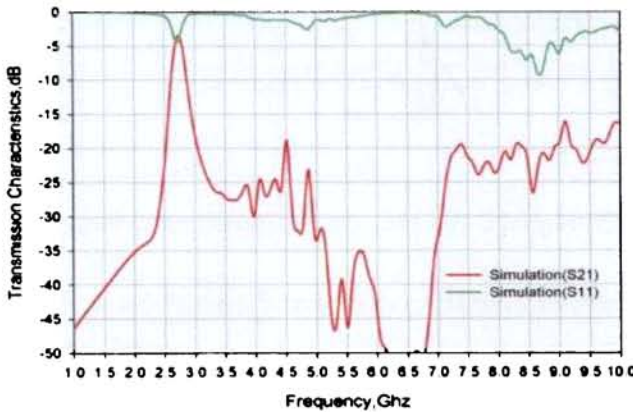
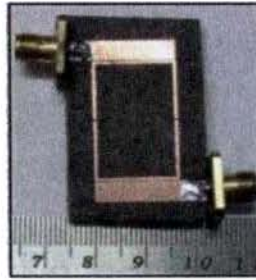


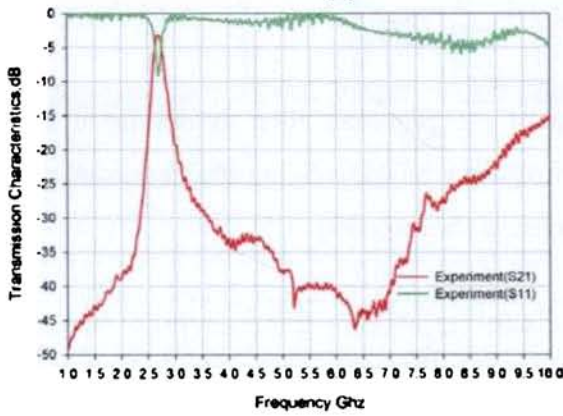
Fig. 4.51 Simulated frequency response for $L \times W = 23.5 \times 16.5 \text{ mm}^2$.

Chapter 4

The photograph of the prototype fabricated on RT Duroid substrate (with $\epsilon_r = 3.2$, substrate height $h=1.6\text{mm}$ and loss tangent of 0.0009), is shown in Fig. 4.52(a). The performance of the filter was experimentally verified using Agilent HP8510c Network analyzer. The measured results are given in Fig. 4.52(b).



(a)



(b)

Fig.4.52 (a) Photograph (b) Measured transmission characteristics

A bandwidth of about 260MHz (-10dB) and a good out of band suppression is observed for the filter. It presents a moderate band with a FBW of 9.6%. The insertion loss and the return loss are 3dB and 8dB respectively. The suppression of the spurious harmonics is more than 20 dB. The size of the filter is $40 \times 25 \text{mm}^2$.

4.3 Compact Bandpass Filter Using Folded Loop Resonator

In this section a compact loop resonator bandpass filter with a good rejection in the stopband is proposed. The technique adopted here to reduce the size is to fold the resonator without affecting its resonant frequency. Apart from reducing size the folding results in the generation of anti resonant modes which could be excited by introducing a slit in the loop. The method adopted to suppress the higher order harmonics is to adjust the length of coupling between the resonator and the transmission line to produce transmission zeroes at $2f_0$ and $3f_0$. The magnetic coupling between the feed lines and folded resonators allow the transmission of the signal from input to output at the resonant frequency. The coupling gap g between the feed line and the resonator is kept small to minimize the insertion loss and increase the Q .

4.3.1 Folded loop resonator

Folded loop resonators are compact structures obtained by folding the closed loop resonator as shown in the Fig.4.53 without affecting the average perimeter of the loop.

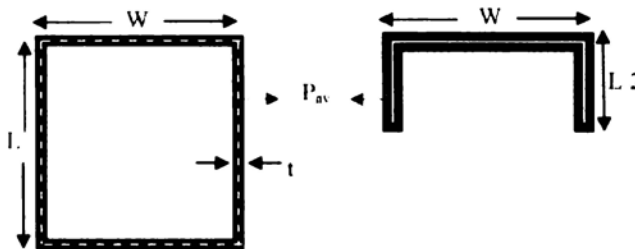


Fig.4.53 Folded closed loop from conventional closed loop resonator

The new filter structure shown in Fig.4.54 has two folded closed loop resonators of same average perimeter as that of the square closed loop and arranged in such a way that they have the same outer perimeter as that of a single square closed loop. The metal

width t ($=0.5\text{mm}$) and the gap distance d ($=0.2\text{mm}$), are kept small to get a narrow passband.

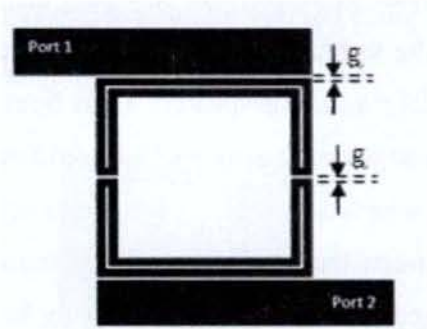


Fig.4.54 Folded loop resonator filter

In order to understand the basic phenomenon underlying the operation of this folded loop, the frequency response (Fig.4.55) is plotted and field configuration for different modes is examined.

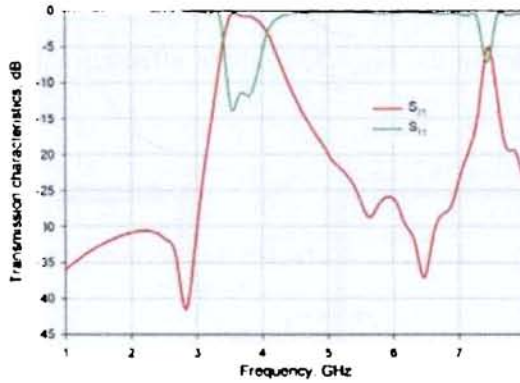


Fig.4.55 Simulated transmission characteristics of folded loop resonator

As can be seen from the plot, modified structure resonates at the same frequency as that of the conventional square loop resonator with a second resonance at twice the resonant frequency. Consequently the same design equation of the closed loop resonator may be used. The magnitude of E field distribution at the two resonant modes is shown in Fig.4.56.

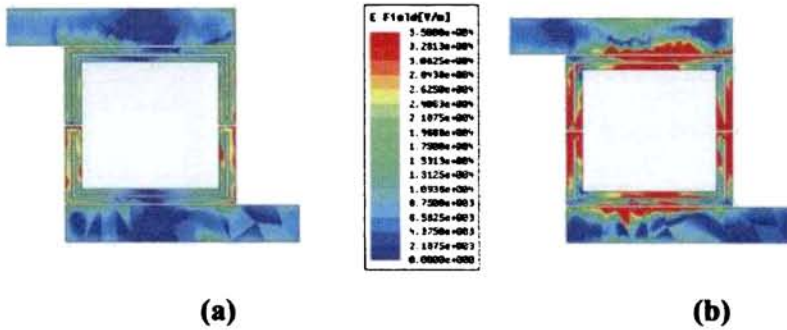


Fig.4.56 E field distribution at (a) 3.8GHz (b) 7.5GHz

The plot in Fig.4.56(a) shows a full wave variation within each folded closed loop and that in Fig.4.56(b) consists of two full waves confined in each of the loops indicating the higher mode ($n=2$). The Fig.4.57 shows the corresponding phase plots of the above filter.

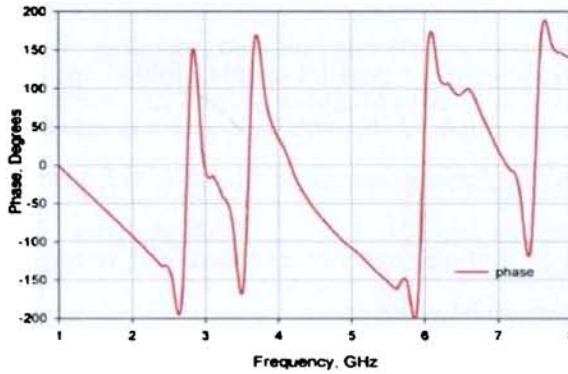


Fig.4.57 Phase plot for folded loop filter

As can be seen from the plot, there are abrupt phase change at four frequencies indicating possibility of four resonances. However, there are only two resonances observed in Fig.4.55. The frequencies which are absent in the plot in Fig.4.55 (i.e., around 2.6GHz and 6GHz) are the anti resonant frequencies that are blocked by the folded loop resonator. These frequencies can be excited by forced boundary conditions

such as opening or shorting the loop. The open boundary condition is obtained by introducing a slit in the loop.

4.3.2 Compact folded open loop resonator filter

Folded open loop resonator is obtained by introducing a slit in the folded closed loop resonator at the center of the folded arm parallel to the coupling length W as shown in Fig. 4.58.

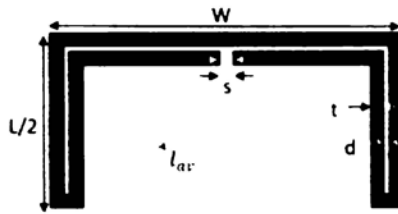


Fig.4.58 Layout of the folded open loop resonator.

The frequency response of the parallel coupled folded open loop resonator filter (Fig. 4.59a) is shown in the Fig.4.59 (b) which depicts a passband at 2.53GHz which was blocked by the folded closed loop resonator.

From the above predictions and observations, the resonant frequency of the folded open loop resonator can be given as

$$f_0 \approx \frac{n + 1}{3} \left(\frac{c}{l_{av} \sqrt{\epsilon_{eff}}} \right) \quad (4.25)$$

$$\text{for } n = 1, 3, 5 \dots$$

where c is the velocity of light in free space, n is the mode number, ϵ_{eff} is the effective permittivity of the substrate given by,

$$\epsilon_{eff} = \frac{\epsilon_r + 1}{2}$$

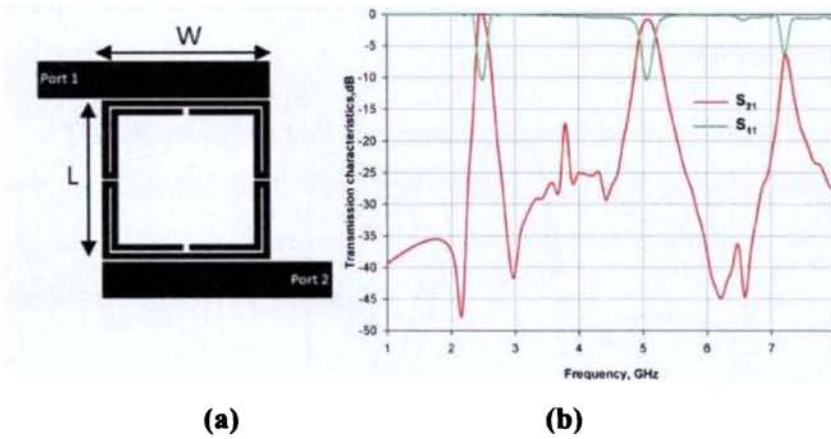


Fig. 4.59 (a) Bandpass filter employing folded open loop resonators ($L \times W = 13 \times 13 \text{ mm}^2$) (b) Simulated transmission characteristics

From these equations, the resonant frequencies for different modes can be calculated. It is evident from the plot that the resonance at 3.8GHz and 6.5GHz are suppressed which are the modes corresponding to mode number $n=2$ and $n=4$.

The relation in (4.25) is validated by designing the filter on different dielectric substrates for resonant frequencies 1, 2 and 4GHz and compared with the simulated frequency in Table 4.2.

| f_{cal} (GHz) | $\epsilon_r = 2.2$ | | $\epsilon_r = 4.4$ | | $\epsilon_r = 10.2$ | |
|--------------------|--------------------|-----------------|--------------------|-----------------|---------------------|-----------------|
| | l_{av} (mm) | f_{sim} (GHz) | l_{av} (mm) | f_{sim} (GHz) | l_{av} (mm) | f_{sim} (GHz) |
| 1 | 159 | 1.04 | 122 | 1.0 | 85 | 1.0 |
| 2 | 79 | 2.06 | 61 | 2.0 | 42.6 | 2.06 |
| 3 | 40 | 4.08 | 30.5 | 4.0 | 21.3 | 4 |

Table 4.2 Comparison of calculated and simulated frequencies

- **Effect of slit width**

The effect of slit width on the resonant frequency has been studied by simulating the structure with varying s . The plot in Fig.4.60 depicts very little effect in the

passband frequency with the slit width variation and thus can be considered for fine tuning of the filter response.

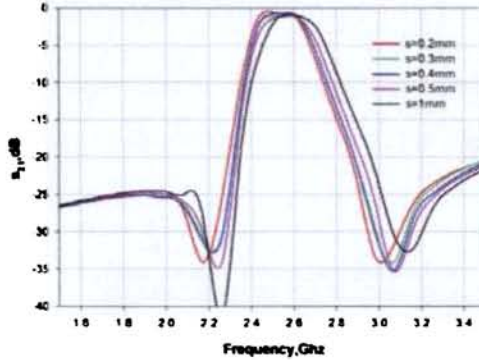


Fig. 4.60 Simulation results for filter with varying slit width

While the configuration is compact and has sharper roll-off than the parallel coupled conventional closed resonator filters, it suffers from the spurious responses which can be suppressed by altering the length of coupling between the microstrip and the folded resonator.

- **Effect of coupling length: Harmonics suppression**

Increasing the side arm length of the folded U resonator along with the input coupling microstrip line, l_{t1} being longer than $\lambda_g/4$, the passband will be almost unchanged, moving the inherent transmission zero f_{tz} to frequency lower than $2f_0$ eliminating the second harmonics.

$$W \approx l_{t1} > \frac{\lambda_g}{4} \quad (4.25)$$

where guide wavelength λ_g is,

$$\lambda_g = \frac{\lambda}{\sqrt{\epsilon_{eff}}}$$

For second harmonics suppression, l_{t1} is also approximately equal to half guide wavelength at $2f_0$.

The characteristics of the proposed filter with different coupling lengths are shown in Fig.4.61. It is worth noticing that as the coupling length, ($W = 20\text{mm}$ ($> \lambda_g/2$ at $2f_0$)), is increased, the transmission zero shifts to the lower frequency removing the second harmonics.

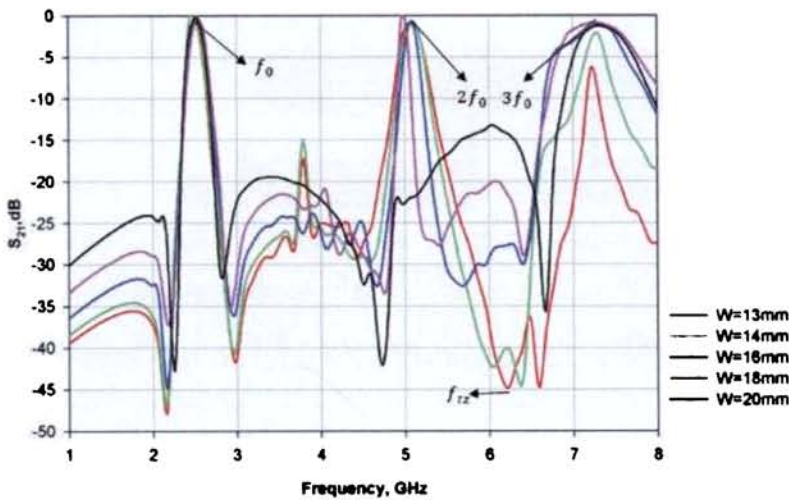


Fig. 4.61 Simulated transmission characteristics for different values of W .

To compare the field distribution of the two configurations with and without second harmonics, the E field distribution plot have been obtained for the $W=13\text{mm}$ and $W=20\text{mm}$ at 2.53GHz and 5.23GHz . They are shown in Fig. 4.62.

The plot in (Fig.4.62 (a)) shows propagation in both the first and second harmonics, whereas the lower figure depicts clearly the absence of field concentration in the loop resonator and the output feed line. That is, the loop resonator is electromagnetically invisible since they exhibit no field density, and thus coupling zero fields to the output port.

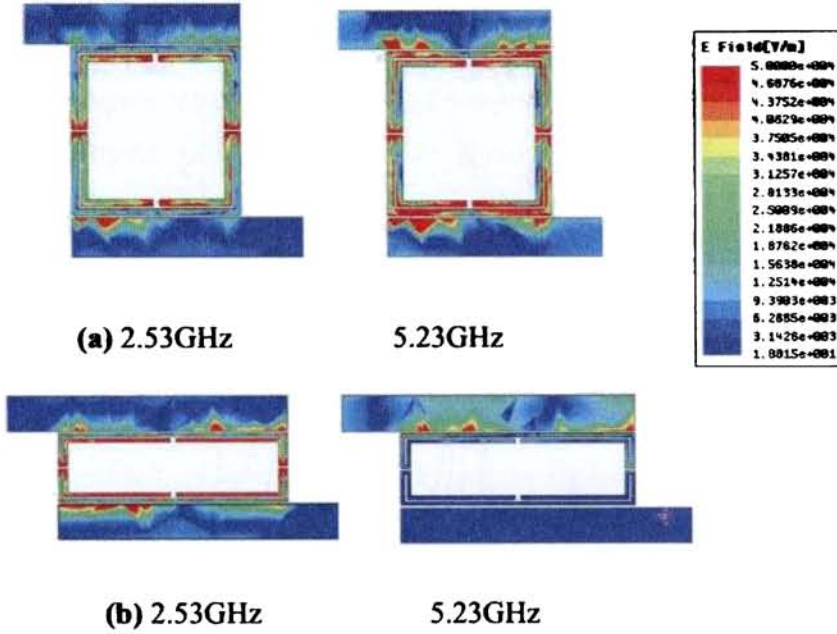


Fig. 4.62 E-field distribution at 2.53GHZ and 5.23GHZ for (a) $W=13\text{mm}$ (b) $W=20\text{mm}$

The next higher harmonics rejection is accomplished when the coupling length of the microstrip line in the lower part l_{t2} of the resonator is shorter than $\lambda_g/4$ or when approximately equal to half guide wavelength at $3f_0$. The coupling length of the output microstrip line l_{t2} is

$$l_{t2} \approx \frac{2}{3} \left(\frac{\lambda_g}{4} \right) \tag{4.26}$$

Figure 4.63(a) shows the schematic of the bandpass filter based on the above design which is simulated using Ansoft HFSS. The results of EM simulation are shown in Fig. 4.63(b).

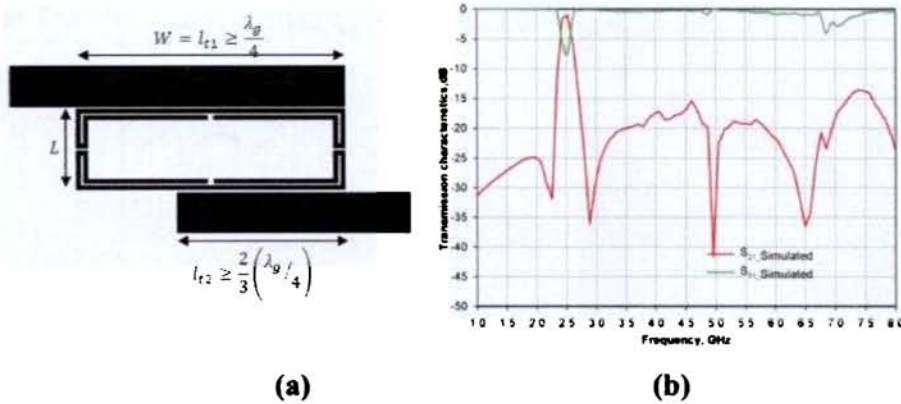


Fig. 4.63 (a) Layout of the proposed filter ($2W \times L = 20 \times 6$, $g = d = 0.2 \text{ mm}$, $s = 0.5 \text{ mm}$, $t = 0.5 \text{ mm}$) **(b)** Simulated transmission characteristics of the prototype filter.

The field distribution plots at 2.53, 5.23 and 7.48 GHz have been simulated to verify the effect of coupling length of the input and output feed lines which produces transmission zeros at their corresponding resonant frequencies. The field distribution in loop resonators of Fig.4.64 (b & c) are not illuminated confirming the absence of field distribution and propagation.

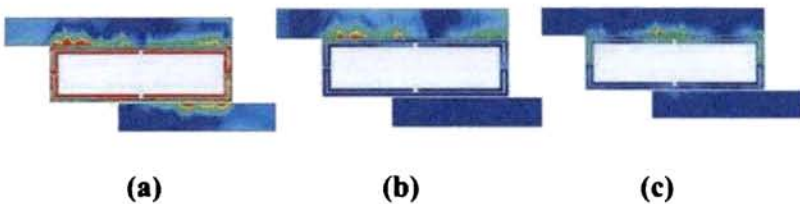


Fig. 4.64 E field distribution at frequencies **(a)** 2.53GHz **(b)** 5.23 GHz **(c)** 7.48 GHz

In order to verify the theoretical predictions, the filter is designed and optimized to operate at 2.5GHz, fabricated on FR4 substrate ($\epsilon_r = 4.4$, $h = 1.6 \text{ mm}$) is shown in Fig.4.65.

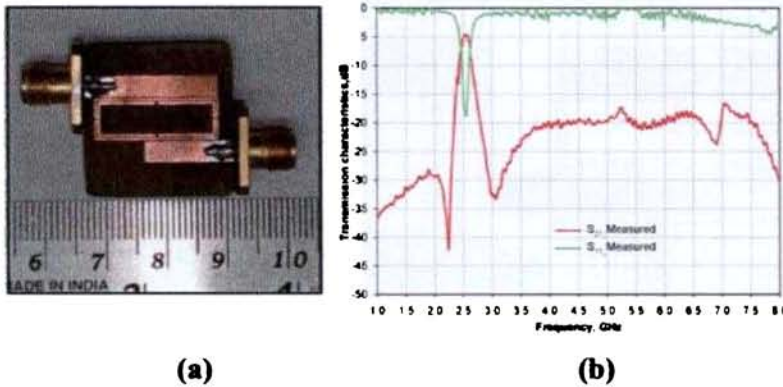


Fig. 4.65 (a) Photograph of the proposed filter (b) Measured transmission characteristics.

The occupied area (without considering the feed lines) is only $0.17 \lambda_0 \times 0.05 \lambda_0$ (λ_0 is the free space wavelength at operating frequency). The performance of the filter is experimentally verified using HP8510c Network analyzer. A passband (-10dB) of about 230MHz with good out of band suppression is obtained.

Good agreement is seen between simulated and measured results (Fig. 4.65), with a clear rejection of propagation in the vicinity of two harmonic frequencies. A -10 dB band width of 230MHz is observed with a FBW of 9% which characterizes the filter as moderate band filter. Around the center frequency of 2.53GHz, the measured insertion loss and the return loss are approximately 4.56dB and 20dB respectively; the high value of insertion loss can be attributed mainly to the dielectric losses and fabrication error as the simulation results show only 0.95dB on a loss less substrate. The suppression of the spurious harmonics is around 20dB.

- **Effect of variable capacitance at the slit**

The passband frequency of the folded loop resonator filter can be tuned by connecting a variable capacitance across the slit s. This was verified by simulation using different capacitance values across the slit and the results are shown in Fig 4.66. It is

seen that the resonant frequency can be controlled in a wide range by varying the capacitance.

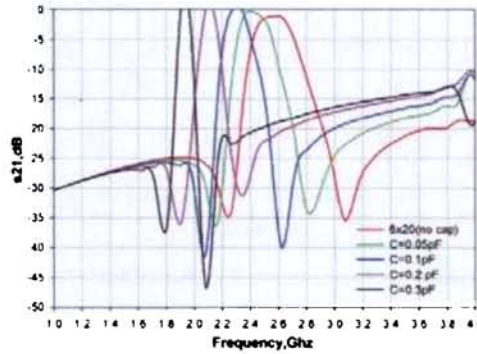


Fig. 4.66 Frequency response of the filter with varying capacitor between the slits

- **Application: Diplexer**

A diplexer can be built by introducing another folded loop resonator parallel coupled to the other side of the input microstrip line as shown in the layout of Fig.4.67.

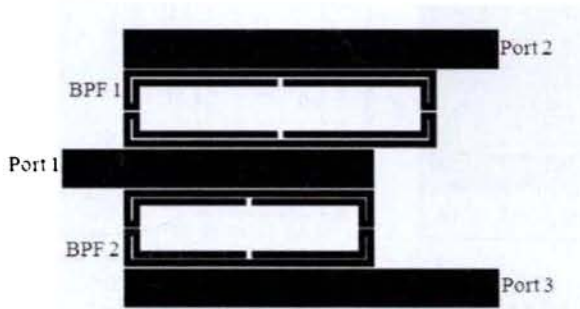


Fig. 4.67 Diplexer using folded open loop filter

The BPF 1 in Fig. 4.3.16 was designed to resonate at 2GHz and BPF2 at 2.5GHz. The simulation results of the diplexer fabricated on a lossless substrate is shown in Fig.4.68.

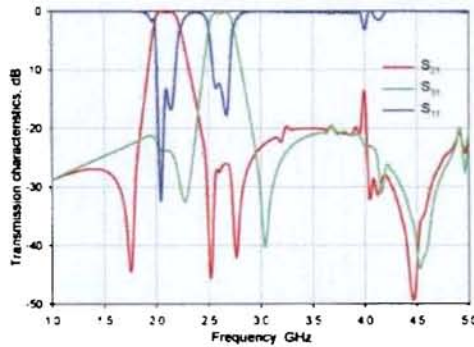


Fig. 4.68 Simulated Transmission characteristics of diplexer

The device has been experimentally tested on a loss FR4 substrate of $\epsilon_r = 4.4$ of thickness 1.6mm having a loss tangent of 0.02. The photograph of the fabricated prototype and the measured results are shown in Fig.4.69. The measured insertion loss is of the order of 3.8dB and 4.5 dB, with a return loss of -35dB and -25 dB for Band I and Band II respectively.

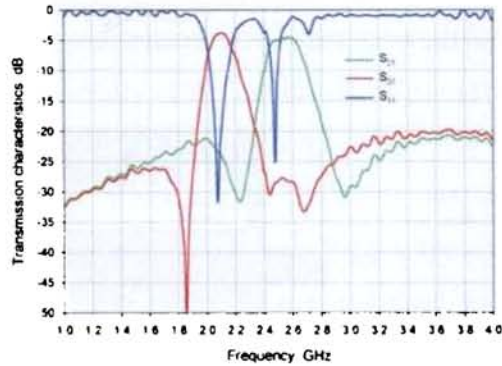
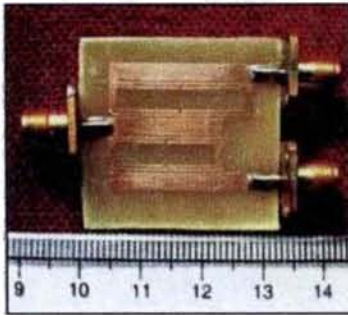


Fig. 4.69 Measured Transmission characteristics of diplexer

4.4 Conclusion

Simple and compact microstrip bandstop filter and bandpass filters are designed and implemented. It is demonstrated that the filters can be tuned electronically by embedding varactor diode in the slit. The filters are very compact and fully planar

therefore it can be easily fabricated using planar circuit technologies like mechanical and photo etching techniques. Empirical formulas are derived for the resonant frequency and for harmonics suppression. The compactness and tunability make this design attractive for printed circuit boards and monolithic microwave integrated circuit technologies.

SRR BASED MICROSTRIP BANDSTOP FILTER

© 2011 by CRC Press, Inc.

ISBN 978-1-4200-8888-8

In this section the propagation characteristics of a microstrip line loaded with an array of SRR as superstrate are investigated. The presence of SRRs over the microstrip line leads to rejection of a narrow band in the vicinity of its resonant frequency. The width and attenuation of the rejected frequency band depends on the height of the superstrate as well as its relative position with respect to the microstrip line.

5.1 Introduction

The split ring resonators (SRRs) have been used in planar circuit technology for the design of novel printed microwave components; particularly in band reject filters. SRRs would be excited by a time varying magnetic field with significant component parallel to the ring axis. Therefore, in microstrip configurations, SRRs have to be etched at the top metal level, in close proximity to the central strip to guarantee efficient magnetic coupling, while in the CPW structures they must be etched underneath the slots (Martin et.al, 2003). SRR particles coupled to the conventional microstrip line where the excitation is by the H-field generated by the line have been investigated by Falcone,(Chap. 5, pp.102-104, 2005). The SRR structure when etched on the same plane of the microstrip line limits the performance due to inefficient magnetic coupling resulting in low stop band attenuation. A more efficient way of coupling is to load the microstrip line with substrate containing SRR array with reduced number of unit cells.

In this section the SRR array as superstrate for bandstop filter application is described. This method also enables the selection of different structures and designs according to the frequency requirements. The variation in coupling strength with the thickness of the superstrate as well as the lateral position of the SRR array from the microstrip line is studied. At the resonant frequency of these particles, due to the electromagnetic coupling between the transmission line and the SRRs, current loops are generated on them and the signal propagation is inhibited.

- **Split ring resonator(SRR)**

SRRs are planar structures with two concentric conducting rings with slits etched on opposite sides (Fig.5.1). It can be considered as an externally driven LC circuit with a resonant frequency that can be tuned by varying the dimensions.

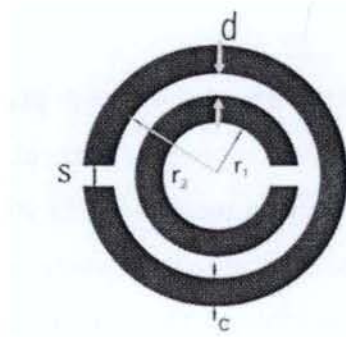


Fig. 5.1 Schematic drawing of an SRR unit cell

A time varying magnetic field applied parallel to the axis of SRR induces rotating currents in the rings, which produces its own magnetic flux to enhance or oppose the incident field. Due to splits in the rings, the SRR unit can be made to resonate at wavelengths much larger than the diameter of the rings. This would not happen in closed rings. The purpose of the second split ring inside and the slit opposite to the first is to generate a large capacitance in the small gap region between the rings, which enables current flow by means of new displacement current. The dimension of the structure is smaller than the free space wavelength resulting in low radiative losses and so very high quality factor.

5.1.1 Transmission characteristics of SRR loaded microstrip Line

The SRR unit cell designed to resonate at 3.7 GHz is placed on a microstrip line as shown in Fig. 5.2. The characteristic of the filter is studied by electromagnetically coupling the SRR unit cell to a microstrip transmission line. The level of rejection depends on the coupling between feed line and resonator and also on the number of resonators. When placed symmetrically above the line (position X_1), no H-field lines penetrate through the axis of the resonator to induce resonance. Thus, the signal propagates from the input port to output port without any attenuation. The H- field lines can have perpendicular incidence on the SRR resonator, when the superstrate is shifted laterally with respect to the transmission line centre along the x-axis(X_1 through X_3). At

X_3 , field lines, both electric and magnetic, interact with the SRR to induce resonance leading to signal inhibition at the resonant frequency. Thus, maximum attenuation level in the rejection band is obtained when placed at position X_3 .

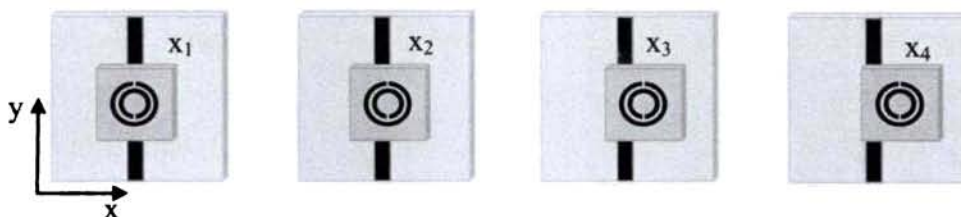


Fig. 5.2 SRR unit cell at various positions with respect to microstrip line

In Fig.5.3, S_{21} plots for different lateral positions of the superstrate are plotted. It is clearly seen that at X_1 the resonance disappears since the SRR is placed symmetrically above the microstrip line.

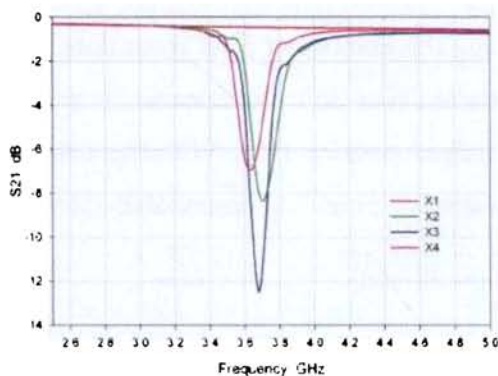


Fig. 5.3 Simulation results of SRR superstrate at different lateral positions

The attenuation increases with the position X_2 through X_3 and decreases at X_4 since it is away from the transmission line. To validate the above fact, current density plots have been obtained by simulation at 3.7GHz by placing the SRR at positions X_1 and X_3 and shown in Fig.5.4. At X_1 (Fig.5.4a), i.e., symmetrically above the microstrip line, the signal propagation is not interrupted as the H-field lines never

penetrate through the SRR axis to excite it. At X_3 (Fig. 5.4b), the SRR particle is adequately excited by the H-field lines at the air-dielectric interface resulting in resonance producing strong attenuation at the resonant frequency.

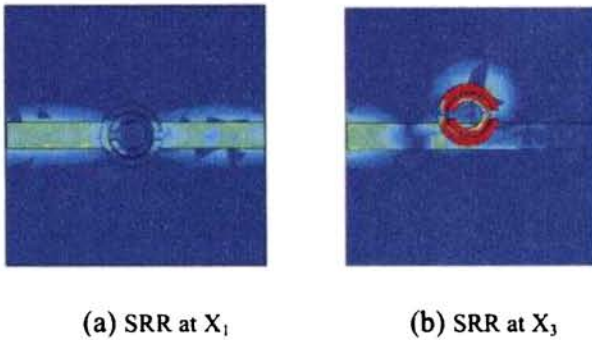


Fig. 5.4 Current density plots for SRR loaded transmission line at position X_1 and X_3 .

The frequency response of the single SRR loaded transmission line can be further enhanced by increasing the number of SRR resonators on the superstrate. The effect of number of SRR resonant cells on the attenuation is also studied by increasing the number cells at the optimized position (X_3). With the size constraints in mind, a minimum number of SRR resonators providing appreciable attenuation are optimized.

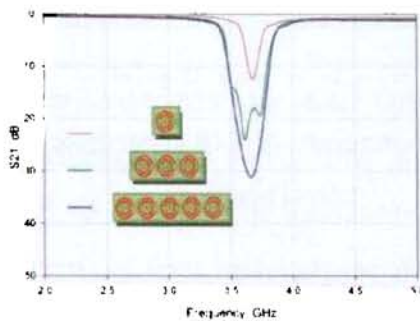


Fig. 5.5 Transmission characteristics of SRR loaded transmission line with varying number of SRR resonators

As depicted in Fig. 5.5, a minimum of 5 SRR cells are required to attain an attenuation of -30dB. The superstrate has the advantage of flexibility of easy coupling gap adjustment and resonator/circuit replacement or modifications. Added advantage of this type of flexible EM coupling is that resonating circuits can be replaced or additional notch resonators can be added, easily without affecting the underlying feed line and port connections, thus achieving properties like multi-frequency operation without much difficulty.

- **SRR array based microstrip bandstop filter**

This section is devoted to design microstrip band reject filter based on the rejection properties of SRR array. When loaded with SRR array, the microstrip line behaves as compact, high Q band reject filters with deep stop band in the vicinity of its resonant frequency. If properly coupled to the host microstrip line, these particles produce rejection levels required in most of practical applications (i.e. >20dB).

A prototype of the SRR array of five unit cells was fabricated by means of etching the pattern on a substrate of relative permittivity $\epsilon_r=2.0$, thickness $t = 0.5, 1, 1.5$ and 2 mm for investigating the variation of the transmission characteristics with height above the microstrip line. A 50Ω microstrip line is fabricated on commercially available FR4 substrate ($\epsilon_r = 4.36, h = 1.6$ mm).

The SRR array was placed over the microstrip line as shown in Fig.5.6 (lateral view). The transmission and reflection coefficients were measured with the aid of Agilent E8362B PNA network analyzer. The effect of lateral of the SRR array over the microstrip line was studied by placing the superstrate of a particular thickness at different lateral positions along the X-axis (X_1, X_2, X_3, X_4) and the transmission characteristics are shown in Fig.5.7.

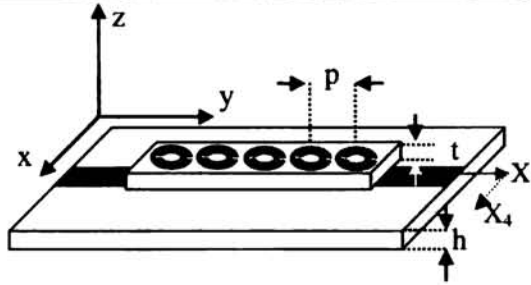


Fig. 5.6 SRR superstrate loaded microstrip line filter ($p=8\text{mm}$, $N=5$, $r_1=1.6\text{mm}$, $r_2=2.7\text{mm}$, $c=.9\text{mm}$, $d=.2\text{mm}$ and $s=1\text{mm}$)

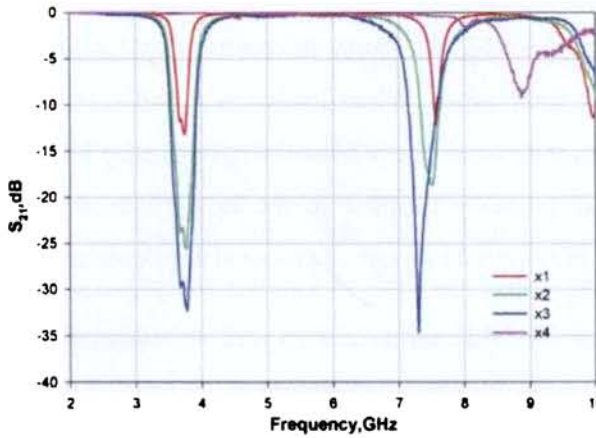


Fig. 5.7 Measured S-parameters of microstrip line loaded with SRR array superstrate at different positions ($t=0.5\text{mm}$)

- **Effect of height above the transmission line**

In order to verify the dependence of thickness, arrays fabricated on different superstrates were placed at the optimum position X_3 and measured. The S_{21} plots are shown in Fig. 5.8. It was observed that the maximum stop band attenuation occurred for minimum value of superstrate thickness ($t=0.5\text{mm}$).

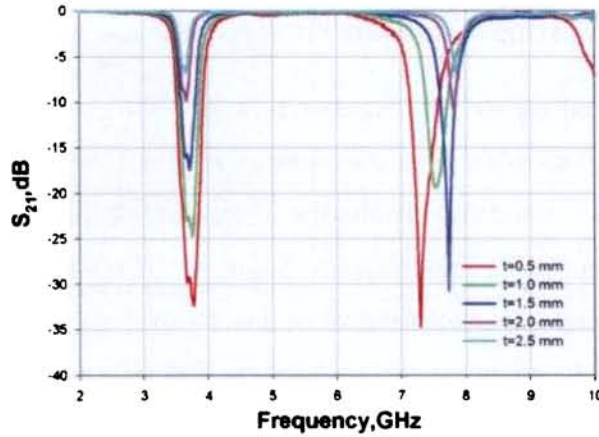


Fig. 5.8 Measured S_{21} -parameters of microstrip line loaded with SRR array superstrate at different heights.

The photograph of the superstrate loaded filter is shown in Fig. 5.9(a). The characteristics of the optimum filter measured in Agilent HP 8510C VNA is shown in Fig. 5.9(b). At the resonant frequency ($f=3.7$ GHz, approx.) S_{21} of -32dB is obtained with 5 SRR elements.

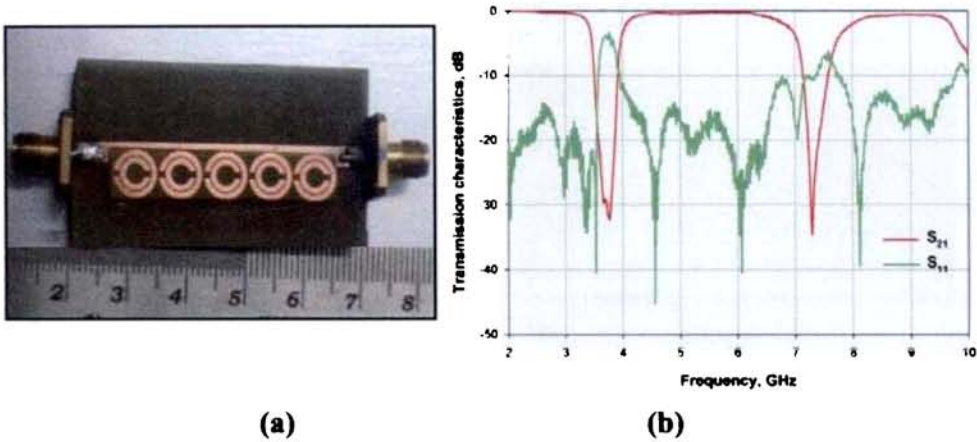
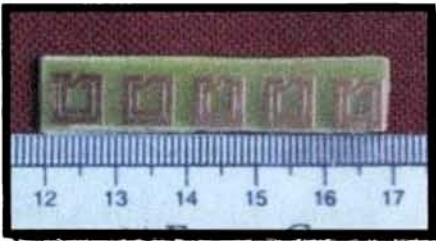


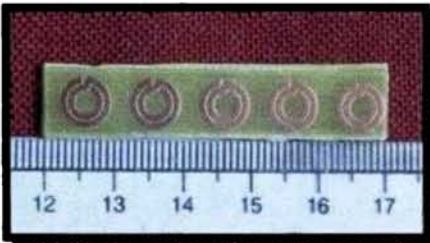
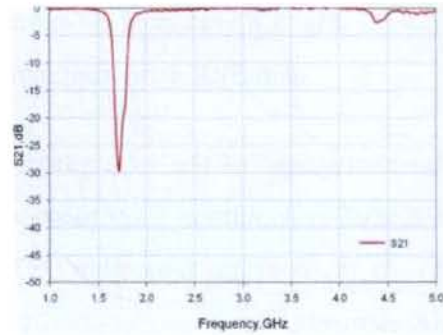
Fig. 5.9 (a) Photograph of the superstrate loaded filter **(b)** Measured S parameters of the optimized filter

- **Superstrate arrays of different element shapes**

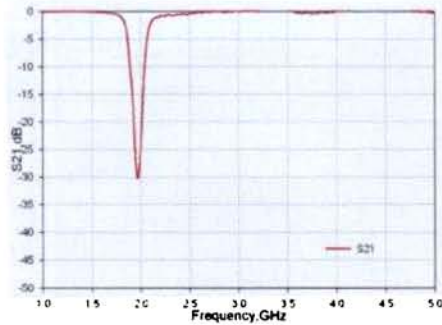
As mentioned earlier, this superstrate method has the additional advantage of flexibility of easy coupling gap adjustment and resonator/circuit replacement or modifications. This method also enables the selection of different structures and designs according to the frequency requirements. Some of the resonator arrays fabricated to illustrate the filtering characteristics when placed over the transmission line at the optimized position to attain maximum coupling and rejection are shown in Fig.5.10 with their frequency response.

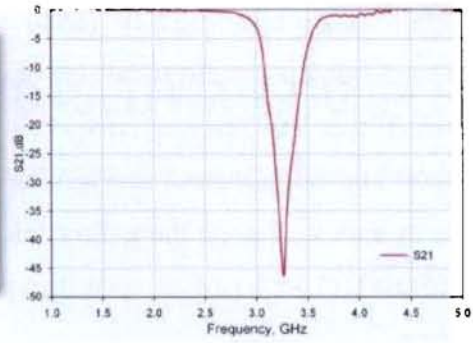
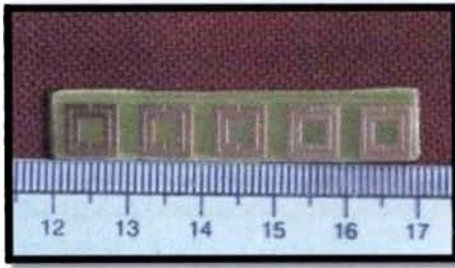


(a) Spiral resonator-Square.

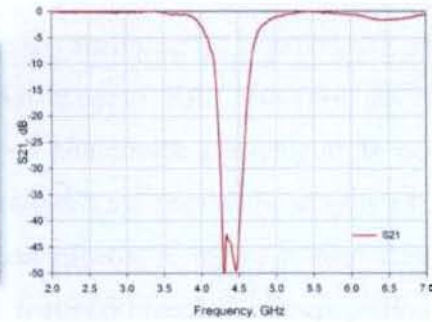
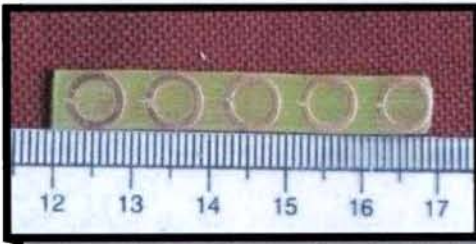


(b) Spiral resonator- Circular

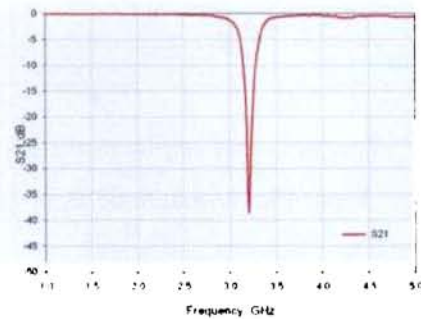
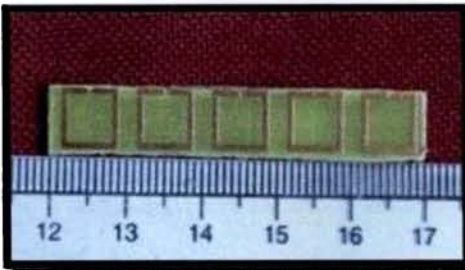




(c) Split ring resonator-Square



(d) Open loop resonator- circular



(e) Open loop resonator-Square

Fig 5.10. Measured transmission characteristics of microstrip line loaded with (a) & (b) Spiral resonators (c) Square SRRs (d) & (e) Open loop resonators

The resonators in Fig.5.10 (a&b) are spiral resonators (SRs) which allow significant reduction in the electrical size of unit cell compared to other ring resonators. It is verified that the resonant frequency of SRs are one half that of its SRR counterparts. The characteristic in Fig.5.10(c) is based on square split ring resonator array with its split axis along the x-direction, to attain narrow bandwidth. The filters in Fig.5.10 (d) and (e) are based on open loop resonator array which are simpler to design and fabricate.

5.2 Conclusion

The transmission characteristics of microstrip line loaded with SRR particles as superstrate are presented. SRR, in the proximity of a microstrip line, inhibits the signal propagation at frequencies determined by its dimensions. Amount of notching and width of the stop band formed are functions of the superstrate height and its relative position with respect to the microstrip line. The frequency of the stop band may be varied by changing the dielectric constant of the superstrate. Our investigation shows that periodic arrangement of SRR over the transmission line gives a band reject filter with appreciable attenuation and low insertion loss.

References

- Falcone F ,*Synthesis and applications of Microwave Metamaterials in Planar Circuit Technology: From Electromagnetic Bandgaps to Left Handed Materials*, chap. 5, pp. 102-103, 2005.
- Martin F., Falcone, F., Bonache, J., Lopetegi, T., Marque's, R., and Sorolla, M.: 'Miniaturized CPW stop band filters based on multiple tuned split ring resonators', *IEEE Microw. Wirel. Compon. Lett.*, 2003, 13, pp. 511–513.

SRR BASED WAVEGUIDE FILTER

© 2011 by CRC Press, Inc. All rights reserved. No part of this publication may be reproduced, stored in a retrieval system, or transmitted, in any form or by any means, electronic, mechanical, photocopying, recording, or by any information storage and retrieval system, without prior written permission from CRC Press, Inc.

This chapter presents the behavior of SRR in waveguide for the development of bandstop and bandpass filters. Use of SRR array for the rejection of a desired band above the cut-off frequency of the waveguide is investigated in the beginning of the chapter. Also the frequency response of the waveguide below cut-off with SRR insert is explored for the development of bandpass filter. This study leads to the phenomenon of waveguide miniaturization.

6.1 Introduction

The classical rectangular waveguide theory is still very much usable in order to build various filter structures, which can meet requirements of the modern technology. The ability of SRRs to inhibit signal propagation in the vicinity of the resonant frequency when properly excited (magnetic field normal to its plane), have already been utilized for the development of several planar filters.

An array of SRR, when placed along the center of the waveguide with the magnetic field parallel to the SRR axis, inhibits the propagation of signal from input port to the output port at the resonant frequency above the waveguide cut off. The same structure can also be used for passing a desired frequency band below the waveguide cut off, in the vicinity of its resonant frequency pointing towards the miniaturization of the waveguide filter. A detailed investigation on the bandwidth characteristics of both stopband and passband with the parameters of the array within the waveguide are carried out. The simulation carried out using Ansoft HFSS has been validated by fabrication and measurement.

- **Transmission properties of SRR in a waveguide**

In this section, the propagation characteristics of a waveguide with array of SRR placed along the axis is discussed. A narrow band rejection is obtained at the first resonant frequency of the SRR, whereas a wide band rejection is obtained at the second resonance.

Rectangular waveguides were one of the earliest types of transmission lines used to transport high frequency signals and are still used today for many high power and low loss systems at microwave and mm wave frequencies. The hollow rectangular waveguide can propagate TE and TM modes, but not TEM waves. Figure 6.1 shows a rectangular waveguide with dimension a and b and parameters ϵ and μ .

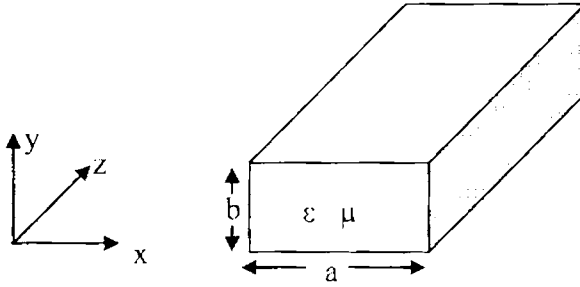


Fig. 6.1 Schematic of rectangular waveguide

The cut-off frequency is given by,

$$f_c = \frac{1}{2\sqrt{\epsilon\mu}} \sqrt{\left(\frac{m}{a}\right)^2 + \left(\frac{n}{b}\right)^2} \text{ Hz} \quad (6.1)$$

where, m and n represent possible modes in x and y directions.

For dominant mode TE_{10} ,

$$f_c = \frac{1}{2a\sqrt{\mu\epsilon}} \text{ Hz} \quad (6.2)$$

SRR array is placed along the center of the waveguide as shown in Fig. 6.2 since the electric field intensity is highest at center of the waveguide, making it possible to achieve greatest interaction of the SRR array with the electric field. Also, as already mentioned, the SRR would be excited by a time varying magnetic field with significant component parallel to the ring axis.

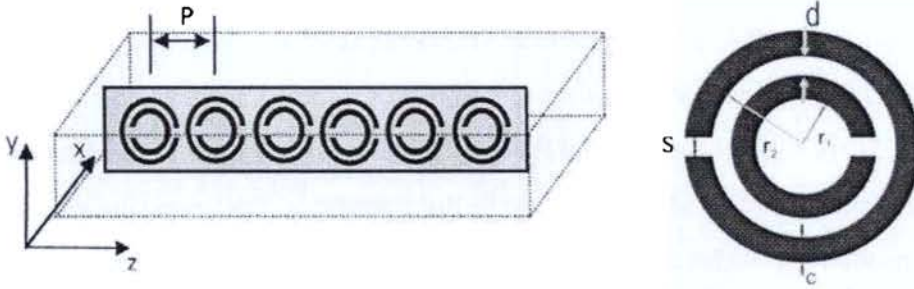


Fig. 6.2 SRR array loaded rectangular waveguide

From basic electromagnetic (Balanis, 1989), it is known that one can resolve fields of the TE waveguide mode into two plane waves (Fig. 6.3(a)). These plane waves propagate along the waveguide in the zigzag fashion due to successive reflections at waveguide walls.

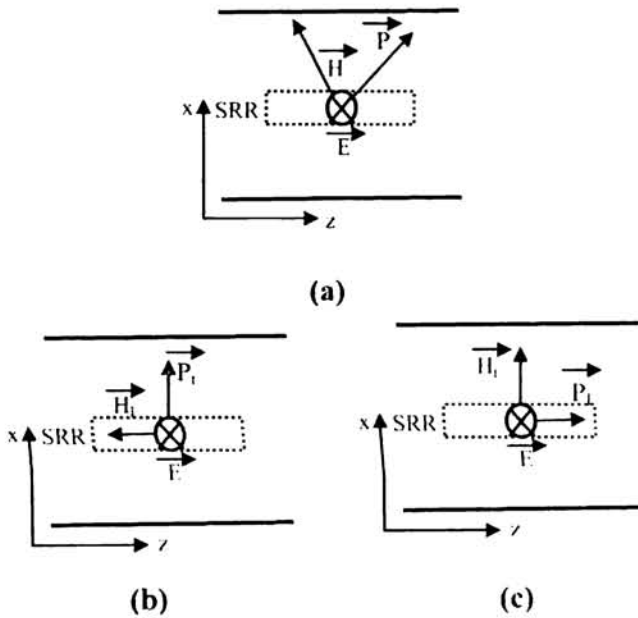


Fig. 6.3 Propagation in the waveguide filled with SRR array (a) The equivalent plane wave (b) The propagation in the transversal direction (c) The propagation in the longitudinal direction.

For each plane wave, the longitudinal components of the magnetic field vector H_1 and the electric field vector E define the transversal component of the Poynting vector P_t (Fig. 6.3(b)). This component of Poynting vector experiences total reflection at the waveguide walls. It causes standing wave in the transversal direction, the existence of which is needed in order to satisfy the boundary conditions. The transverse component of the magnetic field H_t and E produces a Poynting vector in the axial direction as shown in Fig.6.3(c).

The SRR can be thought of as a small capacitively loaded loop antenna (Harbar et al., 2005). The current flowing through the loop antenna (SRR) is induced by the component of the magnetic field vector that is perpendicular to the loop. Hence, it is the transversal component of the magnetic field (H_t), which is perpendicular to the SRR which will give rise to the induced current causing the resonance.

6.1.1 Bandstop characteristics of SRR in waveguide

In this section the band rejection behavior of the SRR array centrally placed in an S-band waveguide is investigated. The SRR unit cell is designed to operate at 3.7 GHz lying in the S-band spectrum. An array of ten SRR unit cells is placed along the axis of the S-band waveguide, which is excited in the TE_{10} mode with two coaxial-to-rectangular waveguide transitions as input and output. The arrangement of SRR array inside the waveguide and its transmission characteristics are illustrated in the Fig.6.4 (a&b) respectively.

The simulation studies using Ansoft HFSSTM showed absorption dips at the designed resonant frequency and at higher resonance. The first resonance is in the S-band while the second resonance in the X-band region.

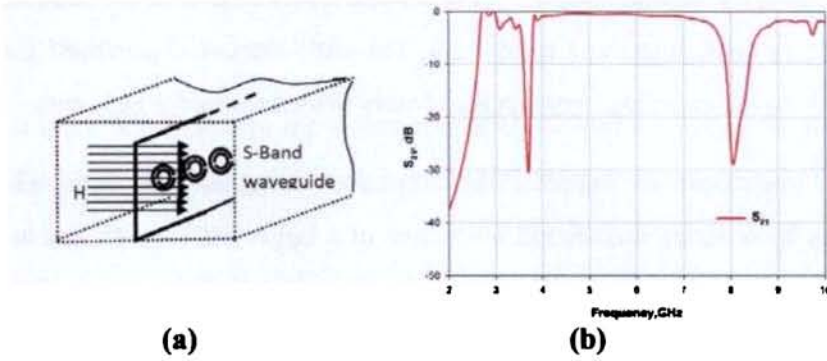


Fig. 6.4(a) SRR array loaded S-band waveguide ($p=10\text{mm}$, $N=10$, $r_1=1.6\text{mm}$, $r_2=2.7\text{mm}$, $d=0.2\text{mm}$, $c=0.9\text{mm}$, $s=0.5\text{mm}$) (b) Transmission characteristics

Since the dimension of the SRR unit cell is very small compared to the waveguide height, very few magnetic field lines penetrate through the SRR to produce considerable attenuation. The level of attenuation and bandwidth can be improved by increasing the number of SRRs along the y axis in the array so that maximum H-field lines penetrate the SRR cells.

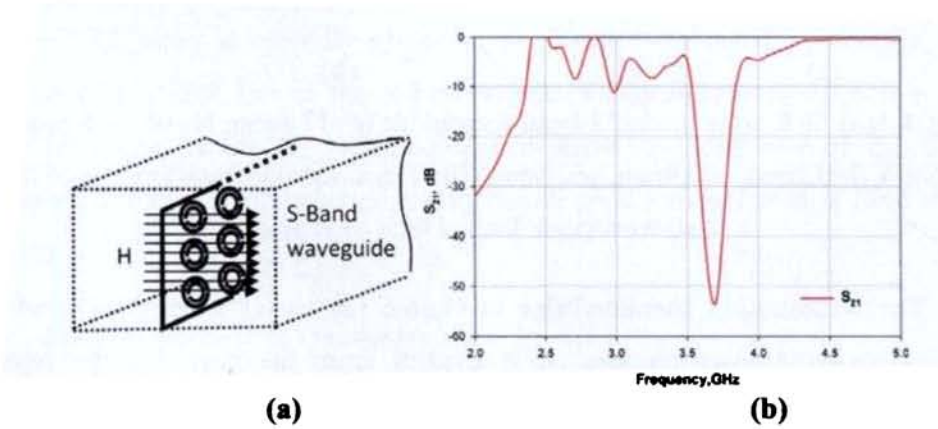


Fig. 6.5 (a) Three rows of SRR array loaded S-band waveguide of SRRs (b) Transmission characteristics

The transmission characteristics in Fig.6.5 shows considerable attenuation at the resonant frequency with improved bandwidth, but with increased passband insertion loss which is due to the coupling between the closely placed resonator elements.

Another technique to improve the stopband characteristics with minimum passband loss is by utilizing the second resonance of a larger SRR which lies in the S-band region. To attain this, an SRR array with 10 unit cells with larger dimension designed to generate the second resonance at 3.7GHz is inserted in the S-band waveguide (Fig. 6.6a).

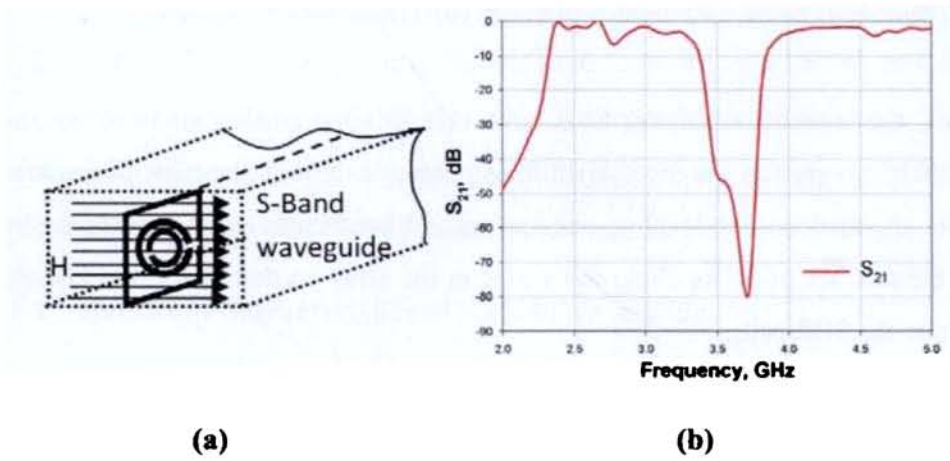


Fig. 6.6(a) SRR array loaded S-band waveguide ($p=17.8\text{mm}$, $N=10$, $r_1=5.5\text{mm}$, $r_2=6.6\text{mm}$, $d=0.2\text{mm}$, $c=0.9\text{mm}$, $s=0.5\text{mm}$) **(b)** Transmission characteristics of the S-band waveguide loaded with SRR array

The transmission characteristics in Fig.6.6 (b) shows a rejection band with minimum passband insertion loss. It is evident from the plot that the rejection characteristic is better than that shown in Fig.6.5 which is due to the enhanced interaction of the H fields with the larger SRR compared to the smaller one.

At higher frequencies, the dimension of SRR becomes extremely small causing fabrication limitations. In order to develop waveguide bandstop filter using SRR at

higher frequencies, SRR of dimension with its second harmonics, lying in the desired frequency region will be a good choice.

Figure 6.7(a) shows the schematic of the X-band waveguide with SRR array having the fundamental resonance at 3.7GHz and second resonance around 7.5GHz.

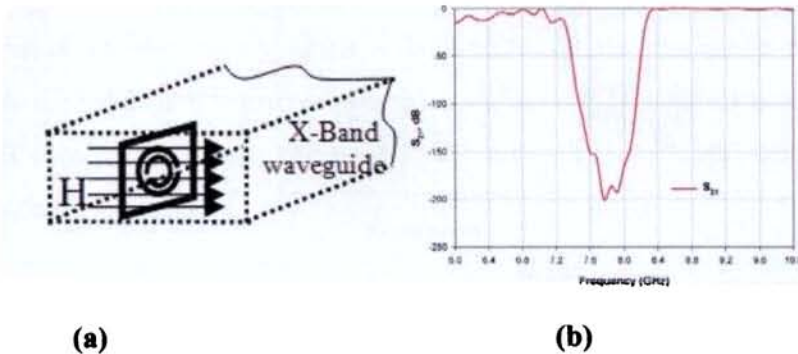


Fig. 6.7 (a) The SRR array in X-band waveguide ($r_1=1.6\text{mm}$, $r_2=2.7\text{mm}$, $d=0.2\text{mm}$, $c=0.9\text{mm}$, $s=0.5\text{mm}$, $p=10\text{mm}$) (b) Enhanced Second resonance in the X-band waveguide

Figure 6.7(b) shows significant attenuation with low passband insertion loss when the SRR array is centrally placed in the X-band waveguide, since the second resonance of the SRR lies in the X-band region where signal propagation is in the lowest TE mode of the X- band waveguide. Here, the diameter of the SRR is comparable to the waveguide height giving rise to good interaction of H field with the SRR array.

- **Effect of number of resonators**

For filter fabrication, the number of resonators for considerable attenuation is optimized by inserting the SRR array with varying number (N) of cells on a single-sided FR4 substrate of dielectric constant 4.4 and height 1.6mm, with a period of 10mm. An absorption dip is observed in the waveguide passband at around 7.8 GHz. The experiment is repeated using arrays with different number of unit cells. It is found that the attenuation is increasing with the number of

unit cells, as shown in Fig. 6.8(a). With $N=12$, the received power level reaches the noise floor of the measuring instrument.

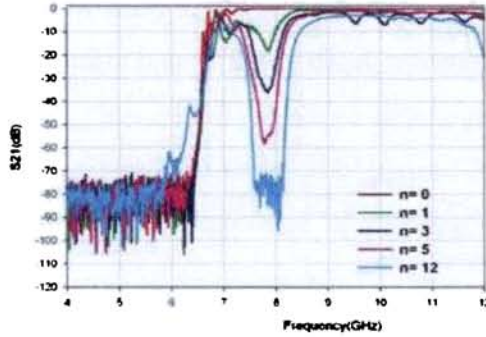


Fig. 6.8 Measured S parameter of standard X-band waveguide filled with SRR array of varying number of unit cells($r_1=1.6\text{mm}$, $r_2=2.7\text{mm}$, $d=0.2\text{mm}$, $c=0.9\text{mm}$, $s=0.5\text{mm}$)

- **Effect of position of the array inside the waveguide**

Now, the SRR array with optimum number of unit cells($N=12$) is moved along the broadside (x -axis) of the waveguide and the transmission characteristics are studied with the distance from the narrow wall. The transmission coefficient S_{21} obtained as the SRR array was moved towards the waveguide wall is given in Fig. 6.9(a).

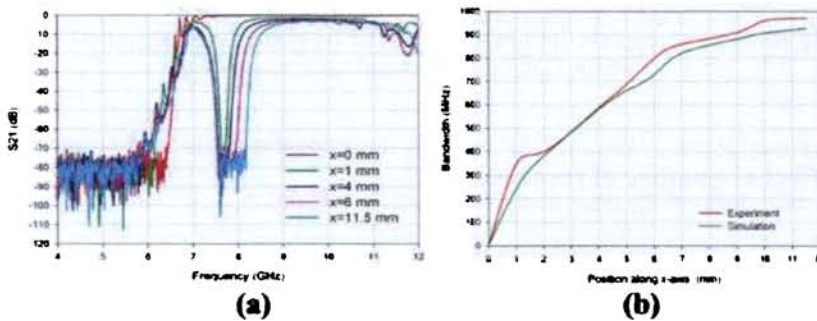


Fig.6.9 (a) Bandwidth variation with position **(b)** Variation in bandwidth vs. position of the SRR array

The width of the stopband varies with the distance x of the SRR array along the x -direction. At the center line of the waveguide, i.e., at $x=11.5\text{mm}$, it was found that the array produces maximum attenuation since the H field lines are exactly perpendicular to the plane containing SRR array producing maximum interaction. Here, $x = 0$ corresponds to the rings in contact with the narrow wall of the waveguide. The bandwidth variation with position of the array within the waveguide is shown in Fig. 6.9, where the bandwidth is narrow near the walls increasing to a maximum at the center. A -10dB absorption dip was observed in the waveguide passband from 7.25GHz, which extended up to 8.5GHz.

6.1.2 Bandpass characteristics of SRR in waveguide: Waveguide miniaturization

A disadvantage of using waveguide filters is the relatively large size required for low-frequency operation. Therefore, physical dimension of the waveguide is an important parameter that needs to be considered.

In this section, a Ku-band waveguide is loaded with periodically arranged SRRs along the waveguide line of symmetry. As discussed in the previous section the wide band nature and bandwidth tunability, with position inside the waveguide of second resonant band, is utilized to generate a wide passband with adjustable bandwidth in the X-band region using a Ku-band waveguide; thus attaining waveguide miniaturization.

A SRR array of 18 unit cells with a period $a=10\text{mm}$ was fabricated on an FR4 substrate of $h= 1.6\text{mm}$, loss tangent=0.02 and dielectric constant 4.4. The SRR array is inserted along the center of the Ku-band waveguide. The length of the inclusion was selected so as to extend till the waveguide adapter port (Fig.6.10) to enable the efficient coupling at the lower frequencies in the vicinity of the resonant frequency of the SRR. Here, in order to obtain passband below waveguide cut off, SRR with resonant frequency below the waveguide cut off is selected.



Fig.6.10 SRR array inserted Ku-band waveguide

The structure is simulated using Ansoft HFSS and results are shown in Fig.6.11. One can notice that the two propagation passbands appear below the waveguide cutoff, one at the fundamental frequency 3.6GHz and other at twice the fundamental resonance (7.0GHz).

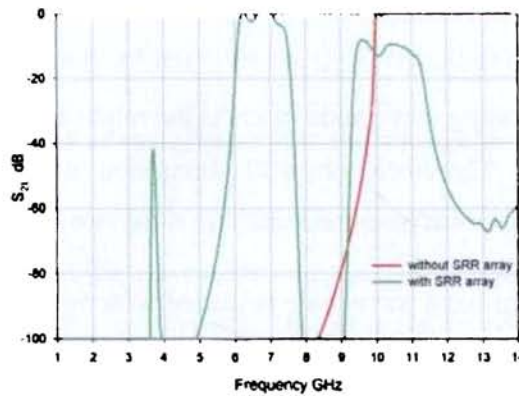


Fig. 6.11 Simulated transmission coefficients of a Ku-waveguide with SRR array

A very narrow band was observed at the resonant frequency with a large insertion loss of about -42dB. Whereas a wider band was obtained at the second resonance with minimum losses. In order to verify the phenomenon of propagation below cutoff, a Ku-band waveguide has been inserted with an array of SRR containing 18 resonators as shown in the photograph of Fig.6.12 (a). In order to allow maximum coupling, the SRR array was extended till the probes of waveguide adapters. The measurement was carried out in Agilent Network Analyzer HP8510C. The measured transmission coefficient (S_{21}) is shown in Fig. (6.12b). The experimental results show a

single passband in the cutoff region at the second resonance. The band corresponding to the fundamental frequency is not visible due to large insertion loss.

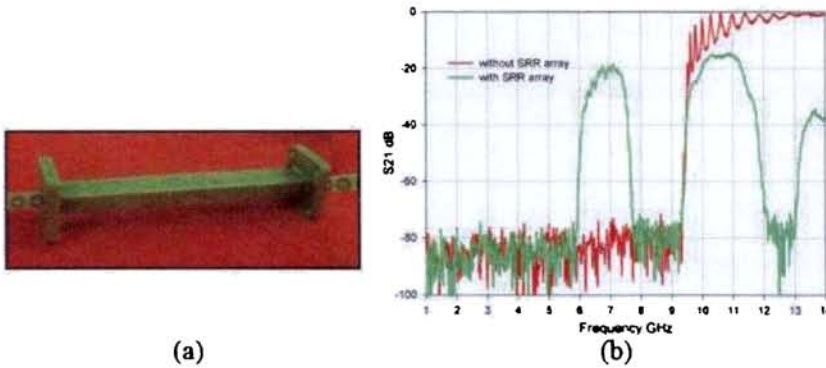


Fig. 6.12(a) Photograph of the Ku- waveguide loaded with SRR array (b) measured transmission coefficient

The large insertion loss is due to the weak coupling of the frequencies below Ku-band cut-off. The wide passband in the X-band region using the Ku-band waveguide proves the role of SRR in miniaturization of waveguide.

6.2 Conclusion

It has been shown both theoretically and experimentally that rectangular waveguide filled with SRR array inhibits the propagation above the cut-off of the waveguide and supports propagation below the cut-off frequency. The attraction of this work is that instead of exploiting the fundamental resonant frequency of the SRR, the second harmonics is utilized to control the bandwidth of the two types of filters.

References

Balanis C. A, *Advanced Engineering Electromagnetics*. New York: Wiley, 1989.

Chapter 6

Hrabar S, Bartolic J, and Sipus Z, "Waveguide Miniaturization Using Uniaxial Negative Permeability Metamaterial," *IEEE Trans on Antennas and Propag.*, vol. 53, no. 1, pp. 110-119, 2005.

CONCLUSIONS

The conclusions drawn from the simulation and experimental investigations carried out on loop resonators for the development of bandstop and bandpass filters are presented in this chapter. A few suggestions for further investigations on this topic are also provided.

7.1 Thesis Highlights

This chapter presents the summary of the investigations carried out and the comments on the results obtained therein. The essence of the thesis is incorporated in chapters 4 through 6. Studies on loop resonator based planar bandstop and bandpass filters, miniaturization techniques and harmonics suppression techniques are carried out in chapter 4. Simple and compact microstrip bandstop filter and bandpass filters are designed and implemented. It is demonstrated that the filters can be tuned electronically by embedding varactor diode in the slit. Empirical formulas are derived for the resonant frequency and for harmonics suppression. The compactness and tunability made these designs attractive for printed circuit boards and monolithic microwave integrated circuit technologies. A different approach for band rejection in planar transmission line is applied with SRR array as superstrate in chapter 5. The investigation shows that periodic arrangement of SRR over the transmission line gives a bandstop filter with appreciable attenuation and low insertion loss. Chapter 6 explores the bandstop and bandpass characteristics of SRR inside the waveguide. It has been shown that rectangular waveguide filled with SRR array inhibits the propagation above the cut-off of the waveguide and supports propagation below the cut-off frequency. The attraction of this work is that instead of exploiting the fundamental resonant frequency of the SRR, the second harmonics is utilized to control the bandwidth of the two types of filters. Suggestions for further investigations and scope for more detailed study in the area are also given at the end of the chapter.

7.2 Compact Planar Loop Resonator Filters

The characteristics of the closed loop resonators lead to the study of open loop resonator for the development of filters compact in size. The characteristics of open loop resonators and the influence of slit on the resonant frequency are studied in the section 4.1.1. The difference in coupling due to the position of the slit with respect to

the transmission line is quantified as an effective permittivity value. This enabled the development of empirical formula for the resonant frequency which is verified by the comparative study of the calculated and simulation studies and tabulated in Table 4.1. In this structure, a minimum of three resonators were required for attaining an attenuation of about -30 dB, which is clearly a drawback. Overall structure is made compact with comparable attenuation using a single resonator side coupled to a transmission line which is bent into a U-shape. This approach produces considerable attenuation level and a narrower bandwidth with a single resonator. The frequency response characteristics, effect of slit width, coupling length and electronic tuning capability of the compact filter are investigated in the section 4.1.2.

7.3 Parallel Coupled Loop Resonators

The bandpass characteristics of the loop resonators placed between two parallel coupled transmission lines is investigated in the section 4.2. Bandpass filter using parallel coupled hairpin resonators are developed for configurations $L < W$ and $L > W$. For configuration $L < W$, the effect of coupling length on the bandwidth is shown in Fig.4.45. The bandwidth of the filter is controlled by the position of upper transmission zero, which is determined by the coupling length W . Filter with minimum bandwidth is optimized. In this case, the higher harmonics are suppressed by integrating bandstop filter at the harmonic frequency. For configuration $L > W$, the effect of coupling length on the bandwidth is shown in Fig.4.50. The harmonics are removed by tuning the transmission zero frequency to correspond to the harmonic frequencies. The transmission zeros are a function of side arm length L and coupling length W . Here configuration of the resonator is carefully selected to eliminate the higher harmonics.

7.4 Compact Bandpass Filter using Folded Loop Resonator

The section 4.3 presented the results of the study performed on the loop resonator by folding it to reduce the size. The characteristics of the folded closed loop resonator placed between two parallel coupled lines are presented in the beginning of the section. Size of the filter is further reduced by introducing a slit in the closed loop to form folded open loop resonator filter. The bandpass characteristics shown of the folded open loop resonator is depicted in Fig.4.59. The effect of coupling length on the harmonics frequencies are investigated and plotted in Fig.4.61. The second harmonics is removed by varying the coupling length W , which tunes the transmission zero value to correspond to the second harmonics without affecting the fundamental frequency band. The third harmonics is removed by varying the length of the second feed line which produces a transmission zero at the third harmonics.

7.5 SRR Based microstrip Bandstop Filter

SRR array as superstrate for bandstop filter application is described in the section 5.1. The band rejection characteristics with variation in coupling strength with the thickness of the superstrate as well as the lateral position of the SRR array from the microstrip are investigated and verified by experiment. The responses of other loop resonator array as superstrate are also examined.

7.6 SRR Based Waveguide Bandstop Filter

Waveguide bandstop filter developed using SRR array are presented in section 6.1.1. The band rejection characteristics at the first and second resonances of the SRR in the waveguide are investigated. The experiments are carried out in X band waveguide on the second resonance for adjusting the attenuation level and bandwidth with different number of resonators and position of SRR array respectively. The results are shown in Fig. 6.8 and Fig.6.9 respectively.

7.7 SRR Based Waveguide Bandpass Filter

The bandpass characteristic of SRR in waveguide below cut-off is studied in section 6.1.2. Since a very narrow band with high attenuation appear at the fundamental resonance presenting a poor bandpass response. Therefore, the second resonance which produces a wider band and comparatively lesser attenuation is utilized. The measured result of the bandpass characteristics in a Ku-band is shown in Fig.6.12.

7.8 Suggestions for future work

This thesis presented the development of microstrip bandstop and bandpass filters with the primary aim of miniaturization and has been successful in attaining the objective to a great extent. Filters can be further miniaturized by the use of high temperature superconductors (HTS). Because of the intrinsic low loss of HTS at microwave frequencies it is possible to reduce the size of filters still retaining performance. The performance of a filter is also improved by the use of superconductors in the sense that the insertion loss can be significantly reduced by improving the filter roll off and reducing the bandwidth.

List of Publications related to thesis work

International Journals

1. **B. Jitha**, C. S. Nimisha, C. K. Aanandan, P. Mohanan, and K. Vasudevan "SRR loaded waveguide band rejection filter with adjustable bandwidth," *Microwave and optical technology letters*, Vol. 48, No. 7, pp. 1427-1429, 2006.
2. C. K. Aanandan, C. S. Nimisha, **B. Jitha**, , P. Mohanan, and K. Vasudevan "Transmission properties of microstrip lines loaded with slit ring resonators as superstrate," *Microwave optical technology letters*, Vol. 48, No. 11, pp. 2280-2282 ,2006.
3. **B. Jitha**, P.C. Bybi, C.K. Aanandan and P.Mohanan, " Microstrip band rejection filter using open loop resonator", *Microwave and optical technology letters*, Vol.50, No.6, pp.1550-1551, 2008.
4. **B.Jitha**, P.C. Bybi, C.K. Aanandan, P.Mohanan and K. Vasudevan, "Compact microstrip bandpass filter using folded U-shaped resonator with harmonic suppression," *PIERL*, 14, pp.69-78,2010.

National Conferences

- 1 **B. Jitha**, C. S. Nimisha, C. K. Aanandan, P. Mohanan, and K. Vasudevan. "Band rejection characteristics of a waveguide with SRR array inserts," *Proc. Of National Symposium on Antennas and Propagation (APSYM2006)*, pp.249-252, 2006.

Other Publications

International Journals

1. P.C. Bybi, Gijo Augustin, **B. Jitha**, Binu Paul, C.K.Aanandan , K. Vasudevan and P.Mohanan, "Compact Monopole Excited Drum Shaped Antenna for AWS/ DCS/ PCS/ DECT/ 3G/ UMTS/ BLUETOOTH Application," *International Journal on Wireless and optical communications*, Vol. 4, No.2,pp. 195-206, 2007.
2. P.C. Bybi, **B. Jitha**, P.Mohanan and C.K.Aanandan, "Wide Band Planar Antenna for New Generation Mobile Applications," *International Journal of Antennas and Propagation*, Vol.2007,pp.1-7, 2007.
3. P.C. Bybi, Gijo Augustin, **B. Jitha**, C.K. Aanandan, K.Vasudevan and P.Mohanan, "A Quasi-omnidirectional antenna for modern wireless communication gadgets", *IEEE Antennas and Wireless Propagation Letters*, Vol.7, pp.504-507, 2008.

International and National Conferences

1. P.C. Bybi, **B. Jitha**, C.K. Aanandan, K.Vasudevan, P.Mohanan, "A Compact wideband Antenna for modern wireless communication systems," *Proceedings of URSI General Assembly 20008, Chicago, USA*.
2. Pradeep, A.; **Jitha, B.**; Mridula, S.; Paul, B.; Aanandan, C.K.; Mohanan, P., "GA optimized SRR calculator," *Proceedings of Recent Advances in Microwave Theory and Applications, 2008. MICROWAVE 2008. International Conference* , pp.800-802, 21-24 Nov. 2008.
3. P.C Bybi, G. Augustin, **B.Jitha**, Binu Paul, C.K. Aanandan, K Vasudevan and P.Mohanan "Compact Drum Shaped Monopole Antenna for New Generation Mobile Applications", *Proc. Of National Symposium on Antennas and Propagation (APSYM2006)*, pp.283-286, 2006.

Resume of the Author

Jitha B

Research Scholar
Centre for Research in Electromagnetics and Antennas
Department of Electronics
Cochin University of Science and Technology
Kochi-22, Kerala, India
Email: jithab@gmail.com

OBJECTIVE

To pursue research activities in the field of microwave filters for present day communication gadgets.

EDUCATION

M.Sc Applied Electronics

PSG college of Arts and Sciences, Coimbatore, TamilNadu, India.
Bharathiyar University
Specialization: Applied Electronics
Duration: 2001-2003
Percentage: 83.68%

B.Sc Electronics

College Of Applied Sciences(IHRD), Calicut,Kerala, India
Calicut University
Duration: 1998-2000
Percentage: 79%

TEACHING EXPERIENCE

1. Seven months teaching experience in College of Applied Sciences(IHRD), Thodupuzha, affiliated to M.G. University.
2. Eight months teaching experience in Gurudev Arts and Science College, Payyanur, affiliated to Kannur University.

Resume of the Author

PERSONAL INFORMATION

| | |
|-------------------|--|
| Date of birth | 11.01.1980 |
| Languages Known | Malayalam, English, Hindi |
| Permanent Address | Thejus, B/H Elayavoor Service Bank, PO Mundayad Kannur. |

REFERENCE

Dr. C.K. Aanandan,
Professor,
Department of Electronics,
Cochin University of Science and Technology,
Cochin 22, Kerala, India
Email: anand@cusat.ac.in
Ph: +91 484 2576418

A

Ansoft HFSS 81

Anti resonant frequencies 157

B

Bandpass filter 9, 46, 130, 145, 150, 154

Bandstop filter 9, 37, 117, 147

Bulk wave 20

C

Closed loop resonator 26, 100, 106, 130

Coaxial resonator 20,24

Coaxial transmission line 11

CSRR 43, 57

D

Diplexer 143

Distributed elements 9, 20

E

Effective dielectric constant 85

F

Filters 4,7,31,

Folded loop resonator 133

Fractional bandwidth 8

H

Hairpin line filter 42

Hairpin resonator 42,121,130

Harmonic suppression 30,40 126,128,138

Helical resonator 17

Highpass filter 7

L

Loop resonator 21,83,85

Lowpass filter 7

Lumped elements 9

M

Microstrip filters 19,38

Microstrip line resonator 5,9,20

Microwave Communication 3

Microwave Filters 31

Microwave Frequency Bands 4

Microwaves 3

Mitered transmission line 101

Moderate band 9

N

Narrow band 9

Network Analyzer 77

Notch filter 32

O

Open loop resonator 21,87

P

Parallel coupling 6,111

Phase velocity 84

Photolithography 76

Planar filter 32,83

Zealand ie3d 72

Planar resonator 18

Propagation constant 85

Q

Q-Factor 115

R

Resonant frequency 80

Resonator 17

S

S parameter 80

SRR 22,35,75,88,149

Stepped impedance resonator 20

Stripline 10,20

Surface acoustic wave 17

T

TEM Wave 84

Transmission line resonator 20

Transmission media 7,9

U

Uniform impedance resonator 84

U-shaped transmission line 101

W

Waveguide 10,17

Wide band 9

Z

- T58 -

